J.S. Rao

# Simulation Based Engineering in Fluid Flow Design

Springer

Simulation Based Engineering in Fluid Flow Design

J.S. Rao

# Simulation Based Engineering in Fluid Flow Design

Springer

J.S. Rao
The Vibration Institute of India
Bangalore
India

ISBN 978-3-319-46381-0 ISBN 978-3-319-46382-7 (eBook)
DOI 10.1007/978-3-319-46382-7

Library of Congress Control Number: 2016952818



Printed on acid-free paper

This Springer imprint is published by Springer Nature
The registered company is Springer International Publishing AG
The registered company address is: Gewerbestrasse 11, 6330 Cham, Switzerland

*To my beloved wife Indira*
*and to the new arrival in the family great grandson Rumi*
*and in memory of my parents*
*Jammi Chikka Rao and Jammi Ramanamma*
*and in memory of my mentor*
*Dr. Nachimuthu Mahalingam*

# Preface

Fluid mechanics is the oldest subject practiced since antique times.

Water and air, together forming fluids, are primary to our life without which this life cannot exist. Therefore, we have always been curious to know more about the behavior of fluids. From earlier times going back to tens of thousands of years, we have been learning to tame water through canals, dams for agriculture and transportation. It is Archimedes of the Alexandrian school 2200 years ago who gave us a basic understanding of hydrostatics and his school produced even hydrodynamics principled through Hero's aeolipile, essentially a steam reaction turbine as we know it today. In the medieval periods, we learned to use wind power from sails and windmills. Things have changed since Newton (simultaneously Leibniz) came up with the discovery of Calculus that ushered in the Scientific Revolution.

During the Science Revolution period, basic governing equations for solids and fluids were derived; however, they remained unsolvable with the numerical tools that were available at that time. Moreover the need for solutions of these equations was not warranted because, even during the industrial revolution, the slow-speed reciprocating steam engines could be designed based only on trial and error and tests. Fluid mechanics was an empirical science that gradually developed from tests and the subject became known as hydraulics.

This scenario changed with the construction of a practical dynamo by Edison and construction of rotating machinery, first an impulse turbine by De Laval and a reaction turbine by Charles Parsons towards the end of the nineteenth century. (Actually Hero of Alexandria built nearly 4000 years ago the first reaction turbine but had no idea what to do with it beyond opening the temple doors using pulleys invented by Archimedes in that period.) The initial sizes of these turbines were so small in size that, producing only a few KWs of power, they could be built by intuition and a trial-and-error approach.

The hydraulics and hydrodynamics approach continued to provide simple solutions and approximate answers with which designs were produced in calculating flow paths and heat transfer. It is these approximate methods that stood the test of time for over a century in determining flow and heat solutions. Combustion problems were solved by tests and the trial-and-error approach until satisfactory solutions were obtained.

Man has quickly learned to adapt to the luxury of electricity and began demanding large-size machines that can produce more power; they in turn demanded designs which needed a better understanding of flow and heat transfer. To achieve these designs, there were no numerical tools to handle the complex physics of fluids.

The invention of digital computer using valves in Philadelphia (ENIAC) during the World War II has changed the scenario gradually; this was accelerated by transistors and subsequently integrated circuits in 1960s and suddenly began a boom for number crunching. The high performance computing that followed gradually replaced engineering approximations through computational fluid dynamics. It is now “Science to Engineering” or “Simulation-Based Engineering Science” through several commercially available codes to do the drudgery arising out of finite element methods or finite volume methods. This has revolutionized the outlook for designs; what used to be months of design time by several skilled engineers is now seconds or minutes of numerical effort.

There are several books dealing with the subject of finite elements or finite volume methods for flow analysis—then why this book?

Industry practices have changed drastically in the recent decade or two by adapting computer-aided methods leaving approximate methods for design analysis practiced during the twentieth century. The flow path is first CAD modeled followed by meshing before applying boundary conditions and setting up the numerical problem to be solved by a solver. These aspects of modeling, meshing and applying boundary conditions belong to a preprocessing stage before a problem is sent to a solver. The results from the solver go to a postprocessor to get what we may call a nearly complete exact picture of velocities, temperatures, pressures, densities, etc., that go into design. Most of the educational institutions across the world still follow basic courses in fluid mechanics developed during the last century. There is a need to bring science upfront in our undergraduate teaching that leads to engineering analysis in a manner that is directly applicable to industry practices. The methods developed during the pre-computer era are now becoming history and can be offered as electives at a later stage for those who want to learn historical aspects. We can now use directly simulation-based engineering science (SBES) with a high performance computing (HPC) background.

The design houses across the world practice cost-cutting methods in preprocessing aspects and even analysis by skilled workers rather than actual designers. A lot of preprocessing work can even be done outside the design companies and to save costs these types of jobs are outsourced to developing countries where engineering colleges mushroomed to cater to this category of jobs. Their standards are to be improved by introducing SBES approach so that they become globally employable.

This book deals with Fluid Mechanics. We begin with a brief historical background from Archimedes times dealing with ancient water wheels, windmills and the medieval period of Leonardo da Vinci. Otto von Guericke’s demonstration of a vacuum was followed by industrial revolution of James Watt', steam engines, Laval and Parsons' steam turbines and jet engines of von Ohain and Frank Whittle. The current state of fluid mechanics from Euler, Navier and Stokes and the present computational fluid mechanics are outlined before we begin with the subject proper.

We begin with fluid statics dealing with pressure in fluids at rest, buoyancy and basics of thermodynamics. Basic physics is next used for fluids in deriving mass balance, force balance and momentum equations, energy equation, kinetic energy, internal energy, shear stresses before giving a summary of fluid flow equations.

We next introduce the modern approach using the SBES, finite volume method. Simple cases of one-dimensional approach for diffusion with convection and pressure velocity coupling are considered. Steady-state one-dimensional incompressible problem and use of Pitot and Venturi tubes are given.

Adiabatic flow, isentropic flow, speed of sound are considered to explain shocks in supersonic flow. Restricting to one-dimensional case in the introductory course, quasi-one dimensional flows in axisymmetric nozzles is explained. One-dimensional converging-diverging nozzle is the basic building block of modern fluid dynamics, beginning with de Laval and Goddard in turbines and rockets. Subsonic and supersonic isentropic examples are given by analytical means first before applying CFD solutions. Though the theory is presented for finite volume method solution only for one-dimensional case to keep the course at introductory level, the CFD example for the nozzles are three-dimensional in nature. It is presumed that the student can see the logical extension from 1D to 3D cases, the details of general 3D finite volume method are left to a later course.

We then proceed to explain turbulence and with Reynolds equations derivations. Nozzle flow with a normal shock in the divergent portion is given next to top it with CFD solution of flow in converging-diverging nozzles with a normal shock.

Coimbatore J.S. Rao
March 2016

# Acknowledgments

I am basically a solid mechanics person through my initial stages after graduation. During the mid-1970s, I began to research about works on excitation forces acting on moving turbo-machine blades which led me to Theodore von Karman's work on isolated airfoils and this aerodynamics was alien to me. I then contacted Prof. William Sears of Ithaca, who had retired and settled in Tucson, Arizona from Rochester, NY. Being 35 years of age at that time, I was nervous about talking to him; true to the character of great teachers, he made me feel at ease and over three to four long-distance calls he explained the physics behind interfering stage flow. I am deeply indebted to Prof. Sears. That was my entry into fluid mechanics.

My large body of dedicated students worked hard in filling the empty areas of the puzzle that was an integrated approach to bringing to life the world of machine components. These students worked long hours in labs, computer centers and my home. They became a part of my family. I am extremely indebted to their devotion to the subject.

I began to realize slowly and steadily that solids, fluids and electromagnetism are interdisciplinary. It was astounding to see that our forefathers, Newton, Euler, Faraday among others have bequeathed us such a rich legacy of science over three centuries. In the absence of computational means, engineering disciplines and practices grew separately over the last century; this scenario is rapidly changing since the last decade or two with basic sciences providing accurate solutions, thus giving rise to simulation-based engineering science to the forefront. This necessitates a rethinking of the approach to inculcate approximate methods to engineering students and replace those by SBES.

My teacher and mentor, Prof. B.M. Belgaumkar, talked to me about this science 54 years ago. Frankly I didn't follow him then. After a continuous exposure to industrial problems in the last two decades I recall his industrial service after retirement in the 1970s. I am very grateful for his guidance in my life.

I am thankful to my colleague Ashok Kumar for helping in solving problems on computer. I am thankful to my Kumaraguru College of Technology office and their help in preparing the materials.

Finally, I would like to express deepest gratitude to Arutselvar Padmabhushan Dr. Nachimuthu Mahalingam. He is a freedom fighter, Gandhian, educationalist, a great Tamil scholar and above all a visionary providing guidance to people like me. He shaped my spiritual part of life in the last decade, particularly during the last 2 years. I have the honor to be associated with him in my academics. I thank him very much for giving me the opportunity to partaking in promoting scientific thinking and temperaments to younger generations of faculty and students. He is no longer with us now and I have the privilege to dedicate this book in his memory.

# Contents

# Chapter 1
# Introduction

**Abstract** This chapter outlines the beginnings of fluid mechanics developments from ancient Indus Valley Civilization to modern day applications of Turbomachinery through science revolution period.

**Keywords** Indus Valley Civilization · Archimedes screw · Hero's aelopile · Water wheels · Vitruvious · Leonardo da Vinci · Scientific revolution · Otto von Guericke · Steam engines · Laval nozzle · Jet engines · Rocket propulsion

The *Pancha Mahabhuta,* or "five great elements", of Hinduism are *Prithvi* or *Bhumi* (Earth), *Ap* or *Jala* (Water), *Agni* or *Tejas* (Fire), *Vayu* or *Pavan* (Air or Wind), and *Akasha* (Aether). Fluid Mechanics is the subject that deals with Water and Air, or Fluids in general. Both air and water form the lifeline of mankind, in general life as we know it on earth. Fluid Mechanics has been classified into hydraulics, which developed from experiments and hydrodynamics that developed through theory.

Hydraulics developed as a purely empirical science with practical techniques beginning in prehistoric times. People began to settle and built villages during Rig-Veda period, nearly 5–7 millennia ago as in ancient Indus Valley Civilization, see Fig. 1.1. Waterways, boats, sails using the wind as a source of energy existed.

Irrigation canals were discovered in Egypt, Greece and Mesopotamia that were constructed in this period. Storage tanks and masonry channels that guide water are said to have begun in Jerusalem. Channels were constructed to transport water as early as 4th century BC, and spread throughout the Roman Empire as given by Nakayama (1998), see Fig. 1.2.

Archimedes (287–212 BC) of Syracuse in Sicily is believed by many to be the first mathematical genius the world has so far produced. The Archimedean screw is illustrated in Fig. 1.3.

The most widely known anecdote about Archimedes tells of how he invented a method for determining the volume of an object with an irregular shape. King Hiero II, who had supplied pure gold to make a crown, doubted the honesty of goldsmith; so asked Archimedes to determine whether some silver had been

 
J.S. Rao, *Simulation Based Engineering in Fluid Flow Design*,
DOI 10.1007/978-3-319-46382-7_1

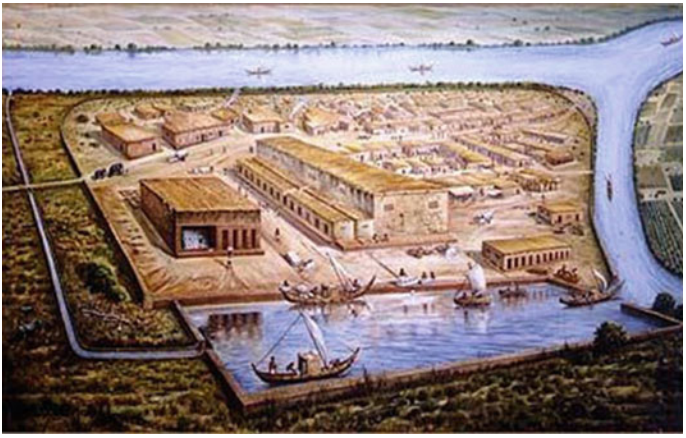

**Fig. 1.1** Indus Valley Civilization (http://www.yokibu.com/communityspeak/wp-content/uploads/2015/08/indus-valley-civilization.jpg)

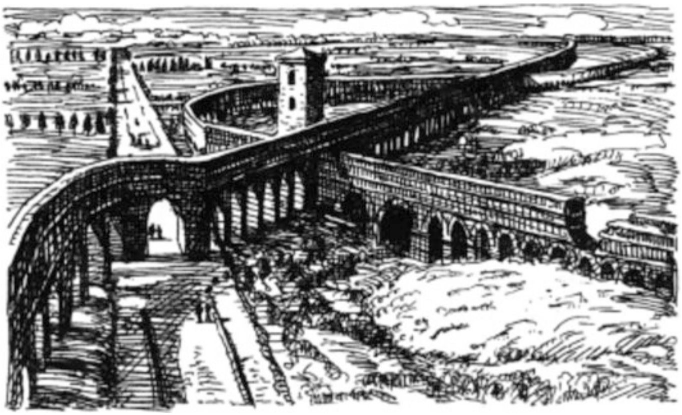

**Fig. 1.2** Restored arch of Roman aqueduct in Campania Plain, Italy, from Yasuki Nakayama, Robert Boucher, Introduction to Fluid Mechanics, Butterworth-Heinemann 1998

substituted without damaging the crown. Archimedes used the "Hydrostatics" principle (known as Archimedes' principle) "a body immersed in a fluid experiences a buoyant force equal to the weight of the fluid it displaces" to solve this problem.

Archimedes received his education at the University of Alexandria, where groups of mathematicians and scientists worked, devoting themselves to the construction of numerous fascinating machines. The greatest and most colorful of what is known as the Alexandrian school of engineers is undoubtedly Hero who lived sometime during the second century BC. His best invention is the *aelopile*, the first

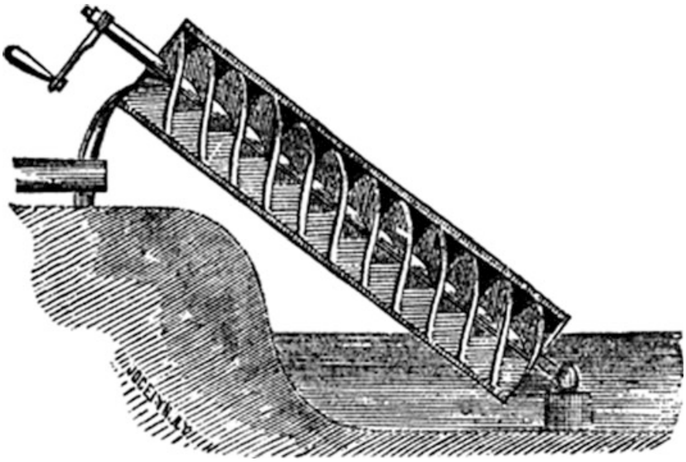

**Fig. 1.3** Archimedean Screw: as the handle a is turned, a certain amount of water is brought into the helical screw, which then brings water up to a reservoir or trough. https://upload.wikimedia.org/wikipedia/commons/8/82/Archimedes_screw.JPG

reaction turbine, which converted heat into mechanical energy through the medium of steam, see Fig. 1.4.

Hero's *aelopile*, the first reaction turbine could not produce useful work, as the speed was not sufficient which would have required a high head of steam. In 1780s James Watt worked on the theoretical operating conditions of a reaction turbine and he concluded that such a turbine could not be built given the state of contemporary technology.

*Water Wheels*: In all likelihood, the earliest tools employed by humankind for crushing or grinding seeds, nuts, and other food-stuffs consisted of little more than a flat rock, upon which the material was crushed by pounding with a stone or tree branch. The archaeological records show that as early as 30,000 years ago, Cro-Magnon artists employed the mortar and pestle to grind and mix the pigments they used to create their magnificent "cave-art."

Far more efficient than the flat rock or even the mortar and pestle was the hand mill, which appears to have long pre-dated the agricultural revolution. The hand mill consists of a flat rock, often hollowed or concave, on which the grain, seeds, or other materials is placed, and a grinding stone, which is rolled across the grain, thus reducing the grain to flour. Although the hand mill is still, today, in use in many parts of the world, approximately 2,000 years ago humankind began to harness water-power to turn the stones that ground its grain. They were probably the first method of creating mechanical energy that replaced humans and animals.

The first description of a water wheel is from Vitruvius, a Roman engineer (31 BC–14 AD), who composed a 10 volume treatise on all aspects of Roman engineering. From classical times, there have existed 3 general varieties of water wheels: the horizontal wheel and 2 variations of the vertical wheel, Fig. 1.5. One of the most remarkable Roman applications of a waterwheel was at Barbegal near


**Fig. 1.4** Hero's *aelopile*-the lower container "*a*" was partly filled with water and was heated. The steam that was then produced was led via pipes "*b*" to a metal sphere "*c*", which could turn on its axle and had exhaust pipes "*d*", whose openings were directed at right angles to the axle. As steam escaped, the sphere rotated because of the steam's reaction

Arles in southern France. Dating from the 4th Century AD, the factory was an immense flour mill which employed 16 overshot water wheels, see Fig. 1.6.

Waterpower was important source of energy in ancient China civilization. One of the most intriguing applications was for iron casting; see Fig. 1.7. According to an ancient text, in 31 AD the engineer Tu Shih invented a water-powered reciprocator for the casting of [iron] agricultural implements. Waterpower was also applied at an early date to grinding grain. Large rotary mills appeared in China about the same time as in Europe (2nd century BC). But while for centuries Europe

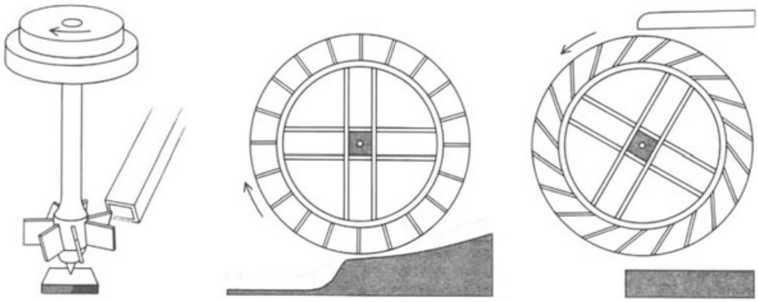

**Fig. 1.5** Types of water wheels norse wheels (*left*) turn millstones directly, undershot wheels (*center*) and overshot wheels (*right*). http://www.waterhistory.org/histories/waterwheels/roman7.jpg

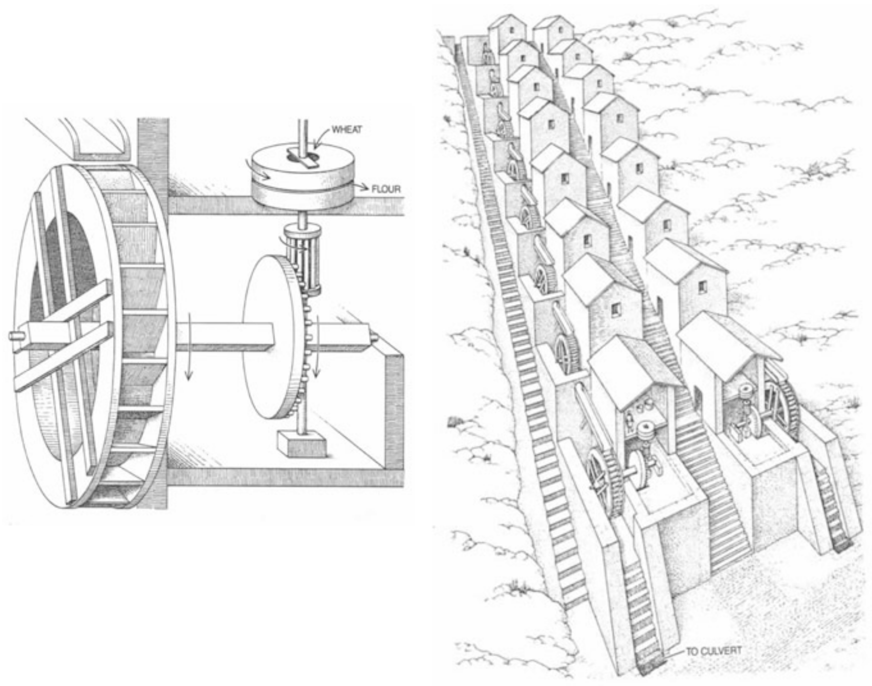


**Fig. 1.6** Flour Mill at Barbegal near Arles in southern France. Dating from the 4th Century AD, the factory was an immense flour mill which employed 16 overshot water wheels. http://www.aquaidwatercoolers.co.uk/wp-content/uploads/2013/12/water-wheels-2.jpg

relied heavily on slave- and donkey powered mills, in China the waterwheel was a critical power supply.

Renaissance engineers studied the waterwheel and realized that the action of water on a wheel with blades would be much more effective if the entire wheel were somehow enclosed in a kind of chamber. They knew very well that only a small

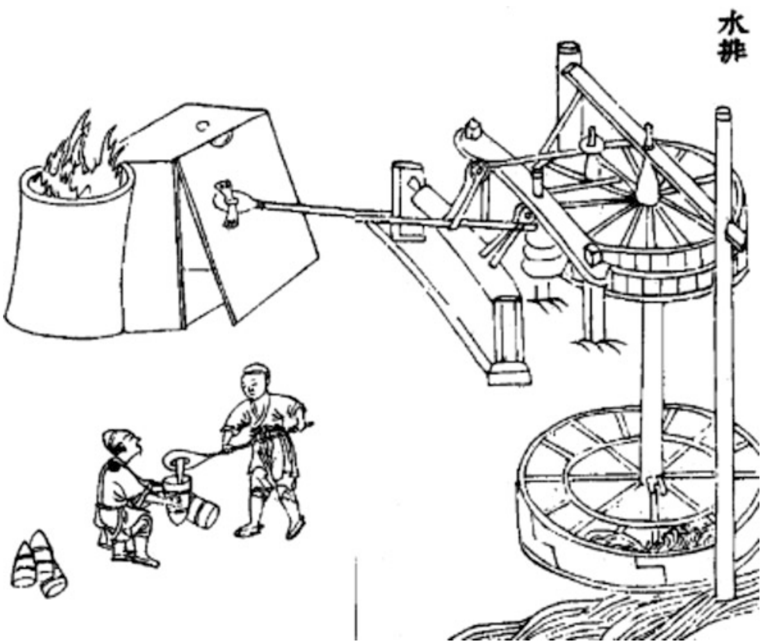


**Fig. 1.7** Water Mill employed in China for iron casting. http://www.waterhistory.org/histories/waterwheels/waterwheelill3.png

amount of the water pushing or falling on a wheel blade or paddle actually strikes it, and that much of the energy contained in the onrushing water is lost or never actually captured. Enclosing the wheel and channeling the water through this chamber would result in a machine of greater efficiency and power. They were hampered, however, by a lack of any theoretical understanding of hydraulics. Both of these problems were resolved to some degree in the eighteenth century, and one of the earliest examples of a reaction turbine was built in 1750 by the German mathematician and naturalist Johann Andres von Segner (1704–1777). In his system, the moving water entered a cylindrical box containing the shaft of a runner or rotor and flowed out through tangential openings, acting with its weight on the inclined vanes of the wheel.

*Wind Mills*: Over 5,000 years ago, the ancient Egyptians used wind to sail ships on the Nile River. While the proliferation of water mill was in full swing, wind mills appeared to harness more inanimate energy by employing wind sails. Prototypes of windmills were probably known in Persia (present day Iran) as early as the 7th century AD with the sails mounted on a vertical axis, see Fig. 1.8. Towards the end of the 12th century, wind mills with sails mounted on horizontal axes appeared in Europe; the first of this kind probably appeared in Normandy, England. These are post mills, where the sails and machinery are mounted on a stout post and the entire apparatus has to be rotated to face the wind.

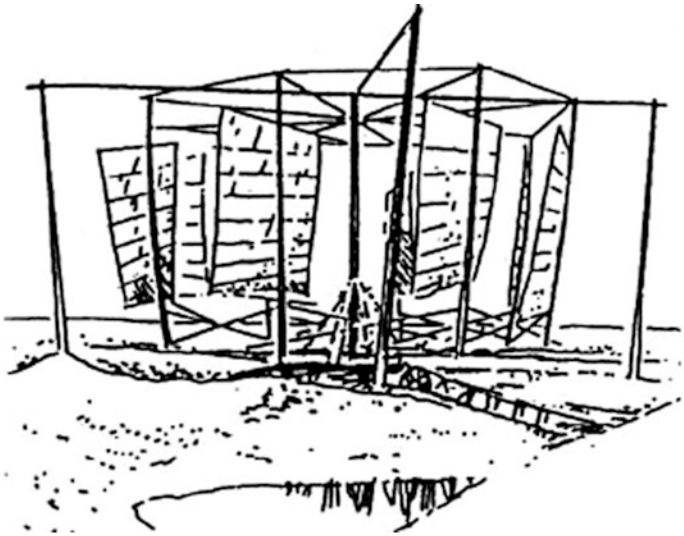

**Fig. 1.8** A sketch of an early Persian Vertical Axis Windmill. http://www.see.murdoch.edu.au/resources/info/Tech/wind/image001.jpg

Two centuries later the tower mill was introduced enclosing the machinery in a stationary tower so that only the cap carrying the sails needed to be turned to the wind.

In 1854 Daniel Halliday obtained the first American windmill patent. His windmill had four wooden blades that pivoted and would self-adjust according to wind speed. It had a tail which caused it to turn into the wind, see Fig. 1.9.

*Renaissance and Scientific Revolution*: Technology has been traditionally the realm of craftsmen working by rough rules of trial and error. The knowledge base was confused in the absence of an understanding on the behavioral motion of solids and fluids. The man of knowledge is a philosopher rather than a scientist.

The reawakening of scientific thought was brought about during the Renaissance Period (1400–1600) and carried over into the period of the scientific revolution. Leonardo da Vinci (1452–1519) is recently credited for some fundamental contributions to solid mechanics, fluid mechanics and mechanical design much before the scientific revolution. During the Renaissance period, Leonardo da Vinci (1452–1519) made significant insights into the laws of natural science well before Newton that ‘a body tries to drop down onto the earth through the shortest path’, and that ‘a body gives air the same force as the resistance which air gives the body’. He discussed the movement of water, eddies, water waves, falling water, the destructive force of water, floating bodies, efflux and the flow in a tube/conduit to hydraulic machinery. He sketched the flow around an obstacle, and Fig. 1.10 shows the development of vortices in the separation region. Leonardo was the first to find the least resistive ‘streamline’ shape.

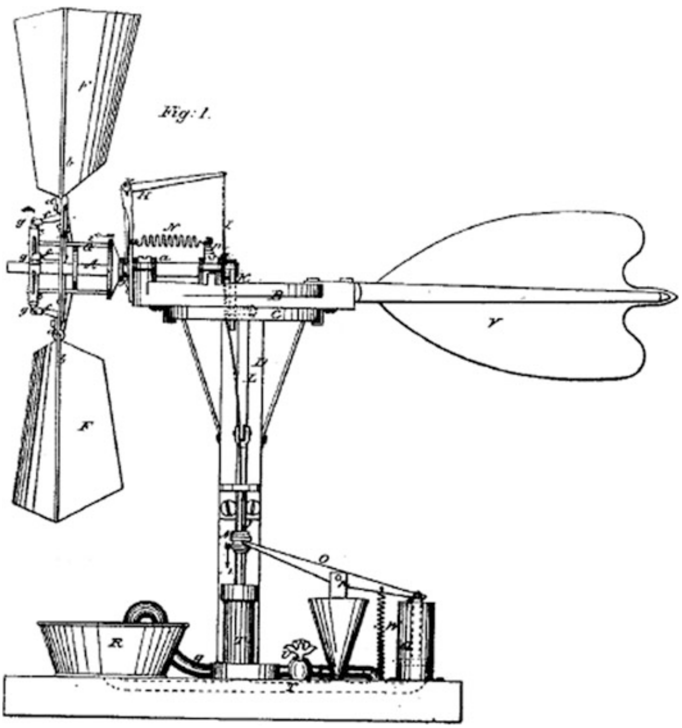


**Fig. 1.9** Early American Wind Mill mounted on horizontal axle. http://image.slidesharecdn.com/homesteaders-solutions-to-farming-problems-25019/95/homesteaders-solutions-to-farming-problems-7-728.jpg?cb=1178176854

**Fig. 1.10** Development of vortices in the separation region from Leonardo da Vinci. http://image.slidesharecdn.com/1-140906130430-phpapp01/95/1history-5-638.jpg?cb=1410008998

*Scientific Revolution*: The event which most historians of science call the scientific revolution can be dated roughly as having begun in 1543, the year in which Nicolaus Copernicus published his *De revolutionibus orbium coelestium*.

Fire or Heat is fundamental to machines where energy is converted into useful mechanical work. Galileo Galilei (1564–1642) is amongst the first to argue in *Il saggitore* and in *Discorsi* that the sensation of heat is caused by the rapid motion of certain specific atoms (Galilean atomic model). Rene Descartes (1596–1650) was more explicit than Galileo and tried to explain all physical phenomena in terms of extension and motion only. Isaac Newton (1642–1727) built upon the work of Johannes Kepler (1571–1630) and Galilei; Galileo's mathematical treatment of acceleration and his concept of Inertia reflect earlier medieval analyses of motion. His development of the Calculus opened up new applications of the methods of mathematics to science. He showed that an inverse square law for gravity explained the elliptical orbits of the planets, and advanced the theory of Universal Gravitation.

Robert Boyle (1627–1691) a disciple of Descartes, made major contributions to heat by retaining his association with chemistry, leading him to his famous law relating the pressure to the volume of an elastic fluid, or gas. Generally speaking, 17th century theories of heat combined the idea of a subtle fluid with that of motion of its constituent corpuscles or atoms. But the atoms remained scientifically inscrutable until Daltonian chemistry (1808) was accepted and the unknown function of their motions was not understood until the concept of energy was established in the 19th century.

Scientific revolution made rapid strides beginning with Newton. Gottfried Leibniz (1646–1716), Pierre Varignon (1654–1722), Jacob Bernoulli (1654–1705), Johann Bernoulli (1667–1748), Daniel Bernoulli (1700–1782). Leonhard Euler (1707–1783) a Swiss mathematician proposed the Euler equations, which describe conservation of momentum for an inviscid fluid, and conservation of mass. Claude Louis Marie Henry Navier (1785–1836) and George Gabriel Stokes (1819–1903) introduced viscous transport into the Euler equations, which resulted in the Navier-Stokes equation.

The credit for making pressure exerted by the atmosphere entirely explicit belongs to Otto von Guericke (1602–1686), who in 1672, published the famous

**Fig. 1.11** Teams of horses trying unsuccessfully to pull apart vacuum-filled copper spheres in a Magdeburg demonstration for Emperor Ferdinand III. http://0.tqn.com/d/inventors/1/S/m/2/Magdeburg.jpg

book in which he described his air pump and the experiments that he made with it from the mid-1650s. His famous demonstration in 1663 is illustrated in Fig. 1.11.

Denis Papin (1647–1712) a French physicist, mathematician and inventor is best known for his pioneering invention of the steam digester, the forerunner of the steam engine. He worked with Robert Boyle from 1676 to 1679, publishing an account of his work in *Continuation of New Experiments* (1680). During this period, Papin invented the *steam digester*, a type of pressure cooker. He first addressed the Royal Society in 1679 on the subject of his digester, and remained mostly in London until about 1687, when he left to take up an academic post in Germany. While in Leipzig in 1690, having observed the mechanical power of atmospheric pressure on his 'digester', he built a model of a piston steam engine, the first of its kind, see Fig. 1.12. The Papin experiment was a metal tube (closed at one end) with a piston inside. Under the piston there was a small quantity of water which, warmed up and transformed in steam, raised the piston which reached the edge of the cylinder where was stopped by a click. A stream of cold water was sprayed onto the cylinder. The steam inside condensed. This produced a partial vacuum and the outside air pressure forced the piston down (active stroke). The tube had three roles: boiler, cylinder and steam condenser. The steam engine will build step by step, separating those three roles.

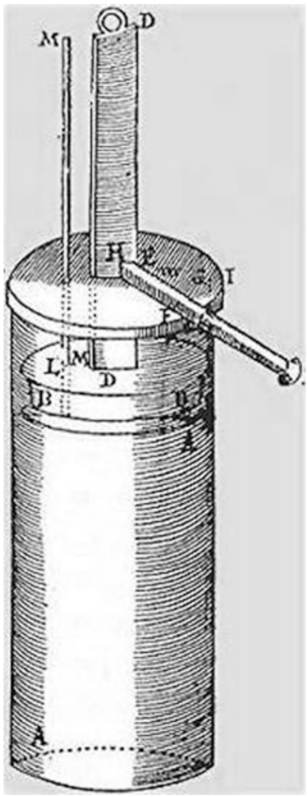

**Fig. 1.12** The first steam engine 1690. https://en.wikipedia.org/wiki/Denis_Papin

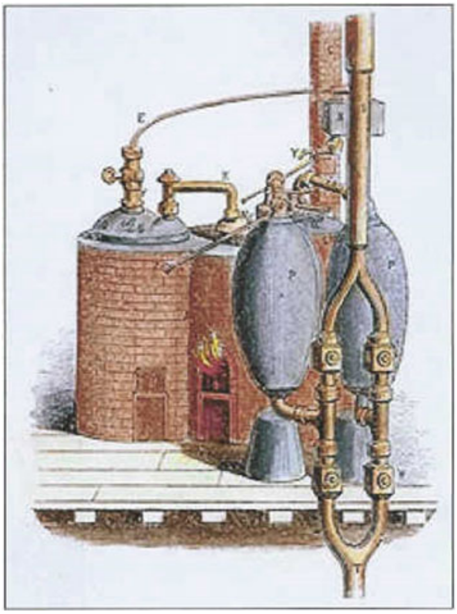

**Fig. 1.13** Thomas Savery 1698 Vacuum Pump. https://en.wikipedia.org/wiki/Thomas_Savery

Thomas Savery (1650–1715) was an English military engineer and inventor who in 1698 patented the first crude steam engine, based on Denis Papin's Digester or pressure cooker of 1679. His machine, Fig. 1.13, consisted of a closed vessel filled with water into which steam under pressure was introduced. This forced the water upwards and out of the mine shaft. Then a cold water sprinkler was used to condense the steam. This created a vacuum which sucked more water out of the mine shaft through a bottom valve.

In 1705 Papin developed a second steam engine with the help of Gottfried Leibniz using steam pressure rather than atmospheric pressure. Papin's steam engine is a break through since Hero's reaction turbine of second century B.C. which never functioned in reality. In the installation at Kassel, Fig. 1.14, steam was fed from boiler "a" to a vessel "b" in which there was a float serving as a piston "c". Papin planned to fill a container "d" in the piston with red-hot scrap iron in order to superheat the steam, but in reality this could not be done. When the steam pushed the piston downwards, the check valve "e" of the container for water to be pumped was closed. Simultaneously the check valve "f" of the ascending pipe "g" was opened and the water was pumped into a cistern "h", from where it flowed to the fountains. When the piston has reached the bottom of "b" a tap "j" on "c" was opened and the steam escaped. Because of the water pressure, "f" was then closed and "e" opened and more water poured in. "k" is a safety valve.

Savery's Vacuum pump installed in a water logged mine is illustrated in Fig. 1.15. It had neither a piston nor a safety valve. Steam from the boiler was fed into a vessel "a" and the water in it was forced out through an ascending pipe "b" by way of check valve "c". When "a" had been emptied, the flow of steam was

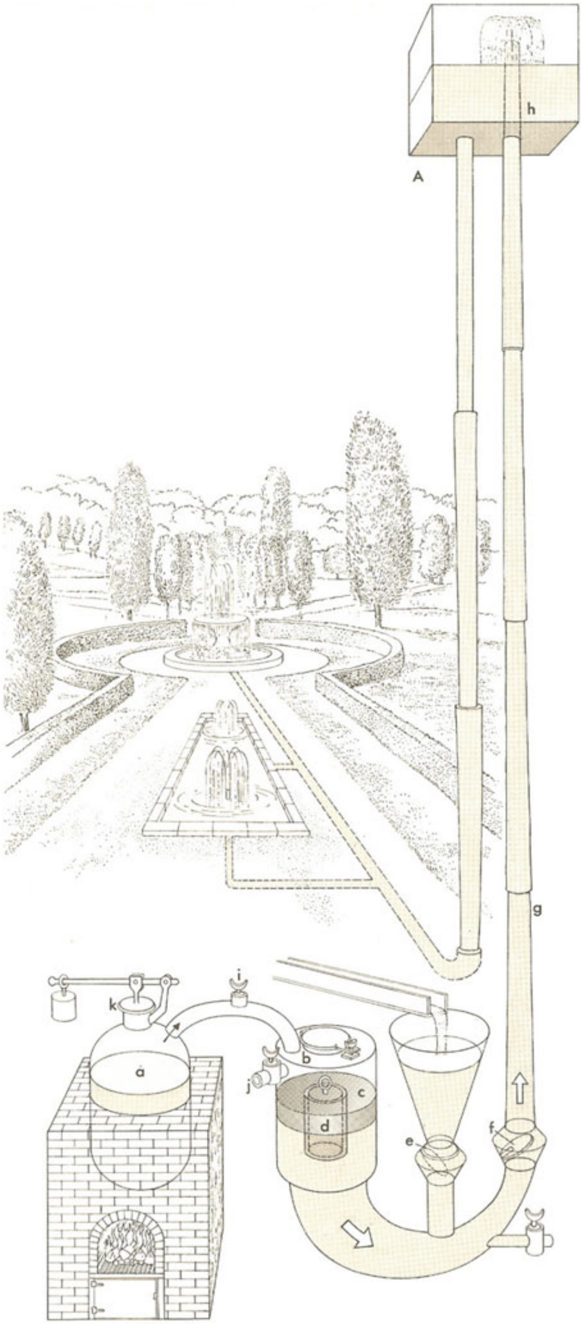


**Fig. 1.14** Papin Steam Engine installed in Kassel gardens of Duke of Hesse

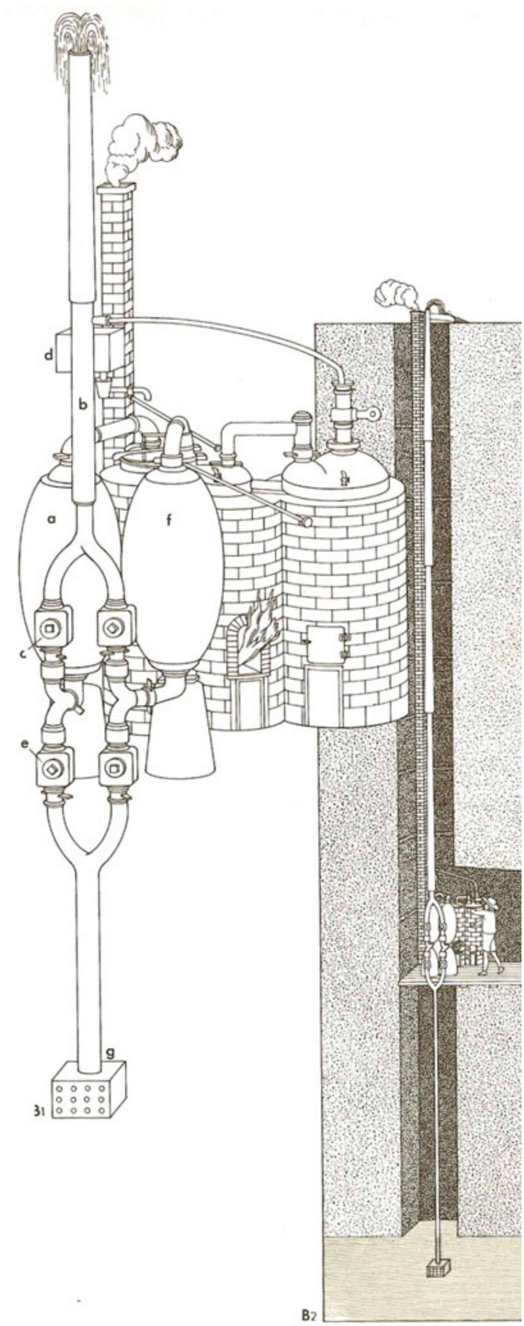


**Fig. 1.15** Thomas Savery Steam Engine in action in a water-logged mine

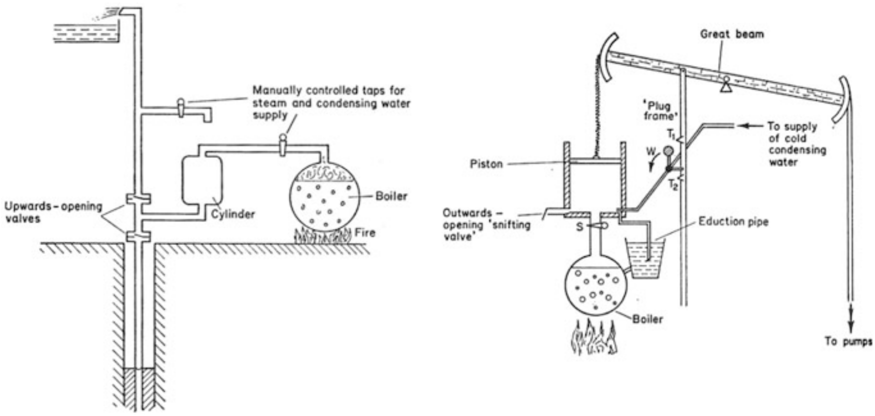


**Fig. 1.16** Improvements in Newcomen Engine 1712 compared with Savery Engine (*left*)

stopped and the vessel was cooled by means of cold water, which was sprayed over it from vessel "d". Since a vacuum was created when the steam was condensed, water was again sucked into "a" by way of a check valve "e". While "a" was being cooled, steam was fed into the water filled vessel "f", which was emptied, cooled and refilled with water "g".

Thomas Newcomen (1663–1729) made explicit provision for the expulsion of air from the cylinder. The snifting valve in Fig. 1.16 opened outwards in such a way that the rush of the steam into the cylinder at the beginning of each cycle carried the accumulated air out with it through the valve. In this way once a cycle, the engine made a wheezing noise—like a man snifting with a cold—as it cleared itself of the air. The movement up and down of the plug frame, a long board hanging from the great beam, causes the tappet, or plug "$T_1$" set in it to trip the weight-operated valve, "W". When the plug frame moves in the opposite direction, another tappet, "$T_2$" resets the valve. A similar mechanism (not shown) controls the steam supply by means of the valve "S". The eduction pipe enables the condensed steam and the warmed condensing water to be returned via a well to the boiler, thus conserving heat.

The Newcomen steam engine was the first practical device to harness the power of steam to produce mechanical work. Newcomen's first working engine was installed at a coal mine at Dudley Castle in Staffordshire in 1712. They were used throughout England and Europe to pump water out of mines starting in the early 18th century, see Fig. 1.17 and were the basis for James Watt's later improved versions.

Glasgow University had one of the Newcomen's engines for its natural philosophy class. In 1763, one hundred years after the birth of Newcomen, this apparatus went out of order and Professor John Anderson gave the opportunity to James Watt (1736–1819) to repair it. After the repair and while experimenting with it, he was struck by the enormous consumption of steam because that at every

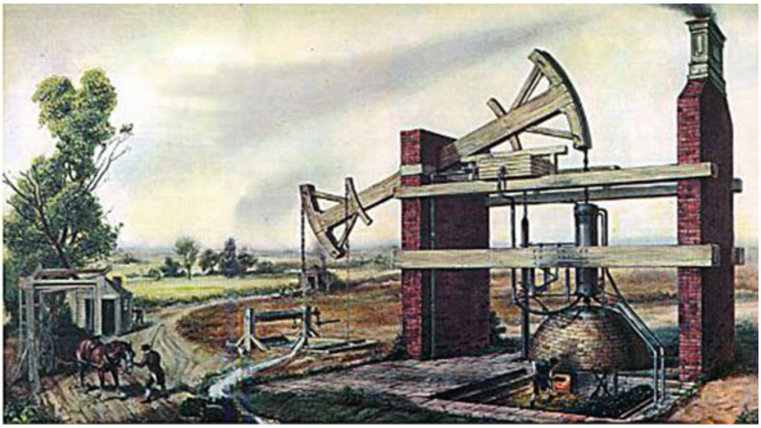

**Fig. 1.17** Newcomen Engine Installation. http://www.altontobey.com/87255.JPG

stroke the cylinder and piston had to be heated to the temperature of boiling water and cooled again. This has prevented the apparatus from making, with the available boiler capacity, more than a few strokes every minute. He quickly realized that the wastage of steam is inherent in the design of the engine and became obsessed with the idea of finding some remedy. From the discovery of Dr. Joseph Black (1728–1799), he deduced that the loss of latent heat was the most serious defect in the Newcomen engine. The work of James Watt is thus the application of science to engineering which led to the birth of the industrial revolution.

Reciprocating machinery has inherent disadvantages at high speeds, they have practically disappeared in the modern day world; there are still steam locomotives operating in a few places, e.g., Fairy Queen, the oldest running vintage steam locomotive in the world built in the year 1855 by the British firm Kinston, Thompson & Hewitson for the British firm East India Railways, see Fig. 1.18, and occasional reciprocating engines for producing small amounts of power in sugar mills, but they are gone. Internal combustion engines still thrive for transportation, power generation …

Instead of external combustion to generate steam, internal combustion and conversion of heat energy to mechanical energy became practical with the availability from extraction of petroleum. The first modern oil refineries were built by Ignacy Łukasiewicz near Jasło in the dependent Kingdom of Galicia and Lodomeria in Central European Galicia, Poland from 1854–56. The first person to build a working four stroke engine, a stationary engine using a coal gas-air mixture for fuel (a gas engine), was German engineer Nicolaus Otto (1832–1891) in 1862. That is why the four-stroke principle today is commonly known as the Otto cycle and four-stroke engines using spark plugs often are called Otto engines.

The achievement of Hero of Alexandria nearly 2200 years ago in demonstrating a rotating machine, a reaction steam turbine, much before the renaissance period still remained a distant dream. Karl Gustaf Patrik de Laval (1845–1913) was a


**Fig. 1.18** For an idyllic weekend trip between Delhi and Alwar, the Fairy Queen comes to the rescue of those bored with the same old blaze ways of traveling around the place

Swedish engineer who built the first steam turbine (impulse turbine), see Fig. 1.19. High pressure steam was blown through nozzles and expanded to low pressure. Its velocity was then greatly increased, and when the steam jets hit the turbine wheel's bent vanes, the wheel was set in motion. The turbine axle is mounted in its bearings fixed in spherical segments.

Charles Algernon Parsons, (1854–1931) was a British engineer, best known for his invention of the reaction steam turbine in 1884 shown in Fig. 1.20.

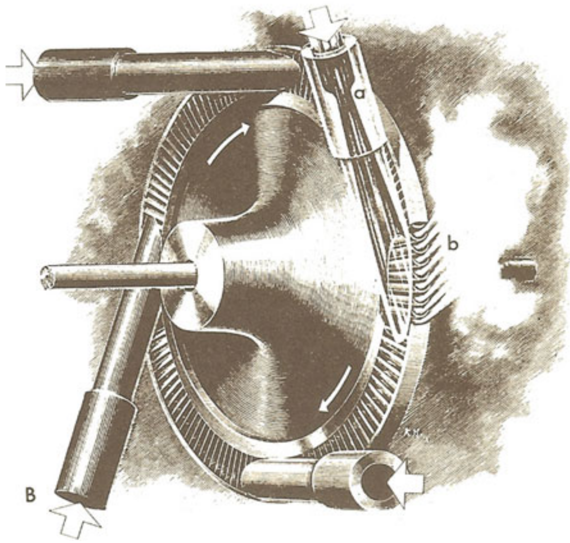


**Fig. 1.19** Laval's impulse steam turbine (1883)

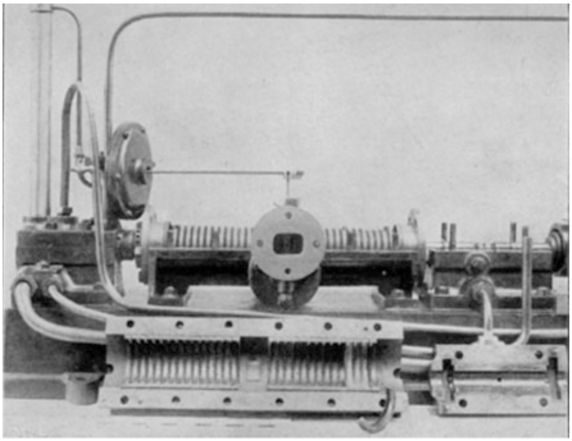

**Fig. 1.20** Parsons' reaction steam turbine (1884)

The steam turbine revolutionized the world; it is a dream come true after 21 centuries and since then mankind has never seen a rapid growth in prosperity. Man has forgotten that he lived in caves first and then settlements under the stars and moonlight. Man has also learnt to have luxury in air-conditioning and refrigeration and travel across seas and countryside.

A major discovery in this period is due to Osborne Reynolds (1842–1912) from his famously studied conditions in which the flow of fluid in pipes transitioned from laminar flow to turbulent flow in 1883. From these experiments came the dimensionless Reynolds number for dynamic similarity—the ratio of inertial forces to viscous forces. Reynolds also proposed what is now known as Reynolds-averaging of turbulent flows, where quantities such as velocity are expressed as the sum of mean and fluctuating components.

The next significant development came with a jet engine, Dr. Hans Von Ohain (1911–1998) studied at the University of Gottingen and when 22 years old he first conceived the idea of a continuous cycle combustion engine in 1933; he patented a jet propulsion engine design similar in concept to that of Sir Frank Whittle (1907–1996) but different in internal arrangement in 1934. After receiving his degree in 1935, Ohain became the junior assistant of Robert Wichard Pohl, then director of the Physical Institute of the University. Dr. Hans von Ohain and Sir Frank Whittle are both recognized as being the co-inventors of the jet engine. Each worked separately and knew nothing of the other's work. While Hans von Ohain is considered the designer of the first operational turbojet engine, Frank Whittle was the first to register a patent for the turbojet engine in 1930. Hans von Ohain was granted a patent for his turbojet engine later in 1936; however, Hans von Ohain's jet was the first to fly in 1939. Frank Whittle's jet first flew in 1941, see Fig. 1.21.

While working at the University, von Ohain met an automotive engineer, Max Hahn, and eventually arranged for him to build a model of his engine. When it was complete he took it to the University for testing, but ran into serious problems with combustion stability. Often the fuel would not burn inside the flame cans, and

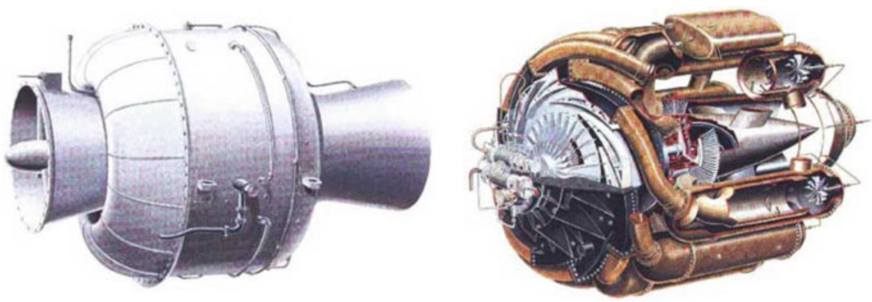

**Fig. 1.21** Hans Von Ohain first Jet Engine (*left*) and Frank Whittle's Jet Engine (*right*)

would instead be blown through the turbine where it would ignite in the air, shooting flames out the back and overheating the electric motor powering the compressor.

In February 1936, Pohl wrote to Ernst Heinkel telling him of the von Ohain design and its possibilities. Heinkel arranged a meeting where his engineers were able to grill von Ohain for hours, during which he flatly stated that the current "garage engine" would never work but there was nothing wrong with the concept as a whole. The engineers were convinced, and in April, von Ohain and Hahn were set up at Heinkel's works at the Marienehe airfield outside Rostock, Germany in Warnemünde.

Once moved, a study was made of the airflow in the engine, and several improvements made over a 2 month period. Much happier with the results, they decided to produce a completely new engine incorporating all of these changes, running on hydrogen gas. The resulting Heinkel-Strahltriebwerk 1 (HeS 1), German for Heinkel Jet Engine 1, see Fig. 1.21, was built by hand-picking some of the best machinists in the company, much to the chagrin of the shop-floor supervisors. Hahn, meanwhile, worked on the combustion problem, an area he had some experience.

Frank Whittle was a Royal Air Force Officer, proposed in a thesis that planes would need to fly at high altitudes, where air resistance is much lower, in order to achieve long ranges and high speeds. Piston engines and propellers were unsuitable for this purpose, so he concluded that rocket propulsion or gas turbines driving propellers would be required: jet propulsion was not in his thinking at this stage. In 1929, Whittle had considered using a fan enclosed in the fuselage to generate a fast flow of air to propel a plane at high altitude. A piston engine would use too much fuel, so he thought of using a gas turbine and patented his idea.

In 1935 Whittle secured financial backing and, with RAF approval, Power Jets Ltd was formed. They began constructing a test engine in July 1936, but it proved inconclusive. Whittle concluded that a complete rebuild was required, but lacked the necessary finances. Protracted negotiations with the Air Ministry followed and the project was secured in 1940. By April 1941 the engine W.2, see Fig. 1.21, was ready for tests and it produced 1600 lb thrust. The first flight Gloster E.28/39 took place on 15 May 1941. By October the Americans had heard of the project and asked for the details and an engine. A Power Jets team and the engine were flown to Washington to enable General Electric examine it and begin construction. The Americans worked quickly and their XP-59A Aircomet was airborne in October 1942, sometime before the British Meteor, which became operational in 1944.

This is an intense application of Fluid Mechanics that led to the jet engine, contrary to much of the early developments of steam turbines and reciprocating machinery which were more dependent on intuition rather than a design starting from Fluid Mechanics. These designs were achieved without the aid of any computational means as known subsequently.

The Laval nozzle in 1883 as given in Fig. 1.19 ushered in another significant application for rocket propulsion. The World's first liquid-fueled rocket was successfully launched on March 16, 1926 by Robert Goddard. A De Laval nozzle was used to generate a high speed jet with a nozzle that alternately converged and diverged central to all rocket propulsion and turbo-machinery, see Fig. 1.22.

All rockets used in space exploration and naval torpedoes essentially use this technology.

Aero-acoustic sound is studied to identify sources in a turbulent flow as simple emitter types referred to as aero-acoustic analogies. They are derived from the compressible Navier–Stokes equations (NSE). The compressible NSE are

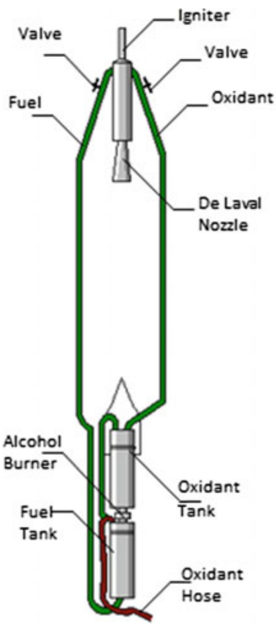


(a) Goddard's Liquid Propellant Rocket

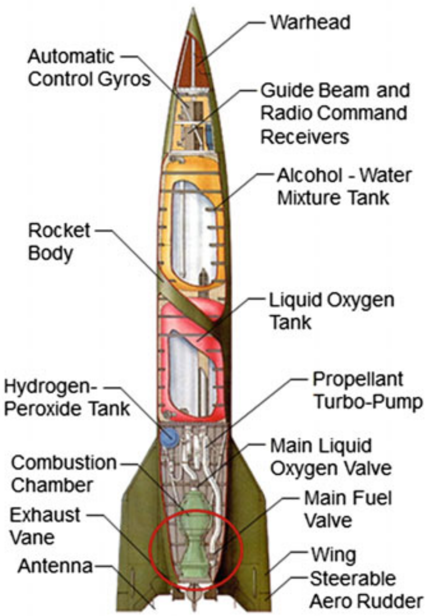


(b) von Braun's V-2 Rocket

**Fig. 1.22** Laval Nozzle in rocket propulsion rearranged into various forms of the inhomogeneous acoustic wave equation. Within these equations, source terms describe the acoustic sources. They consist of pressure and speed fluctuation as well as stress tensor and force terms. Approximations are made to make the source terms independent of the acoustic variables to derive linearized equations describing the propagation of the acoustic waves in a homogeneous, resting medium.

Michael James Lighthill (1924–1998) was a British applied mathematician, known for his pioneering work in the field of aero acoustics. The Lighthill analogy considers a free flow, as for example with an engine jet. The non-stationary fluctuations of the stream are represented by a distribution of quadrupole sources in the same volume. The Ffowcs Williams (1935–)—Hawkings analogy is valid for aero-acoustic sources in relative motion with respect to a hard surface, as is the case in many technical applications, for example in the automotive industry or in air travel. The calculation involves quadrupole, dipole and monopole terms.

Metallic fluids, like mercury, are affected by nearby electromagnetic fields; but they are usually weak enough and therefore their influence can be neglected. However with the emerging fusion reactors containing 10 million times earth's magnetic fields to confine the 100 million degree plasma to a torus path in a high intensity molecular level vacuum chamber, liquids such as Lithium Titanate, magneto-hydrodynamics has become an important study.

Hannes Olof Gösta Alfvén (1908–1995) a Swedish electrical engineer and plasma physicist initiated studies on magneto-hydrodynamics (MHD), plasma physics, including theories describing the behavior of aurorae, the Van Allen radiation belts, the effect of magnetic storms on the Earth's magnetic field, the terrestrial magnetosphere, and the dynamics of plasmas in the Milky Way galaxy.

*Classification and Significant Events*: The science of flow is traditionally classified into hydraulics, which developed from experimental studies, and hydrodynamics that developed through theory. Together they form a single discipline, namely fluid mechanics.

Hydraulics has been practiced as an empirical science since prehistoric times. As man settled to engage in farming, villages are developed and a continuous supply of water and the transport of essential food and materials were needed. This led to the development of hydraulics in the utilization of water channels and ships.

Fluid statics or hydrostatics is the branch of fluid mechanics that studies fluids at rest. It deals with the conditions under which fluids are at rest, i.e., stable equilibrium. Hydrostatics is fundamental to hydraulics. It offers physical explanations for many phenomena such as why atmospheric pressure changes with altitude, why wood and oil float on water, and why the surface of water is always flat and horizontal whatever the shape of its container.

Hydrodynamics deals with fluid motion and is of much recent origin. During the scientific revolution, Euler derived complete theoretical equations for the inviscid flow to describe various flows. The inviscid flow theory results of the force acting on a body or the state of flow did not match well with the experimentally observed values. In the nineteenth century, the derivation of equations of a viscous fluid by Navier and Stokes made a significant difference and competed with methods of hydraulics. The Navier-Stokes equation has convection terms which are nonlinear rendering it difficult to obtain the analytical solution for general flows; specific cases of laminar flow between parallel plates and in a round tube were solved.

In 1869 Gustaf Robert Kirchhoff, a German physicist (1824–87), computed the coefficient of contraction for the jet from a two-dimensional orifice as 0.611. This value coincided very closely with an experimental value for the case of an actual orifice—approximately 0.60. His work connected hydraulics and hydrodynamics and gradually hydrodynamics was accepted.

With the advent of high speed electronic computers and numerical techniques in hydrodynamics, it is now possible to obtain numerical solutions of the Navier-Stokes equation. This way of solution in the present age is Computational Fluid Dynamics, popularly called CFD.

CFD in full form consists of solution of the following.

1. Mass Conservation equation
2. Three Momentum equations from Newton's law
3. Energy equation
4. State equation

Neglecting viscous effects, they are Euler equations for an inviscid flow. In this book we will understand methods of solution of these equations.

If we consider the viscous terms in the momentum equations, we have Navier-Stokes equations, which are very complex and usually solved by using a convenient turbulence model. Then we have Reynolds Averaged Navier-Stokes (RANS) equations.

5. When magnetic fields are present and the liquid under consideration is metallic, then the Navier-Stokes equations should include the Lorentz force arising from the magnetic field. The mass equation remains the same. Besides the equations cited, we have to include Ampere's law, Faraday's law and Ohm's law. This makes the problem more complicated.
6. Turbulent flow induces eddies which are large to start with and they dissipate before the flow becomes laminar—these eddies in the transient flow solution of Navier-Stokes equations form sources for noise and wave propagation equation. With these acoustic sources identified from Navier-Stokes equation solution are used to solve the wave propagation equation in Lighthill's or Ffowcs-Williams and Hawking's equations.
7. The heat carried out in the flow of turbo machinery or internal combustion engines is transferred to the metallic flow path and the way it is dissipated is determined by conjugate heat transfer using CFD; alternatively CFD allows determination of convective heat transfer coefficients enabling a thermal design of machine members.
8. The combustion of fuel inside the flow and the species distribution after combustion leading to pollution analysis is accomplished by CFD.

9. The flow medium may not be a single phase flow, e.g., the medium of water can be in liquid or vapor form leading to cavitation that is important in erosion studies of propeller blades of ships and submarines.
10. Supersonic flows, formation of shocks, separation of flow and even hypersonic flow with chemical reactions can also be simulated by CFD.

CFD is thus the method that most designs prefer to use Fluid Flow problems presently as opposed to Hydraulics or Fluid Dynamics solutions from theory. This subject needs a recap of Mathematics, Physics consisting of Matrix algebra, Vectors and Tensors. You may like to refer to the book *Simulation Based Engineering in Solid Mechanics* by the same author from the same publisher before proceeding further with this book.

# Chapter 2
# Fluid Statics

**Abstract** This chapter deals with Fluid Statics. Starting from properties of fluids, fluid pressure under static conditions is explained. Pascal's law and its applications in Mariotte bottle and hydraulic lever are given. Buoyancy of airships, sea navigating ships are explained. Water storage, dams and sluice gates are next explained. Basic principles of thermodynamics, perfect gases, Vapor pressure and saturation pressure are explained next. The cavitation phenomenon that depends on vapor pressure is next explained. Heat energy aspects, internal energy, enthalpy, specific heats, adiabatic process, reversible process, entropy, Isentropic process are explained while dealing with mechanical energy and heat energy and work done on gases.

**Keywords** States of matter · Fluid pressure · Pascal's siphon · Mariotte bottle · Hydraulic lever · Buoyancy · Airships · Dams · Thermodynamics laws · Boyle's and Charles' laws for perfect gases · Vapor pressure · Saturation pressure and temperature · Cavitation · Internal energy · Enthalpy · Specific heats · Adiabatic process · Reversible process · Entropy · Isentropic process

In this chapter we consider the study of fluids at rest. Popularly fluid statics or hydrostatics is called Hydraulics and is practiced since ancient times for storing water and transportation using canals.

## 2.1 States of Matter

All matter takes three primary states

- Solid—it takes a definite shape and volume, e.g., iron, copper, stone … The size and shape change only slightly under the application of external forces.
- Liquid—is one that takes the shape of its container with a definite volume, e.g., water, kerosene, mercury … They can change their shape very readily. If the



J.S. Rao, *Simulation Based Engineering in Fluid Flow Design*,
DOI 10.1007/978-3-319-46382-7_2

volume of vessel is larger than that of the liquid put into it, there will be a free surface at the top of the liquid.

- Gas—e.g., air, carbon dioxide … Differs from a liquid in that a gas has neither size nor shape. A quantity of gas placed in a container will completely fill that container. There is no free surface. The volume of the gas is the volume of the container.
- There is also a special state—Plasma in which the electrons move out of their designated orbits and even escape making the atoms positively charged.

Liquids and gases are classified as Fluids.

## 2.2 Pressure in Fluids at Rest

A fluid at rest cannot exert any permanent forces tangential to a boundary; therefore any force that it exerts on a boundary must be normal to the boundary. Such a force $F$ is proportional to the area $A$ on which it is exerted, and is called a *pressure*. We can imagine any surface in a fluid as dividing the fluid into parts pressing on each other, as if it were a thin material membrane, and so think of the pressure at any point in the fluid, not just at the boundaries. In order for any small element of the fluid to be in equilibrium, the pressure must be the same in all directions (or the element would move in the direction of least pressure), and if no other forces are acting on the body of the fluid, the pressure must be the same at all neighboring points.

Pascal's Law: The pressure will be the same throughout in a fluid at rest and is the same in any direction at a point. Due to the fundamental nature of fluids, a fluid cannot remain at rest under the presence of a shear stress. If a point in the fluid is thought of as an infinitesimally small cube, then it follows from the principles of equilibrium that the pressure on every side of this unit of fluid must be equal. If this were not the case, the fluid would move in the direction of the resulting force. Thus, the pressure on a fluid at rest is isotropic and allows fluids to transmit force through the length of pipes or tubes; i.e., a force applied to a fluid in a pipe is transmitted, via the fluid, to the other end of the pipe.

We define *pressure* in liquids as a force $F$ that is applied to the surface of a fluid acting over an area $A$ perpendicular to it, and then the average pressure $P$ is $F/A$. In SI units it is force $F$ in Newtons over an area one meter squared, i.e., $N/m^2$, called Pascal, named after the famous scientist Pascal. A Pascal is abbreviated as Pa. The average pressure one Newton over one meter squared is very small, commonly we use Mega Pascals abbreviated as MPa, $N/mm^2$, or even Giga ($10^9$) Pascals, GPa.

In a fluid at rest velocity $V = 0$, all frictional stresses vanish and the state of stress of the system is called *hydrostatic*. The hydrostatic pressure can be determined from a control volume (test volume) analysis of an infinitesimally small cube of fluid $dx' \times dy' \times dz'$ shown in Fig. 2.1.

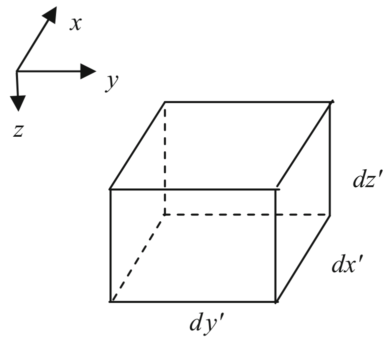


**Fig. 2.1** Infinitesimally small cube of fluid at depth $z'$

Gravity is an example of a *body force* that disturbs the equality of pressure in a fluid. The presence of the gravitational body force causes the pressure to increase with depth, according to the equation $dp = \rho g \times dh$, in order to support the water above. We call this relation the *barometric equation*, for when this equation is integrated, we find the variation of pressure with height or depth.

Let $p$ be the hydrostatic pressure (Pa), $\rho$ the fluid density (kg/m$^3$), $g$ gravitational acceleration (m/s$^2$), $A$ the test area (m$^2$), $z$ the height (parallel to the direction of gravity) of the test area (m), and $z_0$ the height of the reference point of the pressure (m). Then the force acting on any such small cube of fluid is the weight of the fluid column above it; the hydrostatic pressure is obtained from

$$\begin{aligned} p(z) &= \frac{1}{A}\int_{z_0}^{z}\left\{\int\int_{A}\rho(z')g\,dx'dy'\right\}dz' \\ &= \int_{z_0}^{z}\rho(z')g\,dz' \end{aligned} \tag{2.1}$$

For incompressible liquids (unlike gases) the density is constant. The above simplifies to

$$p = \rho g h \tag{2.2}$$

where $h$ is the height $z - z_0$ of the liquid column between the test volume and the zero reference point of pressure. The absolute pressure compared to vacuum is

$$p = \rho g h + p_{\text{atm}} \tag{2.3}$$

Worked Example 2.1:
Determine the maximum height of water that can be supported by atmospheric pressure or maximum height a suction pipe can raise the water. If it is mercury instead of water repeat the calculation.

The density of water is about 1000 kg/m$^3$. The depth of water that corresponds to the normal sea-level atmospheric pressure 101325 Pa can be obtained as $\frac{101325}{1000 \times 9.84} = 10.297$ m.

This is the maximum height that can be supported by atmospheric pressure; or a suction pump can raise the water to a maximum height of 10 m.

Now let's do the same thing with liquid mercury, whose density is 13.5951 times that of water. The height of the mercury column is then $\frac{10.297}{13.595} = 757$ mm, i.e., 30 in Hg.

In practice, it is convenient to measure pressure differences by measuring the height of liquid columns, called *manometery*. The barometer is a familiar example of this, and atmospheric pressures are traditionally given in terms of the length of a mercury column. Corrections are necessary for temperature because mercury density depends on the temperature. Evangelista Torricelli (1608–1647) invented the mercury barometer in 1643, and brought the weight of the atmosphere to light.
Worked Example 2.2:
A U-shaped manometer contains mercury of density $\rho_m = 13534$ kg/m$^3$. The manometer is used to measure pressure $p$ of a fluid in a tank. When connected to the tank, the manometer reads $h$ = 4.5 cm. Determine the pressure in the tank.

$$p = \rho_m gh = 13534 \times 9.80 \times 0.045 = 5968.5\,\text{Pa}$$

*Vacuum*: When pressure is referred to a vacuum, it is an *absolute* pressure, while a *gauge* pressure is referred to the atmospheric pressure. A negative gauge pressure is a (partial) vacuum. When a vacuum is stated to be so many mm, this means the pressure below the atmospheric pressure of about 757 mm Hg. A vacuum of 700 mm is the same thing as an absolute pressure of 57 mm Hg. The mm of mercury is called a *torr* named after Torricelli. 700 torr vacuum means a vacuum of 700 mm.

Pressure is sometimes stated in terms of the height of a fluid. If it is the same fluid whose pressure is being given, it is called *head*, and the factor connecting the head and the pressure is the weight density $\rho g$. As an example 10.297 m head of water multiplied by $\rho g = 1000 \times 9.84$ gives one atmospheric pressure (101325 Pa). It can also be considered energy *availability*. Water with a pressure head of 10 m can furnish the same energy as an equal amount of water raised by 10 m. Note that water flowing in a pipe is subject to *head loss* because of friction.

*Pascal's Siphon*: Blaise Pascal (1623–1662) demonstrated that the siphon worked by atmospheric pressure as shown in Fig. 2.2. The two beakers containing mercury are connected by a three-way tube as shown, with the upper branch open to the atmosphere. As the large container is filled with water, pressure on the free surfaces of the mercury in the beakers pushes mercury into the tubes. When the state shown is reached, the beakers are connected by a mercury column, and the siphon starts, emptying the upper beaker and filling the lower.

*Mariotte's Bottle*: To deliver a constant rate of flow from a closed tank independent of the input pressure and volume of liquid, Edme Mariotte (1620–1684) bottle shown in Fig. 2.3 can be used.

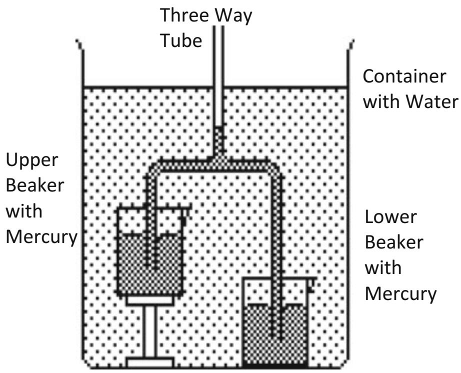


**Fig. 2.2** Pascal's siphon

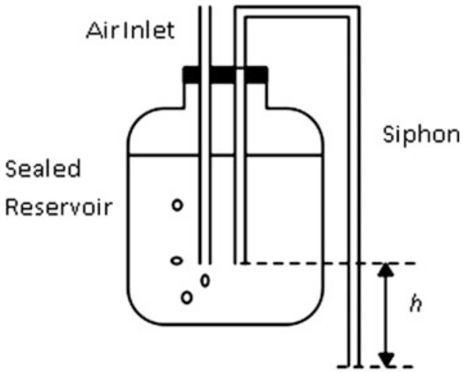


**Fig. 2.3** Mariotte bottle for giving a constant output pressure

The sealed stoppered reservoir is supplied with an air inlet and a siphon. The pressure at the bottom of the air inlet is always the same as the pressure outside the reservoir, i.e. the atmospheric pressure. If it were greater, air would not enter. If the entrance to the siphon is at the same depth, then it will always supply the water at atmospheric pressure and will deliver a flow under constant head height, regardless of the changing water level within the reservoir.

The plug must seal the air space at the top very well. A partial vacuum is created in the air space by the fall of the water level exactly equal to the pressure difference between the surface and the end of the open tube connecting to the atmosphere. The pressure at this point is, therefore, maintained at atmospheric while water is delivered. The head available at the nozzle as shown is equal to $h$ that gives a constant velocity $v = \sqrt{2gh}$.

*Hydraulic Lever*: Consider the devise with a medium of oil as shown in Fig. 2.4. The left side piston of area $a_l$ carries a small input force $F_l$ and the right side piston of area $a_r$ carries a large output force $F_r$.

In operation, when an external force $F_l$ acts downward on the left-hand (or input) piston the incompressible oil in the device produces an upward force of magnitude $F_r$ on the right-hand (or output) piston. Using Pascal's law, we can write

**Fig. 2.4** Hydraulic lever

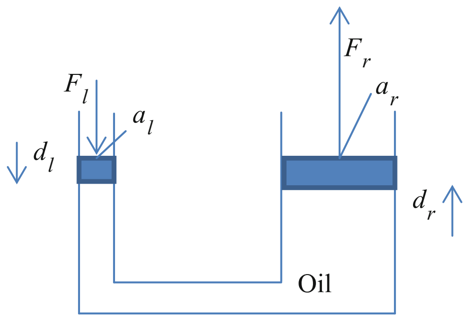


$$F_r = F_l \frac{a_r}{a_i}$$

The above shows that the output force on the right piston $F_r$ is greater than the input force $F_l$ if $a_r > a_l$ as in Fig. 2.4.

If we move the left input piston downward by distance $d_l$, the output piston on the right side moves upward a distance $d_r$, keeping the same volume $V$ of the incompressible liquid displaced at both pistons. Then

$$V = a_l d_l = a_r d_r \Rightarrow$$
$$d_r = \frac{a_l}{a_r} d_l$$

The output piston on the right side moves a smaller distance than the input piston moves. The work done on both the pistons remains same.

The advantage derived out of a hydraulic lever is same as that of mechanical lever of Archimedes. This principle is used in the Bramah hydraulic press, invented in 1785 by Joseph Bramah (1748–1814).

*Forces on Submerged Surfaces*: The hydrostatic pressure acting on the bottom of a vessel is determined solely by the height of the column of liquid as given in Eq. (2.2). What about the sides of a vessel? Simon Stevin (1548–1620) investigated this problem of hydro statics of fluids.

Figure 2.5 shows three water tanks, with one side vertical but the opposite side inclined inwards or outwards. The bottoms of the tanks are of equal sizes and equal heights, filled with water, the pressures at the bottoms are equal, so the vertical force on the bottom of each tank is the same. The tanks do not contain the same weight of water, yet the forces on their bottoms are equal!

**Fig. 2.5** Stevin problem

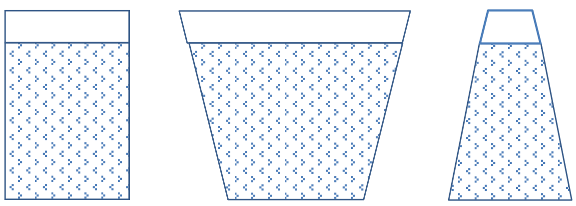

The horizontal forces exerted by the water on the two sides must be equal and opposite, or the tank would scoot off. If the side is inclined outwards, then there must be a downwards vertical force equal to the weight of the water above it, and passing through the centroid of this water. If the side is inclined inwards, there must be an upwards vertical force equal to the weight of the 'missing' water above it. In both cases, the result is demanded by ordinary statics.

## 2.3 Buoyancy

The most widely known anecdote about Archimedes (287–212 BC) faced the question of the honesty of a goldsmith who made a crown for the King. The question arose as to how one could be cetain none of the gold had been substituted by silver. Archimedes found the answer while taking his bath in the tub. He discovered that a body immersed in a fluid experiences a buoyant force equal to the weight of the fluid it displaces and is now known as Archimedes' principle. He used this principle to solvethe King's problem. Expressed mathematically, the buoyancy force $F$ is

$$F = \rho g V \tag{2.4}$$

where $V$ is the volume of fluid displaced.

From the above we note that for any immersed object the volume of submerged portion equals the volume of fluid it displaces. For example if half of a 1000 cc container is submerged 500 cc volume of fluid is displaced, regardless of the container's contents. If we fully submerge the same container one 1000 cc of liquid will be displaced. If we put this container under water there will be gravitational force besides it will be pushed upwards. This upwards force is the buoyancy force equal to the weight of the fluid displaced.

The weight of an object in water is less than the weight of object in air, because of the buoyancy force. The buoyancy force being the weight of the fluid displaced by an object, it is the density of the fluid $\rho$ multiplied by the submerged volume $V$ multiplied by the acceleration due gravity $g$ given in (2.4). Therefore the buoyancy force is greater on a submerged body with greater volume compared with an object of same weight with smaller volume, i.e., with larger density.

Let a body's weight be 10 kg in a vacuum. Let this body displace 3 kg water when lowered into water. It then weighs 10 − 3 = 7 kg. Therefore it is easier to lift the 10 kg body as if it is only 7 kg. Archimedes' principle can be reformulated as follows:

Apparent immersed weight $w_{ai}$ = body weight $w$ − weight of displaced fluid $w_{df}$ or

$$w_{ai} = w - w_{df} \tag{2.5}$$

Dividing both sides by $w_{\mathrm{df}}$

$$\frac{w_{\mathrm{df}} + w_{\mathrm{ai}}}{w_{\mathrm{df}}} = \frac{w}{w_{\mathrm{df}}} \tag{2.6}$$

Equation (2.6) can be rewritten with the left-hand side in densities as

$$\begin{aligned} \frac{\text{body density}}{\text{fluid density}} &= \frac{\text{weight}}{\text{weight of displaced fluid}} \\ \frac{\text{body density}}{\text{fluid density}} &= \frac{\text{weight}}{\text{weight} - \text{apparent immersed weight}} \end{aligned} \tag{2.7}$$

Archimedes realized that a substitution of gold by a cheaper metal cannot be detected by simply weighing the crown, since the crown can be made to weigh the original weight of the gold supplied. Therefore finding the density of the crown would give the answer. Archimedes therefore measured the volume by the amount of water that ran off when the crown was immersed in a vessel filled to the brim and compared the result with pure gold. The two being not the same it was deduced that the crown was adulterated.

Equation (2.7) allows the calculation of density of the immersed object relative to the density of the fluid without measuring any volumes.

Worked Example 2.3:

Consider the case of a 1 m long circular wood of area 1000 $cm^2$ (60 kg weight) having a density of 600 $kg/m^3$. If you drop this wood into water, buoyancy will keep it afloat. Determine the cross-sectional area under water.

Density of water is 1000 $kg/m^3$.
Weight of water displaced will be 60 kg.
Volume of water displaced is 60/1000 = 0.06 $m^3$
Area of 1 m long water is 0.06 $m^2$
Cross-sectional area of wood under water is 600 out of 1000 $cm^2$.

In the case of a ship, its weight is balanced by pressure forces from the surrounding water, allowing it to float like the log of wood above. If more cargo is loaded onto the ship, it would sink more into the water, displacing more water. In turn the ship receives a higher buoyancy force to balance the increased weight.

In general the horizontal and vertical (buoyancy as above) components of the hydrostatic force acting on a submerged surface are given by the following:

$$\begin{aligned} F_H &= p_c A \\ F_V &= \rho g V \end{aligned} \tag{2.8}$$

where

$p_c$ is the pressure at the center of the vertical projection of the submerged surface
$A$ is the area of the same vertical projection of the surface

$\rho$ is the density of the fluid
$g$ is the acceleration due to gravity
$V$ is the volume of fluid directly above the curved surface

## 2.3.1 Application of Buoyancy Principle to the Stability of a Ship

In Fig. 2.6 G is the center of gravity of the ship and its weight W acts through G. The force exerted by the water on the bottom of the ship when it is upright acts through the center of gravity B of the displaced volume $V$, i.e., the center of buoyancy. $\rho g V = W$; G is above B since the CG of the ship will be higher than the CG of the displaced water; this can lead to the ship to capsize.

When the ship heels by an angle Δθ, a wedge-shaped volume of water is added on the right, and an equal volume is removed on the left, so that $V$ remains constant. The center of buoyancy is then moved to the right to point B′.

Taking moments of the volumes about the y-axis

$$V \times (BB') = V \times (0) + \text{Moment of the shaded volume} - \text{Moment of the equal compensating volume.} \tag{2.9}$$

In the displaced volume shown shaded to the right, let $dA$ be the elemental of area in the $y = 0$ plane; the volume of this element is $x \times \Delta\theta \times dA$. It can be seen that the volume to the left of $x = 0$ is same but negative. The moment of this elemental area is

Fig. 2.6 Ship stability from buoyancy

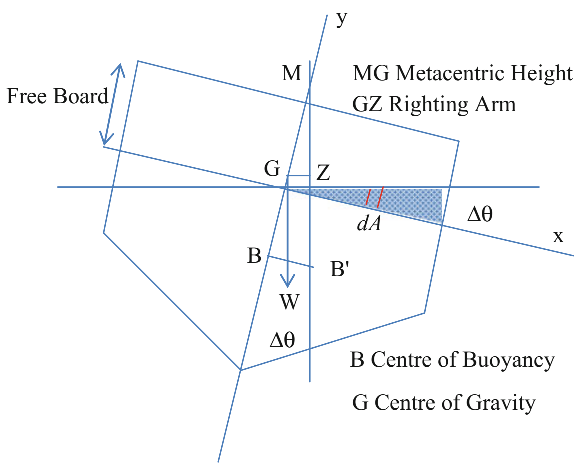

$$x^2 \times \Delta\theta \times dA = I \times \Delta\theta \tag{2.10}$$

where $I = \int x^2 dA$ is the moment of inertia of the water-level area of the ship. (Note that the contributions from $x > 0$ and $x < 0$ are both positive.)

$$\begin{aligned} &\therefore V \times (\mathrm{BB}') = I\Delta\theta \\ &\Rightarrow \\ &\frac{\mathrm{BB}'}{\Delta\theta} = \frac{I}{V} \end{aligned} \tag{2.11}$$

From Fig. 2.6 $\frac{\mathrm{BB}'}{\Delta\theta} = \mathrm{MB}$ and MB = MG + GB. This gives

$$\mathrm{MG} = \frac{I}{V} - \mathrm{BG} \tag{2.12}$$

where M is metacenter and MG is the metacentric height from the center of gravity.

When the ship is displaced to the position shown in Fig. 2.6, a restoring moment given by the weight $W$ times the GZ (= MG × Δθ), acts making it stable. GZ is called the *righting arm*.

When a ship rolls it has an inertia torque given by the product of its polar mass moment of inertia and angular acceleration. The restoring torque and the inertia torque keep the dynamic equilibrium. The frequency of vibration depends on the restoring torque; for the same inertia, if the restoring torque is small, i.e., its angular stiffness is small and the natural frequency is small or long rolling period. A small GM means a small restoring torque, and so a long roll period.

A ship with a small GM is said to be *tender*; a passenger ship may have a roll period of 28 s making it comfortable. A ship with a large GM and a short roll period is called *stiff*. Metacentric heights GM are typically 1–2 m.

### *2.3.2 Balloons and Airships*

The buoyancy principle is a perfect application to be applied to balloons. The balloon or airship needs to be filled with a gas lighter than air so that the buoyancy from air (as compared to water in the case of ship) can make the balloon float. The first hot air balloon ascended first in 1783 with a paper envelope made by Joseph-Michel Montgolfier (1740–1810) and Jacques-Étienne Montgolfier (1745—1799). They used a fire balloon; initially they used crumpled paper and lit under the bottom of the box to observe the levitation. Their first demonstration is illustrated in Fig. 2.7.

Such “fire balloons” were then replaced with hydrogen-filled balloons, and then with balloons filled with coal gas, which was easier to obtain and did not diffuse through the envelope quite as rapidly. Methane would be a good filler, with a density 0.55 that of air.

**Fig. 2.7** Montgolfier brothers' public demonstration in 1783. https://upload.wikimedia.org/wikipedia/commons/6/6b/Early_flight_02562u_(2).jpg

Balloons are naturally stable, since the center of buoyancy is above the center of gravity in all practical balloons. Natural rubber balloons with hydrogen have been used for meteorological observations; Helium is a good substitute for hydrogen as it is not inflammable. Submarines are other examples that utilize Archimedes and Pascal principles.

### *2.3.3 Hydrostatics of Dam*

A dam or retainer wall is constructed to store water. This stored water at a height can be used to convert hydraulic head to electricity. One of the largest hydroelectric power plants in the world shown in Fig. 2.8 has a capacity of 12,600 MW and located on the border between Brazil and Paraguay on the Parana River. Three Gorges Dam in China has the highest generating capacity of 22,500 MW.

The electric power is generated from the head of the water which is led through penstocks through the height of the dam to a hydraulic turbine which drives a generator, see Fig. 2.9. This is enabled through sluice gates which allow the flow to take place and thus produce power. The sluice gate design is based simply on principles of hydrostatics.

Consider the dam of area $A$ at an angle $\theta$ as shown in Fig. 2.10. The axis $y$ is taken along the dam downwards with $x$ axis perpendicular as shown. Taking the pressure

**Fig. 2.8** Dam on the Parana River on the border between Brazil and Paraguay. http://3.bp.blogspot.com/_AqMeNIWSpns/SlDiw3lNZ2I/AAAAAAAAArI/SEKeTqC90ew/s320/Itaipu+dam+wallpapers,+7+wonders+of+the+world+images.jpg

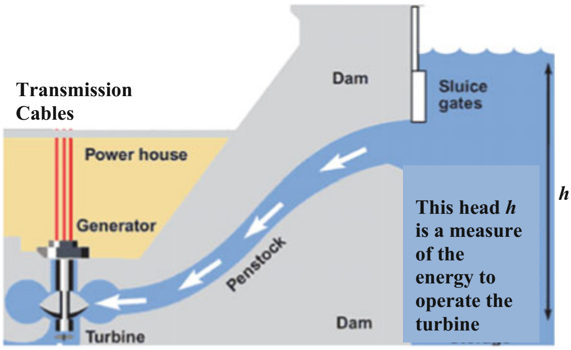


**Fig. 2.9** Sluice gates allow water from reservoir to penstocks

acting on the surface to be zero, i.e., disregarding the atmospheric pressure, the pressure $dp$ at a depth $h$ or a distance $y$ along the dam can be written from (2.2) as

$$dp = \rho g y \sin\theta \tag{2.13}$$

The force $dF$ on an element of area $dA$ is

$$dF = \rho g y \sin\theta \times dA \tag{2.14}$$

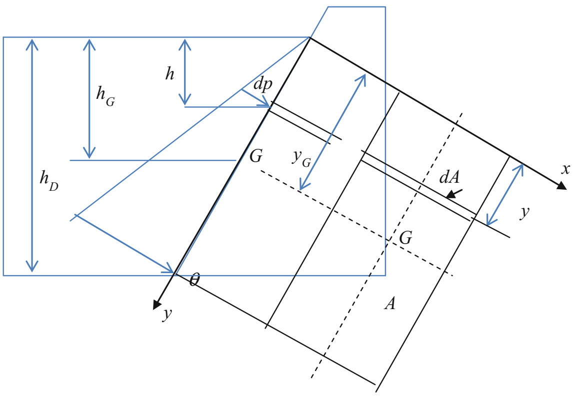


**Fig. 2.10** Hydrostatic forces on a gate

The total force $F$ on the underwater area of the dam wall $\boldsymbol{A}$ is:

$$\begin{aligned} F &= \int_A dF = \rho g \sin\theta \int_A y dA \\ &= \rho g \sin\theta \times y_G A = \rho g h_G A \end{aligned} \tag{2.15}$$

This force $F$ above is the product of the pressure at the centroid G and the underwater area $A$ of the dam.

Worked Example 2.4:
Consider now a rectangular sluice gate similar to the retaining wall but vertical and hinged at the top water level as shown in Fig. 2.11.

The hydrostatic force acting normal to the gate has to be countered by a force $P$ at the bottom such that the torque about the hinge of the hydrostatic forces is equal and opposite to the reaction $P$ times the height of the sluice gate $h_s$.

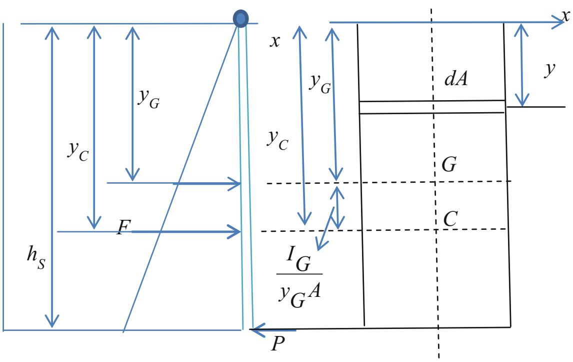


**Fig. 2.11** Sluice gate forces

The force $F$ acting on the whole plane of the gate from Eq. (2.15) is $\rho g y_G A$. The force acting on the elemental area $dA$ is $\rho g y \times dA$, the moment of this force about the hinge axis $xx$ is $\rho g y^2 dA$ and the total moment on the gate is

$$M_{xx} = \int \rho g y^2 dA = I_{xx} \rho g \tag{2.16}$$

where $I_{xx} = \int y^2 dA$ is the second moment of area of the sluice gate about $xx$ axis.

Let $C$ be the center of pressure as shown in Fig. 2.11, where the net hydrostatic load can be considered to act, then

$$M_{xx} = I_{xx} \rho g = F y_C \tag{2.17}$$

Using parallel axis theorem $I_{xx} = I_{GG} + A y_G^2$ the above becomes

$$\left(I_{GG} + A y_G^2\right) \rho g = F y_C \tag{2.18}$$

$$\begin{aligned} \left(I_{GG} + A y_G^2\right) &= A y_G y_C \\ y_C = \tfrac{\left(I_{GG} + A y_G^2\right)}{A y_G} &= y_G + \tfrac{I_{GG}}{A y_G} \end{aligned} \tag{2.19}$$

The second moment of area about GG axis is $I_{GG} = \frac{1}{12} b h_s^3 = \frac{1}{12} A h_s^2$ we have

$$y_C = y_G + \frac{1}{12} \frac{h_s^2}{y_G} \tag{2.20}$$

$$\begin{aligned} \rho g y_G A \left( y_G + \tfrac{1}{12} \tfrac{h_s^2}{y_G} \right) &= P h_s \Rightarrow \\ P = \tfrac{\rho g y_G A}{h_s} \left( y_G + \tfrac{1}{12} \tfrac{h_s^2}{y_G} \right) \end{aligned}$$

The above derivations help us in design of dams, penstocks, gates etc. In a similar way this formulation will also be useful in the design of valves in pipelines.

## 2.4 Basics of Thermodynamics

Thermodynamics is the scientific treatment of mechanical actions or relations of heat. The basic principles of thermodynamics are the laws governing the energy from one form to another. Among the many consequences of these laws are relationships between the properties of the matter and the effects of changes in pressure and temperature. Thermodynamics is based on observations of common experience that have been formulated into thermodynamic laws.

We first define a system, e.g., a fixed mass of gas, a block of ice or the hot plate used for cooking. The region outside the system is called the surroundings. An open system may exchange mass, heat and work with the surroundings. A closed system may exchange heat and work but not mass with the surroundings.

It is a common experience for us to talk of a body when we touch it that it is hot, e.g., boiling water or cold, e.g., a block of ice. This is a primitive way of expressing the condition of a body, as it is a relative measure of a system with respect to human body. Thermodynamics can refine this primitive way of expression by a precise concept of temperature.

Let's construct a mercury-in-glass thermometer that has its pressure held constant. This thermometer forms a system by itself. It can be used to measure the temperature of another system, the mercury changes in its volume under constant pressure until an equilibrium state is reached with the system, whose temperature is being measured. Bodies in thermal equilibrium are said to have the same temperature.

### 2.4.1 Zeroth Law

Consider a large body of water in thermal contact through a wall with large body of another fluid, say alcohol, both in the state of equilibrium that is they both have the same temperature. When a mercury-in-glass thermometer is used to measure the temperature of either of these fluids, it will register the same volume of the mercury. This fact of experience is commonly known as Zeroth law of Thermodynamics, namely, *If two bodies A and B are separately in thermal equilibrium with a third body C, then A and B are in equilibrium with each other.*

### 2.4.2 Hydrostatics of Gases

A fluid medium can be considered to consist of particles, a collection of molecules, atoms, ions, and electrons etc., which are more or less in random motion. As these particles are all under an electronic structure a force field exists in the space between them. Such a force field is called intermolecular force field. If the fluid medium is a gas and that its particles sufficiently separated such that the intermolecular forces are negligible, it is called a *perfect gas*. For temperatures and pressures normally encountered in the compressible flows of our common interest, the particles in the medium are generally apart by a distance of ten molecular diameters or more. Hence we will be concerned in our compressible flow studies with such gases that can be considered as perfect in nature. The density of a gas changes with pressure; for example the atmospheric pressure changes with the height so also the density.

Boyle's-Charles' law for gases states that

$$pv = RT \tag{2.21}$$

where $p$ is the pressure of a gas, $v$ the specific volume, $T$ the absolute temperature and $R$ the gas constant. This is the equation of state for a perfect or ideal gas, and $v = \frac{1}{\rho}$. The value of $R$ varies for different gases, for air it is 287.1. Gases at considerably higher temperatures than the liquefied temperature can be considered to be a perfect gas.

Worked Example 2.5:
The pressure inside a room with dimensions 6 × 8 × 6 m contains air at a pressure 0.1 MPa and temperature 22 °C. Determine the density, specific gravity, and mass of the air treating air as ideal gas with a gas constant 287 Pa m$^3$/kg °K.

The density is determined from $\rho = \frac{p}{RT} = \frac{0.1 \times 10^6}{287 \times 295} = 1.1811\,\text{kg/m}^3$.

Dividing the density with density of water, specific gravity of air therefore is 0.0011811.

Mass of air in the room is 6 × 8 × 6 × 1.1811 = 340 kg.

## 2.4.3 Vapor Pressure

There is one-to-one correspondence between temperatures and pressures. At a given pressure, the temperature at which a pure substance changes phase is called the *saturation temperature* $T_{sat}$. Similarly, at a given temperature, the pressure at which a pure substance changes phase is called the *saturation pressure* $P_{sat}$. Table 2.1 gives Saturation (or vapor) pressure of water at various temperatures.

**Table 2.1** Saturation (or vapor) pressure of water as a function of temperatures

| Temperature | Pressure |
|---|---|
| $T$, °C | $P_{sat}$ kPa |
| 0 | 0.611 |
| 5 | 0.872 |
| 10 | 1.23 |
| 15 | 1.71 |
| 20 | 2.34 |
| 25 | 3.17 |
| 30 | 4.25 |
| 40 | 7.38 |
| 50 | 12.35 |
| 100 | 101.3 (1 atm) |
| 150 | 475.8 |
| 200 | 1554 |
| 250 | 3973 |
| 300 | 8581 |

At an absolute pressure of 1 standard atmosphere, 101.325 kPa, the saturation temperature of water is 100 °C. Conversely, at a temperature of 100 °C, the saturation pressure of water is 1 atm. The *vapor pressure* $P_v$ of a pure substance is defined as the pressure exerted by its vapor in phase equilibrium with its liquid at a given temperature. This is a property of the pure substance, and turns out to be identical to the saturation pressure $P_{sat}$ of the liquid.

It should be noted that vapor pressure and partial pressure are different. *Partial pressure* is defined as the pressure of a gas or vapor in a mixture with other gases. As an example atmospheric air is a mixture of dry air and water vapor, and atmospheric pressure is the sum of the partial pressure of dry air and the partial pressure of water vapor. The partial pressure of water vapor constitutes a small fraction less than 3 % of the atmospheric pressure which is mostly nitrogen and oxygen. The partial pressure of a vapor must be less than or equal to the vapor pressure if there is no liquid present. However, when both vapor and liquid are present and the system is in phase equilibrium, the partial pressure of the vapor must equal the vapor pressure, and the system is said to be saturated.

Worked Example 2.6:
A bucket of water is left at 25 °C left in a room with dry air at 1 atm. The vapor pressure of water at 25 °C is 2.4 kPa. When will the evaporation stop?

The water will begin evaporating and continue evaporating until all the water evaporates away if there is not enough water to establish phase equilibrium in the room.

Or the evaporation stops when the partial pressure of the water vapor in the room rises to 2.4 kPa at which point phase equilibrium is established.

Worked Example 2.7:
At what temperature does water boil in a pressure cooker operating at 3 atmospheres pressure? Also at what temperature does water boil at an elevation of 2000 m.

Vapor pressure increases with temperature as given in Table 2.1. Therefore, a substance at higher temperatures boils at higher pressures. Let us use linear interpolation from Table 2.1. Two atmospheres pressure is 304 − 101.3 = 202.7 kPa. From Table 2.1 we find that a 50 °C rise at 100 °C raises the saturated pressure from 101.3 to 475.8 kPa, i.e., 374.5 kPa. For a rise of 202.7 kPa, the temperature rise is $\frac{202.7}{374.5} \times 50 = 27$ °C. Therefore water boils at 127 °C in the pressure cooker. The correct value is 134 °C.

At 2000 m elevation the atmospheric pressure is only 81 kPa (0.8 atm). Using linear interpolation as above, $\frac{(101.3-81)}{(101.3-12.35)} \times 50 = 11.4$ °C giving the boiling temperature equal to 88.6 °C. The correct value is 93 °C.

*Cavitation*: When the liquid pressure in a flow drops below the vapor pressure *cavitation* occurs resulting in unplanned vaporization. In Impeller tip regions on suction sides of the pumps the pressure can fall below vapor pressure of the flow medium. For example, water at 15 °C will flash into vapor and form bubbles forming cavities when the pressure drops below its saturation pressure 1.71 kPa. The cavitation bubbles collapse as they are swept away from the low pressure regions, generating extremely high-pressure waves. Cavitation causes poor performance and even the erosion of impeller blades, is called cavitation. The pressure spikes resulting from the large number of bubbles collapsing near a solid surface over a long period of time causes erosion, surface pitting, fatigue failure, and the eventual destruction of the components or machinery.

### 2.4.4 Internal Energy

The subject of Thermodynamics itself does not define the concepts of energy or work; they are adopted from the subject of Mechanics. The principle of conservation of energy is also taken as axiomatic.

Now, consider an isolated system (no exchange with surroundings) with a finite volume of gas, formed from any part of a given system. It will have a definite amount of energy trapped in the molecules of the system in the form of kinetic energy and potential energy. This trapped energy is called *internal energy*.

The internal energy per unit mass is defined as *specific internal energy* denoted by $e$ and it is a state variable depending only on the initial and final states of a system undergoing a change.

### 2.4.5 Enthalpy

For a given system *enthalpy* is defined as the sum of internal energy and the system's volume multiplied by pressure exerted by the system on the surroundings.

Enthalpy per unit mass is defined as *specific enthalpy*, $h$, which is written as

$$h = e + pv \tag{2.22}$$

Specific enthalpy is a commonly used quantity and it repeatedly appears in a discussion of thermodynamics. Enthalpy depends only on the initial and final states of a system undergoing a change, therefore a state variable in contrast to heat and work which are path functions.

The specific internal energy and specific enthalpy for a perfect gas are functions of temperature only, i.e.,

$$\begin{aligned} e &= e(T) \\ h &= h(T) \end{aligned} \tag{2.23}$$

### 2.4.6 Specific Heats

The *specific heat* is defined as the amount of heat required to raise unit mass of a material by one degree, i.e., $\frac{\text{J}}{\text{kg}^{\circ}\text{K}}$. As we are concerned with gases here, there are two different ways by which we can perform the heating operation, one at constant volume and the other at constant pressure.

Consider a system of gas with its mass enclosed at a constant volume, any heat added is used solely to raise the gas temperature, hence the heat added increases the internal energy of the gas, $e$. The specific heat under these conditions is defined by *specific heat at constant volume* and denoted by $c_v$. The change in the specific internal energy then is written as

$$de = c_v dT \tag{2.24}$$

For a calorically perfect gas the $c_v$ is independent of temperature $T$ and therefore

$$e = c_v T \tag{2.25}$$

For air under standard conditions, $c_v = 718 \frac{\text{J}}{\text{kg}^{\circ}\text{K}}$.

In a similar manner, now consider a system of gas which is allowed to expand and maintain a constant pressure due to any imposed change. Application of heat to such a system raises the temperature and in order to keep the pressure same, its volume also changes simultaneously. The change in the volume of the gas results in mechanical work on the surroundings, for example the piston carrying a constant load with gas in a cylinder. Thus it is necessary to supply the heat required to increase the temperature of the gas by one degree K as in the case of constant volume before, in addition the amount of heat equivalent to the mechanical work done against the surroundings. The total heat required is the *specific heat under constant pressure*, denoted by $c_p$. Now by definition of specific enthalpy in (2.22)

$$dh = c_p dT \tag{2.26}$$

For a calorically perfect gas the $c_p$ is independent of temperature $T$ and therefore

$$h = c_p T \tag{2.27}$$

For air under standard conditions, $c_p = 1005 \frac{\text{J}}{\text{kg}^{\circ}\text{K}}$.

For most of the compressible flow problems, the temperatures normally encountered are moderate and the gases can be considered as calorically perfect and therefore the specific heats are taken constant. The *specific heat ratio* is denoted by $\gamma$

$$\gamma = \frac{c_p}{c_v} \tag{2.28}$$

For a perfect gas

$$\begin{aligned} &pv = RT \Rightarrow h - e = RT \Rightarrow c_pT - c_vT = RT \\ &\therefore c_p - c_v = R \end{aligned} \tag{2.29}$$

Eliminating $c_v$ in (2.28), we get

$$c_p = \frac{\gamma R}{\gamma - 1} \tag{2.30a}$$

Similarly

$$c_v = \frac{R}{\gamma - 1} \tag{2.30b}$$

## 2.4.7 *Polytropic Form for Pressure-Specific Volume Relation*

In general the pressure and specific volume relation is expressed in a polytropic form $pv^n$ = constant and the exponent $n$ for different state processes can be represented as in Fig. 2.12.

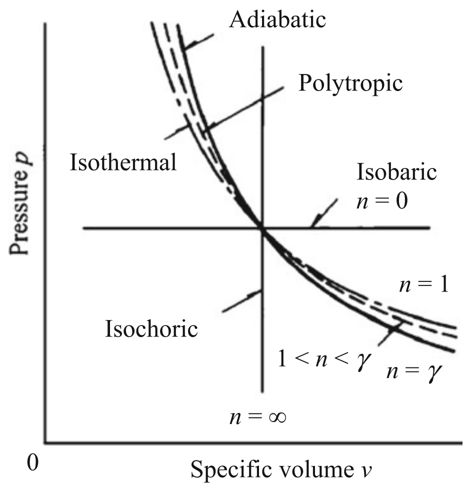


**Fig. 2.12** Polytropic Exponent $n$ in state relation for gases

In Fig. 2.12, $\gamma$ is ratio of specific heats $c_p$ and $c_v$. Therefore for gases it is not possible to integrate the pressure simply as in the case of a liquid. Referring to the sea level ($z$ = 0) pressure $p$ and density $\rho$ with a subscript 0, we can write

$$\frac{p}{\rho^n} = \frac{p_0}{\rho_0^n} \tag{2.31}$$

We can write the expression for the density in the following form

$$\rho^n = \frac{p}{p_0}\rho_0^n \Rightarrow \rho = \rho_0\left(\frac{p}{p_0}\right)^{\frac{1}{n}} \tag{2.32}$$

From Eq. (2.1) with the sea level as datum, we can write

$$\frac{dp}{dz} = -\rho g \Rightarrow dz = -\frac{dp}{\rho g} \tag{2.33}$$

Substituting for $\rho$ from (2.32) we have

$$\begin{aligned} dz &= -\frac{dp}{\rho g} = -\frac{1}{g}\frac{p_0^{\frac{1}{n}}}{\rho_0}p^{-\frac{1}{n}}dp \\ &= -\frac{1}{g}\frac{p_0}{\rho_0}\left(\frac{p_0}{p}\right)^{\frac{1}{n}}d\left(\frac{p}{p_0}\right) \end{aligned} \tag{2.34}$$

From sea level as datum, integrating

$$z = \int_0^z dz = \frac{1}{g}\frac{n}{n-1}\frac{p_0}{\rho_0}\left[1 - \left(\frac{p}{p_0}\right)^{\frac{n-1}{n}}\right] \tag{2.35}$$

Rearranging the above, we get the pressure at $z$ in terms of sea level value

$$\frac{p(z)}{p_0} = \left(1 - \frac{n-1}{n}\frac{\rho_0 g}{p_0}z\right)^{\frac{n}{n-1}} \tag{2.36}$$

From (2.32), we can get a similar relation for the density

$$\frac{\rho}{\rho_0} = \left(\frac{p}{p_0}\right)^{\frac{1}{n}} = \left(1 - \frac{n-1}{n}\frac{\rho_0 g}{p_0}z\right)^{\frac{1}{n-1}} \tag{2.37}$$

For absolute temperature $T_0$ at sea level and $T$ at the point of height $z$, we can write

$$\frac{p}{\rho T} = \frac{p_0}{\rho_0 T_0} = R \\ \Rightarrow \\ \frac{T}{T_0} = \frac{p}{p_0}\frac{\rho_0}{\rho} \tag{2.38}$$

With the help of (2.36) and (2.37)

$$\frac{T}{T_0} = \frac{p}{p_0}\frac{\rho_0}{\rho} = \frac{\left(1 - \frac{n-1}{n}\frac{\rho_0 g}{p_0}z\right)^{\frac{n}{n-1}}}{\left(1 - \frac{n-1}{n}\frac{\rho_0 g}{p_0}z\right)^{\frac{1}{n-1}}} = \left(1 - \frac{n-1}{n}\frac{\rho_0 g}{p_0}z\right) \tag{2.39}$$

From the above, we can obtain a relation for temperature as a function altitude given by

$$\begin{aligned} \frac{dT}{dz} &= -\frac{n-1}{n}\frac{\rho_0 g}{p_0}T_0 \\ &= -\frac{n-1}{n}\frac{g}{R} \end{aligned} \tag{2.40}$$

The sea level values in general are $p_0 = 101.325$ kPa, $T_0 = 288.5$ K and $\rho_0 = 1.225$ kg/m$^3$. The polytropic exponent $n$ then is 2.235. One can show that the temperature decreases by 0.65 °C every 100 m of height in the troposphere up to approximately 1 km high, but is constant at −50.5 °C from 1 to 10 km height.

### 2.4.8 First Law of Thermodynamics

Consider a closed system; say a fixed mass of gas. Its internal energy can be altered only by an exchange of energy from its surroundings through the boundary. Such an exchange can take place in three different ways by

1. mass transfer
2. heat transfer or
3. work exchange

For a closed system no mass transfer can take place. Therefore its state can be changed either by heat addition or by work done on the system by its surroundings. This is the First Law of Thermodynamics.

Let the amount of incremental heat added be $\delta q$ and the work done on the system be $\delta w$, then the change in the specific internal energy $de$ is

$$de = \delta q + \delta w \tag{2.41}$$

Since $e$ is a state variable, it is an exact differential.

### 2.4.9 Adiabatic Process

A special case of the First Law is when no heat is added or taken away. The process is then called an *adiabatic process*. For an adiabatic process, therefore, $\delta q = 0$. Then the change in internal energy is simply equal to the work done by the surroundings of the system.

$$de = \delta w \tag{2.42}$$

This case is similar to solids when the work done by external forces is equal to the internal energy, called *strain energy*.

### 2.4.10 Irreversible Process

Any process that occurs in nature follows the Ist Law of Thermodynamics, however many processes that satisfy the first law may never occur. There is ample evidence that processes prefer to proceed in one direction.

James Prescott Joule conducted an experiment in 1845 to find the Mechanical Equivalent of Heat. In his experiment he used a falling weight, in which gravity does the mechanical work, to spin a paddle-wheel in an insulated (adiabatically) barrel of water which increased the temperature. The total effect of the experiment was to increase the internal energy of the water and to lower the weight, keeping the surroundings unchanged. He estimated a mechanical equivalent of 4.41 J/cal (Nm/cal).

This process cannot be reversed, i.e., water cannot be restored to original state and raise the weight to the original height without making additional changes to the surroundings. Hence the process is *irreversible* (Fig. 2.13).

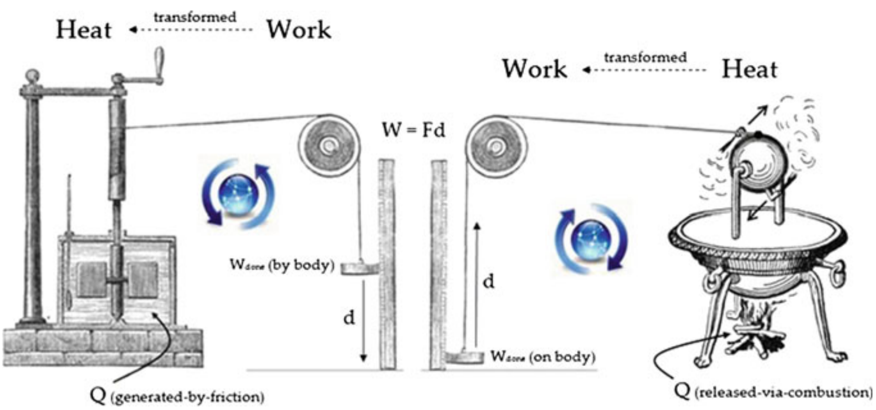


**Fig. 2.13** Joule's apparatus to find mechanical equivalent of heat and demonstrate the irreversibility. http://image.wikifoundry.com/image/1/f04TM0t9WI4ADVjQGYm8MA78738/GW666H312

### 2.4.11 Reversible Process

Thermodynamics makes use of an idealization, called *Reversible Process*. This is a limiting case of the natural or irreversible process. Reversible process is one in which no dissipative phenomenon (e.g., effects of viscosity) occur. A reversible process may be imagined to proceed through a succession of equilibrium states and may be reversed by an infinitesimal change in the external conditions.

Consider as an example a gas cylinder fitted with a frictionless piston. Let the piston be moved slowly, such that the pressure gradients are absent and that the gas is in equilibrium at all the times. The pressure difference between the gas in the cylinder and the external surroundings need be infinitesimal only at any given time to cause a motion of the frictionless piston. Under such restrictive conditions of a reversible process, we can write

$$\delta w = -pdv \tag{2.43}$$

Hence the first law for a reversible process can be written as

$$de = \delta q - pdv \tag{2.44}$$

### 2.4.12 Entropy and Second Law of Thermodynamics

The discussion on irreversible process in Sect. 2.4.10 led to the II Law of Thermodynamics, which is essentially a statement on the preferred direction of a given process.

Consider a block of ice that is brought into contact with a hot iron plate. It is a common knowledge that ice melts from the heat of the iron plate and the plate cools; hat transfer takes place from the hotter iron plate to cooler ice block.

The First Law of Thermodynamics does not define this process in a unique manner; instead it can allow a process, though physically not possible, wherein the ice block becomes cooler further by giving away heat to hot iron plate, making it hotter. The nature has a preference to this process in which heat flows from a hotter body to a cooler body.

Rudolf Clausius laid the foundation for the second law of thermodynamics in 1850, which states "It is not possible that at the end of a cycle of changes, heat has been transferred from a colder to a hotter body without providing some other effect". Though Clausius statement explains the fact that some processes allowed by the First Law cannot occur in nature, it is not a mathematical statement.

### 2.4.13 Entropy

For understanding the mathematical consequences of the II Law and ascertaining the proper direction of a given process, a state variable *entropy* $s$ is defined as follows.

Incremental amount of heat $\delta q_{\text{rev}}$ added reversibly to a system is expressed as

$$\delta q_{\text{rev}} = T ds \tag{2.45}$$

For an irreversible process, where $\delta q$ is the heat added, the above becomes

$$\begin{aligned} \delta q &= T(ds - ds_{\text{irrev}}) \Rightarrow \\ ds &= \frac{\delta q}{T} + ds_{\text{irrev}} \end{aligned} \tag{2.46}$$

$ds_{\text{irrev}}$ is the entropy generated due to any irreversible process phenomenon, e.g., viscous effects occurring in the system. The dissipative phenomenon always increases the entropy, i.e.,

$$ds_{\text{irrev}} \geq 0 \tag{2.47}$$

For a reversible process, $ds_{\text{rev}} = 0$ therefore Eq. (2.46) leads to

$$ds \geq \frac{\delta q}{T} \tag{2.48}$$

For an adiabatic process, the above simplifies to

$$ds \geq 0 \tag{2.49}$$

The above two equations are mathematical expressions of the Second Law.

The II Law tells us the direction in which a process can take place. Specifically it tells us that a process in which generation of entropy is not positive, i.e., the entropy cannot increase, cannot take place even if it satisfies the Ist Law. The process should yield a net increase in the entropy from one state to another state. In the example of ice block and hot iron plate, we find that there is a net increase in the entropy only when ice receives heat from the hot plate, or

$$ds = \frac{\delta q}{T_{\text{ice}}} + \frac{-\delta q}{T_{\text{plate}}} > 0$$

On the other hand, if we conceive a process by which ice block gives away its heat, thus lowering its temperature further, and the hot plate receives heat, increasing its temperature further, i.e., heat transfer takes place from colder to a hooter body, the entropy change is negative, or

$$ds = \frac{-\delta q}{T_{\text{ice}}} + \frac{\delta q}{T_{\text{plate}}} < 0$$

and the II Law prohibits this direction of the process.

### 2.4.14 Entropy Calculation for Any Process

Let us assume that heat is added in a reversible manner, Eq. (2.44); using (2.45), we can write

$$Tds = de + pdv \tag{2.50}$$

From the definition of enthalpy, Eq. (2.22)

$$dh = de + pdv + vdp$$

Therefore Eq. (2.50) becomes

$$Tds = dh - vdp \tag{2.50a}$$

Equations (2.50) and (2.50a) are essentially the same, they are alternate forms of the first law expressed in terms of entropy.

Consider now a perfect gas and according to the definitions of specific heats given in (2.24) and (2.26), we write the above (2.50) and (2.50a) as

$$ds = c_v \frac{dT}{T} + \frac{pdv}{T} \tag{2.51}$$

$$ds = c_p \frac{dT}{T} - \frac{vdp}{T} \tag{2.51a}$$

Equation (2.51) can be further written using $\frac{p}{T} = \frac{R}{v}$ from the perfect gas equation

$$ds = c_v \frac{dT}{T} + R\frac{dv}{v} \tag{2.52}$$

Let a thermodynamic process take place with initial and end states represented by 1 and 2 respectively, then

$$s_2 - s_1 = c_v \int_{T_1}^{T_2} \frac{dT}{T} + T \int_{v_1}^{v_2} \frac{dv}{v} \Rightarrow$$
$$s_2 - s_1 = c_v \ln \frac{T_2}{T_1} + R \ln \frac{v_2}{v_1} \tag{2.53}$$

In a similar manner (2.51a) gives

$$s_2 - s_1 = c_p \ln \frac{T_2}{T_1} - R \ln \frac{p_2}{p_1} \tag{2.54}$$

We note from the above two equations that the entropy is a function of two thermodynamic variables, either $p$ and $T$ or $v$ and $T$.

### 2.4.15 Isentropic Process

We now consider a third thermodynamic process without any change in the entropy of the system, called *isentropic process*. For a reversible process as given in Eq. (2.44), the quantity of heat transferred is directly proportional to the system's entropy change. Systems which are thermally insulated from their surroundings undergo processes without any heat transfer and such processes are denoted as adiabatic as given in Sect. 2.4.9. Thus, an isentropic process is one which is both reversible and adiabatic, so that $ds = 0$. For an isentropic process, Eq. (2.54) gives

$$c_p \ln \tfrac{T_2}{T_1} - R \ln \tfrac{p_2}{p_1} = 0 \Rightarrow$$
$$\tfrac{p_2}{p_1} = \left(\tfrac{T_2}{T_1}\right)^{\frac{c_p}{R}} \tag{2.55}$$

Using Eq. (2.30a)

$$\frac{p_2}{p_1} = \left(\frac{T_2}{T_1}\right)^{\frac{\gamma}{\gamma-1}} \tag{2.56}$$

Similarly (2.53) gives

$$\frac{v_2}{v_1} = \left(\frac{T_2}{T_1}\right)^{-\frac{1}{\gamma-1}} \tag{2.57}$$

By definition of specific volume

$$\frac{\rho_2}{\rho_1} = \frac{v_1}{v_2} \tag{2.58}$$

Equation (2.57) can then be written as

$$\frac{\rho_2}{\rho_1} = \left(\frac{T_2}{T_1}\right)^{\frac{1}{\gamma-1}} \tag{2.59}$$

Therefore, for an isentropic process

$$\frac{p_2}{p_1} = \left(\frac{\rho_2}{\rho_1}\right)^{\gamma} = \left(\frac{T_2}{T_1}\right)^{\frac{\gamma}{\gamma-1}} \tag{2.60}$$

The above relation is essentially a combination of the first law of thermodynamics and the definition of entropy and hence it is basically an energy relation for an isentropic process. Though an isentropic process seems to be highly restrictive that it has to be adiabatic and reversible, it is of immense use in practical compressible flows.

As an example consider the flow between two adjacent blades in a turbomachine, which is like the flow through nozzle. In the regions adjacent to the walls of the nozzles, a thin boundary layer is formed, within which, the viscosity, thermal conduction and diffusion are predominant. Entropy increases substantially within such a boundary layer. Barring this thin boundary layer, the entire flow field is adiabatic and reversible, i.e., isentropic in nature. Hence the importance of isentropic process in the compressible flow problems.

## Exercises 2

1. Derive a relation for hydrostatic pressure of a given liquid with density $\rho$ as a function of its height above the datum. Use acceleration due to gravity $g$. Show that the atmospheric pressure at sea level is 757 mm of mercury. The density of mercury is 13595.1 kg/m$^3$.
2. What is absolute pressure and how do you relate it to gauge pressure. How do you express vacuum? Express a vacuum of 600 torr as an absolute pressure.
3. Determine the head of water equivalent to one atmospheric pressure 101325 Pa.
4. Determine the pressure at the bottom of a sea which is 6000 m deep.
5. Describe how a Pascal siphon works? Using this principle describe an apparatus for giving a constant output pressure.
6. Describe a Bramah hydraulic press and derive the relation between input and output pressures, similar to a mechanical lever.
7. Three water tanks of same height have side walls inclined from vertical at 130°, 90° and 75° respectively. If they contain a liquid of same height, show that the forces at the bottom are all same.

8. Determine the pressure at point $P$ in the figures shown. $p_0$ is atmospheric pressure.

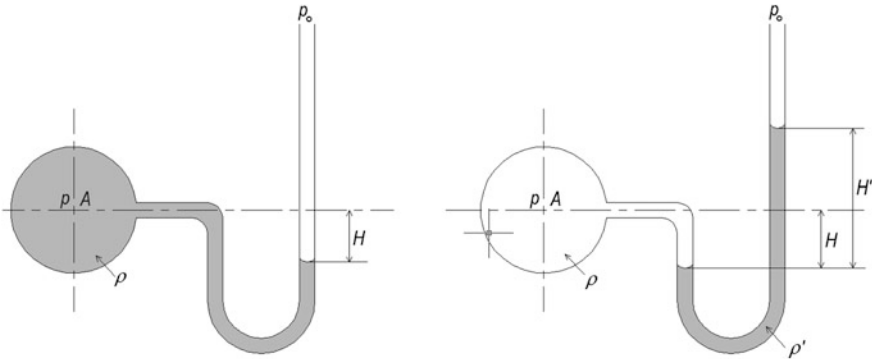


9. A barometer at a location gives a reading 750 mm Hg. If the density of mercury is 13,600 kg/m$^3$ determine the atmospheric pressure at this location.
10. The gage pressure in a liquid at a depth of 3 m is 28 kPa. What will be the gage pressure in the same liquid at a depth of 12 m?
11. The vacuum gage reading on a tank shows 28 kPa at a location where the barometric reading is 750 mm Hg. What is the absolute pressure in the tank? The density of mercury is 13,500 kg/m$^3$.
12. It was decided to use the basic barometer in measuring the height of a building. At the top of the building the barometer read 720 mm Hg and at the bottom it is 750 mm Hg. What is the height of the building? The density of air is taken an average value in this height which is 1.15 kg/m$^3$.
13. Determine the force acting on the lower stay of the water gate 2 m high and 1 m wide shown in the figure.

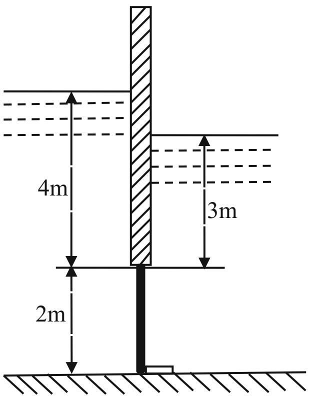

14. What is the force in magnitude and the location acting on a unit width of the dam wall? The water is 15 m deep and the wall is inclined at 60°.
15. The piston of a vertical piston–cylinder device containing a gas has a radius 20 cm and weighs 50 kg. Determine the pressure inside the cylinder. If some heat is transferred to the gas and its volume is doubled, what will be the change of pressure inside the cylinder?
16. A tank $H$ m depth is filled with saline water whose density varies with depth $z$ from the free surface given by $\rho = \rho_0\sqrt{1 + \tan^2\frac{\pi z}{4H}}$. $\rho_0$ is the density of water at the free surface. If $H$ is 4 m determine the gage pressure at the bottom of the tank.
17. A car sunk in a lake 10 m deep. The front seat door is at a height of 25 cm from the lake bottom and is of width 100 cm and height 40 cm. When submerged there is no leakage of pressure of air from the cabin that remained with atmospheric pressure. Determine the hydrostatic force at the center of pressure of the door. If the driver rolled the glass pane a little to make the pressure inside and outside the car same, what will be the hydrostatic pressure at the new center of pressure of the door.
18. A concrete block 0.4 × 0.4 × 5 m of density 2300 kg/m$^3$ is lowered into salt water of density 1025 kg/m$^3$. Determine the tension in the crane rope when the block is completely immersed in water.
19. What is internal energy and enthalpy of a perfect gas? On what state quantity the specific values of internal energy and enthalpy depend on.
20. Define specific heat. Discuss two different ways of performing the heating process and obtain the relations for specific internal energy and specific enthalpy of a perfect gas.
21. Define specific heat under constant volume and specific heat under constant pressure. Show that specific internal energy and specific enthalpy are functions of temperature alone.
22. For a perfect gas show that the specific heats are related to the gas constant $R$. Derive also expressions for the specific heats in terms of specific heat ratio and the gas constant.
23. What are different possible polytropic forms for pressure—specific volume relations? For a general polytropic law $pv^n$ constant obtain a relation for temperature of air as a function altitude.
24. The sea level values for pressure, temperature and density of air are $p_0$ = 101.325 kPa, $T_0$ = 288.5 K and $\rho_0$ = 1.225 kg/m$^3$. Determine the polytropic law. Assuming that this law is valid for the first kilo meter height, find the decrease in temperature for every 100 m.
25. For a closed system state the first law of thermodynamics. Discuss the special case of adiabatic process. What is the change in internal energy for such a system?
26. Describe Joule's apparatus to find mechanical equivalent of heat and demonstrate the irreversible Process using the first law of thermodynamics.
27. Discuss a reversible process and express the first law for a reversible process.

28. State the II Law of Thermodynamics as a statement on the preferred direction of a given heat transfer process. Discuss Clausius statement “It is not possible that at the end of a cycle of changes, heat has been transferred from a colder to a hotter body without providing some other effect”.
29. Define entropy that ascertains the proper direction of a given process in accordance to II law.
30. Derive a relation for change in entropy of a system in terms of initial and final states of thermodynamic variables pressure and temperature. For an isentropic process derive a relation for pressure ratio in terms of temperature or density ratios using specific heat ratio.

# Chapter 3
# Fluid Dynamics

**Abstract** The dynamic aspects of fluids, with the state variables, viz., pressure, temperature, velocity, density and their relations with energy, are considered in mass conservation and Newton's laws as first derived by Euler. Both Lagrangian and Eulerian formulations are discussed. Using thermodynamics laws and heat, the energy equation in flow is considered in addition to Euler's equations. The kinetic energy as well as internal energy in the flow is accounted. No viscous forces are considered in this chapter

**Keywords** State variables · Pressure · Velocity · Density · Temperature · Lagrangian and Eulerian formulation · Euler equation · Energy equation · Normal and shear stresses

In Chap. 2 we studied fluids at rest. Pressure, density and volume of the fluid are the state quantities that described the fluid at rest. When the fluid moves the velocity of the fluid is the main consideration. In early studies we were concerned with the flow of water in rivers and canals. In fluids at rest, the head played a significant role that defined the pressure. Fluids at a higher level from a given datum have more head energy or potential energy.

Engineering is essentially conversion of thermal energy to kinetic energy to give motion to mechanical parts and utilize their motion to move vehicles; on surface of land or sea or move as submarines under the sea or aircraft and space craft, run dynamos, transport fluids etc. We can site several examples:

1. Penstock pipes are used to take water at a high head from a Dam. The potential energy of the water behind the Dam retaining wall is transported through the penstocks to a hydraulic turbine; the water head energy is converted to kinetic energy and the water impinging on the turbine wheel rotates and drives a dynamo; see Fig. 3.1.
2. In the modern era of oil production from sea fields, long pipelines are used to transport oil over long distances, for example a pipeline linking Caspian Sea to Persian Gulf is shown in Fig. 3.2.

 
J.S. Rao, *Simulation Based Engineering in Fluid Flow Design*,
DOI 10.1007/978-3-319-46382-7_3

**Fig. 3.1** A Penstock carrying water from a dam to power house to run hydraulic turbines. http://www.nebrownstone.com/blog/wp-content/uploads/2015/08/DSC_0019-1024x576.jpg

**Fig. 3.2** Oil pipeline linking caspian sea to persian gulf. https://www.streetwisereports.com/images/piping.jpeg

3. A Heat Exchanger is commonly adopted to exchange heat from one fluid to another, e.g., hot gases from a Furnace are taken to a Plenum and made to pass through the plenum Shell containing Baffles and in this process exchange heat to

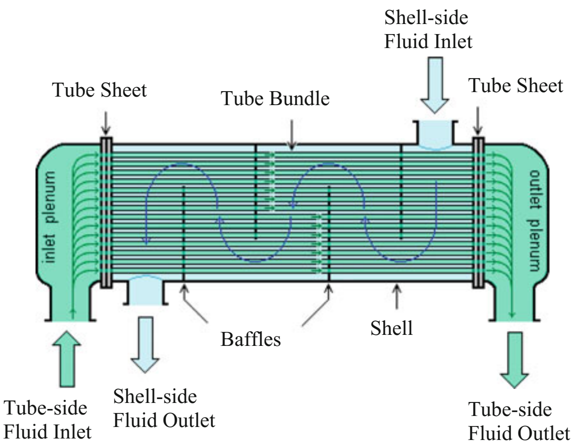


**Fig. 3.3** Heat exchanger between fluids

water flowing through a Tube Bundle to produce steam for a turbine in a power plant, see Fig. 3.3.

4. In the automobile internal combustion engine, air is sucked in during the suction stroke, compressed in the compression stroke, diesel oil injected which ignites at the highly compressed air, expands and provides the power to the engine crank shaft in the expansion stroke and in the last stroke the burnt gases are exhausted before the next four stroke cycle begins. The flow of air, combustion process etc. are all a part of liquid flow, see Fig. 3.4.
5. In an aircraft engine, air is sucked, compressed and taken to a combustion chamber where kerosene is burnt and the hot gases transfer the heat energy to a turbine which provides the power. These actions are performed in a pure

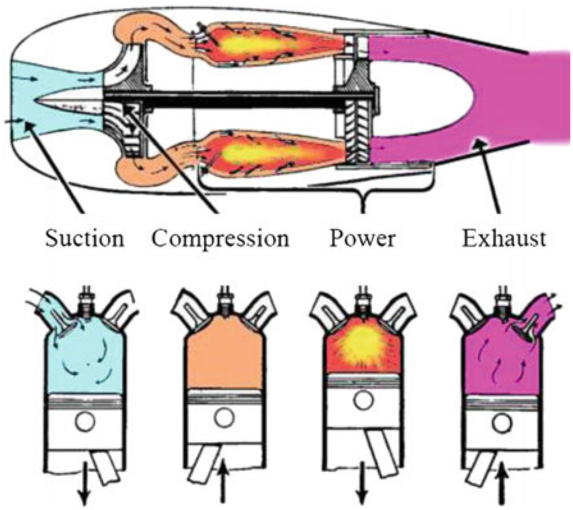


**Fig. 3.4** Internal combustion engines—aircraft turbomachine and automobile piston engines (flow in a diesel engine)

rotating machine with a compressor and turbine as compared to the piston reciprocating system in an internal combustion engine as compared in Fig. 3.4. The flow of air through the compressor stages, diffuser, combustion chamber and then through the turbine stages is all a complex flow.

## 3.1 Characteristics of Fluids

The principal difference in the mechanical behavior of fluids compared to solids is that when a shear stress is applied to a fluid it experiences a continuing and permanent distortion. Fluids offer no permanent resistance to shearing, and they have elastic properties only under direct compression: in contrast to solids which have all three elastic moduli, fluids possess a bulk modulus only. Thus, a fluid can be defined unambiguously as a material that deforms continuously and permanently under the application of a shearing stress, no matter how small.

The inability of fluids to resist shearing stress gives them their characteristic ability to change shape or to flow; their inability to support tension stress is an engineering assumption, but it is a well-justified assumption because such stresses, which depend on intermolecular cohesion, are usually extremely small.

Because fluids cannot support shearing stresses, it does not follow that such stresses are nonexistent in fluids. During the flow of real fluids, the shearing stresses assume an important role, and their prediction is a vital part of engineering work. Without flow, however, shearing stresses cannot exist, and compression stress or pressure is the only stress to be considered.

Fluid particles are made of molecules which consist of a given atomic structure. The molecular level behavior is of no importance to engineering applications and what we are interested is the behavior of the fluid as a continuum. Therefore the fluid is described in terms of macroscopic properties length scales of one micron or larger. A point in a fluid can be thought as the smallest possible fluid element whose macroscopic properties are not affected by the molecular level structure. The state quantities to describe the behavior of a liquid in motion are:

- Velocity $\mathbf{u}$—a vector with three components $u_x$, $u_y$ and $u_z$ at any given location.
- Pressure $p$—is a scalar as it is isotropic in nature. Pressure and fluid velocities are always calculated together. The pressure is used to determine the forces as we have done in Fluid Statics. Fluid velocities then show structure of flow.
- Density $\rho$—is also a scalar
- Temperature $T$—is also a scalar

The above properties may be thought of as averages taken over a fairly large number of molecules. Figure 3.5 shows one typical element in a flow of size $\delta x \times \delta y \times \delta z$ whose center is located at a position $(x, y, z)$ in the right-handed coordinate system shown. This element is labeled with its six vertices marked as $N$, $S$, $E$, $W$, $T$ and $B$.

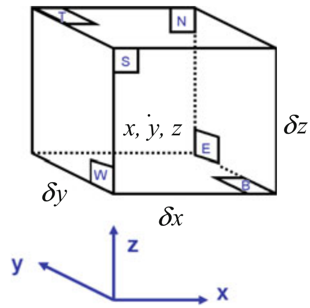


**Fig. 3.5** Fluid element $\delta x\ \delta y\ \delta z$ at $(x, y, z)$

*Lagrangian Description*: We can consider the fluid flow to comprise a large number of the finite sized fluid particles which have mass, momentum, internal energy, and other properties. For each of these particles, mathematical laws can then be written. Such a method of describing the Physics of Fluids is called Lagrangian description of fluid motion, see Fig. 3.6. An element thus taken is considered to move along with the flow on a path line.

*Eulerian Description*: Another way of depicting the fluid motion is the Eulerian description, in which a fixed control volume (or a cell) is taken through which the fluid streamlines pass. In the Eulerian description of fluid motion, we consider how flow properties change at the element that is fixed in space and time $(x, y, z, t)$, rather than following individual fluid particles, see Fig. 3.7.

In this book we will use Eulerian model for development of the Finite Volume method for solution of Fluid flow problems.

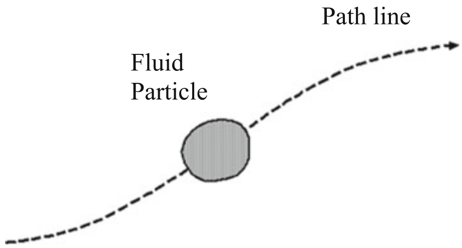


**Fig. 3.6** Lagrangian model for fluid motion

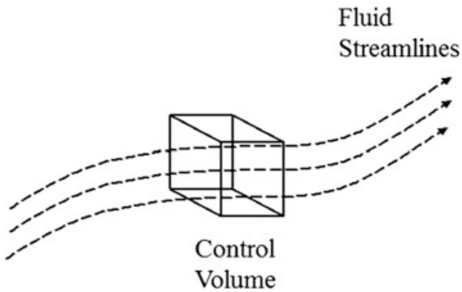


**Fig. 3.7** Eulerian Model for Fluid Motion

*Fluid Properties at faces*: We can use Taylor series expansion with only one term to determine the properties on the faces in Fig. 3.5 in terms of the properties at the center of the finite volume. Or we can consider that the variation of pressure in $x$ direction is given by the partial derivative of $p$ with respect to $x$, that is $\frac{\partial p}{\partial x}$. The net change over the distance $\frac{1}{2}\delta x$ is $\frac{\partial p}{\partial x}\frac{1}{2}\delta x$. The west face is in the negative direction of $x$ axis and the east face is in the direction of $x$ axis, therefore the pressure $p$ in the center ($x$, $y$, $z$) decreases on the west face and increases on the east face. The properties on the west and east faces for the pressure can be written as

$$\begin{aligned} p_w &= p - \frac{\partial p}{\partial x}\frac{1}{2}\delta x \\ p_E &= p + \frac{\partial p}{\partial x}\frac{1}{2}\delta x \end{aligned} \tag{3.1}$$

Similarly for south and north faces

$$\begin{aligned} p_S &= p - \frac{\partial p}{\partial y}\frac{1}{2}\delta y \\ p_N &= p + \frac{\partial p}{\partial y}\frac{1}{2}\delta y \end{aligned} \tag{3.2}$$

and for bottom and top surfaces

$$\begin{aligned} p_B &= p - \frac{\partial p}{\partial z}\frac{1}{2}\delta z \\ p_T &= p + \frac{\partial p}{\partial z}\frac{1}{2}\delta z \end{aligned} \tag{3.3}$$

In a similar way we can write the other state properties, viz., temperature, density and velocity on the six faces in Fig. 3.5.

## 3.2 Mass Balance

The mass of the gas has to be conserved; whatever enters from west, south and bottom surfaces should leave from the east, north and top surfaces (unless some mass is injected into this finite volume). Figure 3.8 shows the mass balance conditions.

The $x$ component of velocity on the west face is taken on similar lines in Eq. (3.1), which is

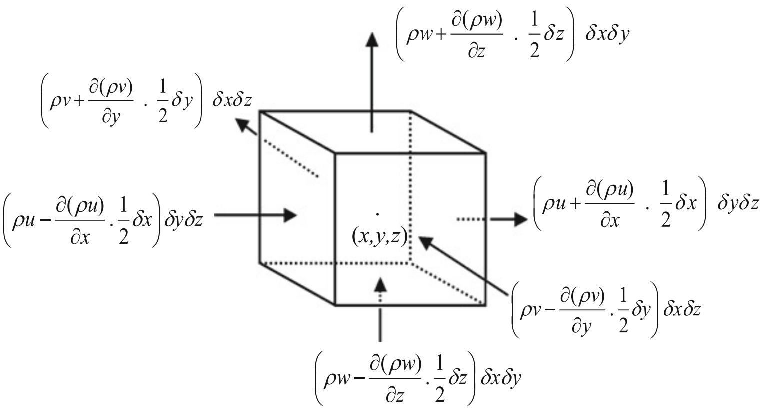


**Fig. 3.8** Mass balance conditions

$$u_W = u - \frac{\partial u}{\partial x}\frac{1}{2}\delta x. \tag{3.4}$$

The mass input from the west face is given by the $x$ component of velocity $u$ on the west face multiplied by the density $\rho$ times the area $\delta y\ \delta z$ of this face, which is

$$\begin{aligned} m_W &= \rho u_W \delta y \delta z \\ &= \left(\rho u - \frac{\partial(\rho u)}{\partial x}\frac{1}{2}\delta x\right)\delta y \delta z \end{aligned} \tag{3.5}$$

The mass output from the East Face is correspondingly given by

$$\begin{aligned} m_E &= \rho u_E \delta y \delta z \\ &= \left(\rho u + \frac{\partial(\rho u)}{\partial x}\frac{1}{2}\delta x\right)\delta y \delta z \end{aligned} \tag{3.6}$$

We can likewise determine the mass flow in from south and out through north and from bottom to top surfaces and they are indicated in Fig. 3.8.

The mass balance equation can now be written as: Rate of increase of mass in fluid element equals the net rate of flow of mass into element. The rate of increase is:

$$\frac{\partial}{\partial t}(\rho \delta x \delta y \delta z) = \frac{\partial \rho}{\partial t}\delta x \delta y \delta z \tag{3.7}$$

Now we can sum up all the inflows, outflows noted in Fig. 3.8 and the rate of increase above to give

$$\frac{\partial \rho}{\partial t} + \frac{\partial(\rho u)}{\partial x} + \frac{\partial(\rho v)}{\partial y} + \frac{\partial(\rho w)}{\partial z} = 0 \tag{3.8}$$

The above equation can be written in vector notation as

$$\frac{\partial \rho}{\partial t} + div(\rho \mathbf{u}) = 0$$

or (3.9)

$$\frac{\partial \rho}{\partial t} + \nabla \cdot (\rho \mathbf{u}) = 0$$

In Eq. (3.9) $\frac{\partial \rho}{\partial t}$ is the change in density; and Net flow of mass across boundaries gives the Convective term $div(\rho \mathbf{u}) = \frac{\partial(\rho u)}{\partial x} + \frac{\partial(\rho v)}{\partial y} + \frac{\partial(\rho w)}{\partial z}$.

For incompressible fluids, the density $\rho$ is constant, therefore $\frac{\partial \rho}{\partial t} = 0$ and the continuity Eq. (3.8) becomes

$$div\, \mathbf{u} = 0 \tag{3.10a}$$

The above can also be written in other forms, full notation or in tensor form.

$$\frac{\partial u}{\partial x} + \frac{\partial v}{\partial y} + \frac{\partial w}{\partial z} = 0 \tag{3.10b}$$

$$\frac{\partial u_i}{\partial x_i} = 0 \tag{3.10c}$$

Considering an incompressible flow, we have the equation that connects the three components of velocity $u$, $v$ and $w$. While this equation is not sufficient to solve a fluid dynamics problem, it imposes a condition between them. A simple case is one dimensional flow in the $x$ direction with $v$ and $w$ equal to zero. Then we get $\frac{du}{dx} = 0$, i.e., the velocity is constant.

## 3.3 Force Balance and Momentum Equations

Physics tells us that the fluid element under consideration should be in equilibrium at any instant of time; i.e., the forces, static and dynamic together should be in balance. The element is subjected to pressures on all six faces, i.e., forces (pressure multiplied by area) should be in equilibrium. In Hydrostatics the liquid is not in motion, here the element has a velocity, the rate of change of this with time, the acceleration and therefore Newton's laws would apply between the force and acceleration.

The forces on the element are of two types;

1. Normal to the plane or Direct and
2. In-plane or shear forces

The normal force arises out of the pressure on each surface and the shear forces arise out of shear stresses. Because of motion of liquid, there is a shear stress between the layers of the liquid. In Hydrostatics they are not present because the liquid is at rest. For fluids in motion, the shear stresses are off-diagonal elements in the stress tensor given by

$$[\tau] = \begin{bmatrix} & \tau_{xy} & \tau_{xz} \\ \tau_{yx} & & \tau_{yz} \\ \tau_{zx} & \tau_{zy} & \end{bmatrix} \tag{3.11}$$

The stress notation is same in solids or fluids. In (3.11) the first subscript denotes the outward normal of the surface and the second subscript the direction in which the shear stress acts on that surface. For equilibrium it is necessary that shear stress $\tau_{xy}$ acting in $y$ direction on surface with normal in $x$ direction is same that stress $\tau_{yx}$ which acts in $x$ direction on the surface with normal in $y$ direction. We follow the Taylor's series expansion as before to obtain the terms for the six faces in terms of the values at the center of this volume, viz., $(x, y, z)$. Figure 3.9 shows for simplicity the forces in the direction $x$ only arising out of these stresses on all six faces. Note that the normal pressure forces on west and east faces are only present for the $x$ direction.

Summing up all the forces in Fig. 3.9 we get the net force $F_x$ in $x$ direction on the element

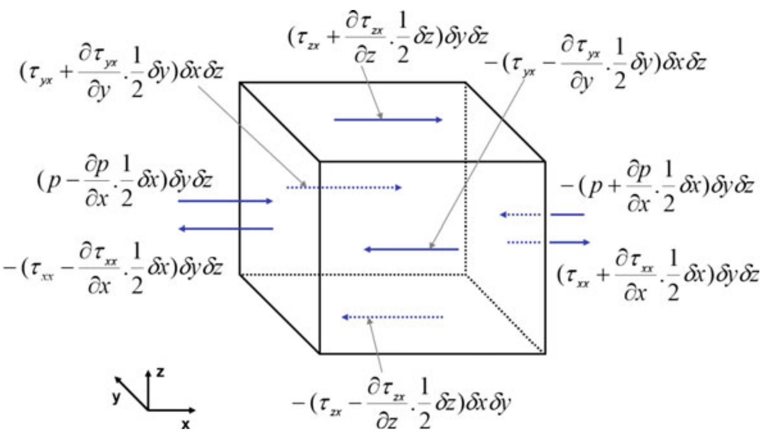


**Fig. 3.9** Forces in $x$ direction on the fluid element

$$F_x = \left( \frac{\partial(-p + \tau_{xx})}{\partial x} + \frac{\partial \tau_{yx}}{\partial y} + \frac{\partial \tau_{zx}}{\partial z} \right) \delta x \delta y \delta z \tag{3.12}$$

Now that we have the force field on the element, we can apply Newton's II law. We first note that $u$ varies not only with time but also in $x$, $y$, $z$ directions. Therefore we take the total derivative, denoted by $D$ of $u$ with time $t$

$$\frac{Du}{Dt} = \frac{\partial u}{\partial t} + \frac{\partial u}{\partial x}\frac{dx}{dt} + \frac{\partial u}{\partial y}\frac{dy}{dt} + \frac{\partial u}{\partial z}\frac{dz}{dt} \tag{3.13}$$

In general we define the total derivative of $\phi$ with time as

$$\frac{D\phi}{Dt} = \frac{\partial \phi}{\partial t} + \frac{\partial \phi}{\partial x}\frac{dx}{dt} + \frac{\partial \phi}{\partial y}\frac{dy}{dt} + \frac{\partial \phi}{\partial z}\frac{dz}{dt} \tag{3.14}$$

In addition to the forces given in Fig. 3.9, there may be other forces acting on the element, e.g., the body forces. Let all these forces be represented by $S_M$, a source term which has three components in $x$, $y$, $z$ directions given by $S_{Mx}$, $S_{My}$, $S_{Mz}$. Newton's law for $x$ direction is

$$\begin{aligned} \rho \delta x \delta y \delta z \frac{Du}{Dt} &= \left( \frac{\partial(-p + \tau_{xx})}{\partial x} + \frac{\partial \tau_{yx}}{\partial y} + \frac{\partial \tau_{zx}}{\partial z} + S_{Mx} \right) \delta x \delta y \delta z \Rightarrow \\ \rho \frac{Du}{Dt} &= \frac{\partial(-p + \tau_{xx})}{\partial x} + \frac{\partial \tau_{yx}}{\partial y} + \frac{\partial \tau_{zx}}{\partial z} + S_{Mx} \end{aligned} \tag{3.15}$$

Writing similarly for $y$ and $z$ directions, we get

$$\rho \frac{Dv}{Dt} = \frac{\partial \tau_{xy}}{\partial x} + \frac{\partial(-p + \tau_{yy})}{\partial y} + \frac{\partial \tau_{zy}}{\partial z} + S_{My} \tag{3.16}$$

$$\rho \frac{Dw}{Dt} = \frac{\partial \tau_{xz}}{\partial x} + \frac{\partial \tau_{yz}}{\partial y} + \frac{\partial(-p + \tau_{zz})}{\partial z} + S_{Mz} \tag{3.17}$$

The shear stress the source terms are ignored as an approximation; Replacing $\frac{dx}{dt} = u$, $\frac{dy}{dt} = v$ and $\frac{dz}{dt} = w$, we can now write all three Eqs. (3.15)–(3.17) as

$$\begin{aligned} \rho\left( \frac{\partial u}{\partial t} + u\frac{\partial u}{\partial x} + v\frac{\partial u}{\partial y} + w\frac{\partial u}{\partial z} \right) &= -\frac{\partial p}{\partial x} \\ \rho\left( \frac{\partial v}{\partial t} + u\frac{\partial v}{\partial x} + v\frac{\partial v}{\partial y} + w\frac{\partial v}{\partial z} \right) &= -\frac{\partial p}{\partial y} \\ \rho\left( \frac{\partial w}{\partial t} + u\frac{\partial w}{\partial x} + v\frac{\partial w}{\partial y} + w\frac{\partial w}{\partial z} \right) &= -\frac{\partial p}{\partial z} \end{aligned} \tag{3.18}$$

The above are Euler's momentum equations.

## 3.4 Energy Equation

In Sects. 3.2 and 3.3 we addressed two aspects, mass and force balance that led to one continuity equation and three momentum equations. The fluid flow as we discussed earlier has energy, its main purpose is to transport the energy and mass. Fluids carry heat, the main form of energy and therefore the temperature in the flow is an important aspect of the flow besides the state quantities of pressure, velocity and density that have been accounted for in the mass balance and momentum equations. Fluid flow has two forms of energy, the heat energy or internal energy, $i$, and the kinetic energy $\frac{1}{2}(u^2 + v^2 + w^2)$ by virtue of its motion. We usually treat the potential energy (gravitation) separately and include as a source term. The total energy in the flow can be written as

$$E = i + \frac{1}{2}\left(u^2 + v^2 + w^2\right) \tag{3.19}$$

According to First law of thermodynamics, the rate of change of energy of a fluid particle is equal to the rate of heat addition plus the rate of work done. The rate of increase in the energy is $\rho \frac{DE}{Dt}$.

*Work done in the flow*: The work done in the flow is the forces multiplied by velocity and considering first the $x$ direction as in Fig. 3.9; we can have the work done as shown in Fig. 3.10.

We can similarly write the work done by the forces in $y$ and $z$ directions. We add up all these works and divide by $\delta x \delta y \delta z$ to get the work done per unit volume by the surface stresses:

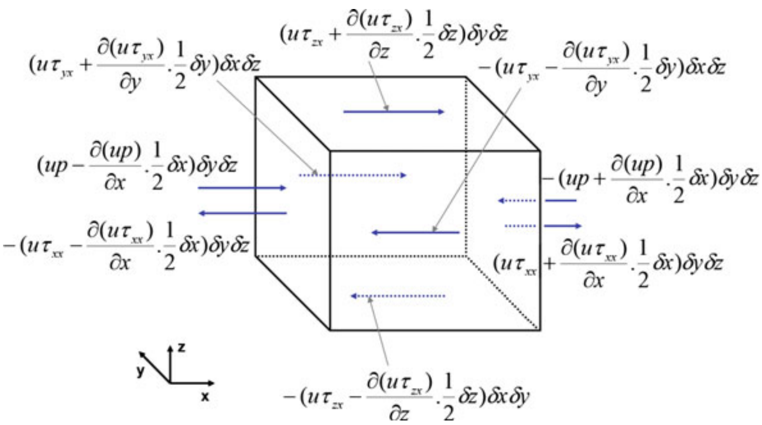


**Fig. 3.10** Work done by the forces in $x$ direction

$$\text{work done per unit volume} = -div(p\mathbf{u}) + \frac{\partial(u\tau_{xx})}{\partial x} + \frac{\partial(u\tau_{yx})}{\partial y} + \frac{\partial(u\tau_{zx})}{\partial z} + \frac{\partial(v\tau_{xy})}{\partial x} + \frac{\partial(v\tau_{yy})}{\partial y} + \frac{\partial(v\tau_{zy})}{\partial z} + \frac{\partial(w\tau_{xz})}{\partial x} + \frac{\partial(w\tau_{yz})}{\partial y} + \frac{\partial(u\tau_{zz})}{\partial z} \tag{3.20}$$

*Recap on Heat*:
Heat and energy are of same form and measured as Joules with 1 Joule (J) = 1 Watt second (Ws), = 1 Nm. Power is rate of heat measured in Watts, 1 W = 1 J/s = 1 Nm/s. A more convenient unit is 1000 W or 1 kW.

Heat flux $\boldsymbol{q}$ kW/m$^2$ rate of heat or power conducted into a control volume through a given surface. It is a vector with three components $q_x$, $q_y$ and $q_z$.

Heat capacity $C$ is the measure of the heat energy required to increase the temperature of an object by a certain temperature interval. Heat capacity is an extensive property because its value is proportional to the amount of material in the object; for example, a bathtub of water has a greater heat capacity than a cup of water.

Heat capacity is usually expressed in units of J/°K. For instance, one could write that the gasoline in a 55-gallon drum has an average heat capacity of 347 $\frac{\text{kJ}}{^\circ\text{K}}$.

Specific heat of a material, $c$ is a measure of heat energy required to increase temperature of a unit mass by a certain temperature interval and is expressed $\frac{\text{kW hr}}{\text{kg}\,^\circ\text{C}}$.

The specific heat is typically measured under constant pressure and denoted $c_p$. However, fluids are typically also measured at constant volume denoted $c_v$. Measurements under constant pressure produces greater values than those at constant volume because work must be performed in the former.

Thermal conductivity, $k$, of a material is its ability to conduct heat. It is used primarily in Fourier's law for heat conduction. It is defined as the quantity of heat, $Q$, transmitted in time $t$ through a thickness $L$, in a direction normal to a surface of area $A$, due to a temperature difference $\Delta T$, under steady state conditions and when the heat transfer is dependent only on the temperature gradient. $k$ = heat flow rate × distance/(area × temperature difference). The units are

$$k = \frac{Q}{t} \times \frac{L}{A \times \Delta T} = \frac{\frac{\text{kWhr}}{\text{hr}} \times \text{m}}{\text{m}^2 \times {}^\circ\text{C}} = \frac{\text{kW}}{\text{m}^\circ\text{C}}.$$

Alternately, it can be thought of as a flux of heat (energy per unit area per unit time) divided by a temperature gradient (temperature difference per unit length). The units are

$$k = \frac{Q}{A \times t} \times \frac{L}{\Delta T} = \frac{\frac{\text{kWhr}}{\text{hr}} \times \text{m}}{\text{m}^2 \times {}^\circ\text{C}} = \frac{\text{kW}}{\text{m}^\circ\text{C}}.$$

Thermal diffusivity of a material $\alpha$ is defined by $\alpha = \frac{k}{\rho c}$ where $\rho$ is the density of the material. The units are $\frac{\mathrm{m}^2}{\mathrm{hr}}$.

Heat transfer due to convection is described by Newton's Law of Cooling,

$$
\begin{aligned}
Q_{\text{convection}} &= hAdT \text{ Heat convected to surrounding fluid W} \\
h &= \text{Convective heat transfer coefficient W/m}^2\text{K} \\
A &= \text{Area of solid in contact with fluid m}^2 \\
dT &= \text{Temperature difference between solid and surrounding fluid} \left(T_s - T_f\right) \text{K}
\end{aligned}
$$

The rate of heat transferred to the surrounding fluid is proportional to the object's exposed area $A$, and the difference between the solid temperature $T_s$ and the mean fluid temperature $T_f$. Velocity of the fluid over solid is also a major contributing factor to enhance the rate of heat transfer.

Convection heat-transfer coefficient $h$ plays main role in heat transfer by convection. Heat transfer rates by convection are expressed in terms of $h$. It depends on following factors ($h$ is directly proportional to these factors):

1. Exposed area of solid
2. Temperature difference between solid and fluid
3. Fluid velocity

Whenever, the surface of a solid is in contact with a fluid medium, heat is transferred by convection currents. The convection process may be natural or free convection (buoyancy forces within the fluid) or it can be due to forced convection (pumping action). Convective heat transfer $q_h$ is expressed in kW/m$^2$. For convenience $q_h = h(T - T_\infty)$, $h$ is heat transfer coefficient $\frac{\mathrm{kW}}{\mathrm{m}^2\,{}^\circ\mathrm{C}}$ where $T_\infty$ is far field or ambient temperature.

*Energy flux due to heat conduction*: The rate of heat conducted into the control volume is expressed as heat flux $\boldsymbol{q}$ (kW/m$^2$). The heat flux vector $\boldsymbol{q}$ has three components, $q_x$, $q_y$, and $q_z$. As in Eqs. (3.1)–(3.3) we can write

$$
\begin{array}{ll}
q_{xw} = q_x - \frac{\partial q_x}{\partial x}\frac{1}{2}\delta x & q_{xw} = q_x + \frac{\partial q_x}{\partial x}\frac{1}{2}\delta x \\
q_{yS} = q_y - \frac{\partial q_y}{\partial y}\frac{1}{2}\delta y & q_{yN} = q_y + \frac{\partial q_y}{\partial y}\frac{1}{2}\delta y \\
q_{zB} = q_z - \frac{\partial q_z}{\partial z}\frac{1}{2}\delta z & q_{zT} = q_z + \frac{\partial q_z}{\partial z}\frac{1}{2}\delta z
\end{array}
\tag{3.21}
$$

The heat fluxes entering and leaving the finite volume are shown in Fig. 3.11. Summing all terms in Eq. (3.21) and dividing by $\delta x\ \delta y\ \delta z$ gives:

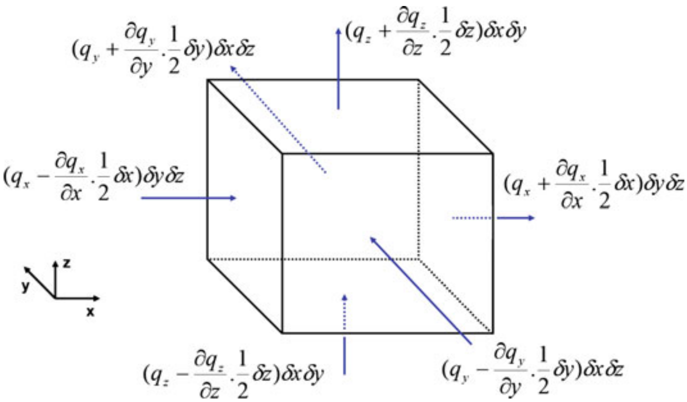


**Fig. 3.11** Heat flux in and out of the finite volume

$$\text{net rate of heat transfer of particle per unit volume} = -\frac{\partial q_x}{\partial x} - \frac{\partial q_y}{\partial y} - \frac{\partial q_z}{\partial z} = -div\,\mathbf{q} \tag{3.22}$$

The heat flux $\boldsymbol{q}$ is related to local temperature gradient and according to Fourier's law this is:

$$q_x = -k\frac{\partial T}{\partial x} \quad q_y = -k\frac{\partial T}{\partial y} \quad q_z = -k\frac{\partial T}{\partial z} \tag{3.23}$$

where $k$ is the thermal conductivity (kW/m/K). In vector form the above is

$$\mathbf{q} = -k\,grad\,T \tag{3.24}$$

$$\text{Note} : grad\phi = \nabla\phi = i\frac{\partial\phi}{\partial x} + j\frac{\partial\phi}{\partial y} + k\frac{\partial\phi}{\partial z}$$

Using (3.24) in (3.22) we get the net rate of heat transfer of the fluid particle per unit volume.

$$-div\,\mathbf{q} = div(k\,grad\,T) \tag{3.25}$$

According to I Law of Thermodynamics, setting the total derivative for the energy in a fluid particle equal to the previously derived work in (3.20) and energy flux terms in (3.25) and including any source term of energy $S_E$ (potential energy, sources due to heat production from chemical reactions, etc.) results in the following energy equation:

$$\rho\frac{DE}{Dt} = -div(p\mathbf{u}) + \left[\frac{\partial(u\tau_{xx})}{\partial x} + \frac{\partial(u\tau_{yx})}{\partial y} + \frac{\partial(u\tau_{zx})}{\partial z} + \frac{\partial(v\tau_{xy})}{\partial x} + \frac{\partial(v\tau_{yy})}{\partial y} + \frac{\partial(v\tau_{zy})}{\partial z} + \frac{\partial(w\tau_{xz})}{\partial x} + \frac{\partial(w\tau_{yz})}{\partial y} + \frac{\partial(w\tau_{zz})}{\partial z}\right] + div(k\,grad\,T) + S_E \tag{3.26}$$

## 3.5 Kinetic Energy

The kinetic energy of the fluid is by virtue of its mass and velocity. Separately, we can derive a conservation equation for the kinetic energy of the fluid. Multiply the $u$-momentum equation by $u$, the $v$-momentum equation by $v$, and the $w$-momentum equation by $w$ and add the results to get the equation for the kinetic energy:

$$\rho\frac{D[\frac{1}{2}(u^2+v^2+w^2)]}{Dt} = -\mathbf{u}.grad\,p + u\left(\frac{\partial\tau_{xx}}{\partial x} + \frac{\partial\tau_{yx}}{\partial y} + \frac{\partial\tau_{zx}}{\partial z}\right) + v\left(\frac{\partial\tau_{xy}}{\partial x} + \frac{\partial\tau_{yy}}{\partial y} + \frac{\partial\tau_{zy}}{\partial z}\right) + w\left(\frac{\partial\tau_{xz}}{\partial x} + \frac{\partial\tau_{yz}}{\partial y} + \frac{\partial\tau_{zz}}{\partial z}\right) + \mathbf{u}.\mathbf{S}_M \tag{3.27}$$

## 3.6 Internal Energy

Expanding the energy Eq. (3.26)

$$\rho\frac{DE}{Dt} = -p\,div(\mathbf{u}) + \tau_{xx}\frac{\partial u}{\partial x} + \tau_{yx}\frac{\partial u}{\partial y} + \tau_{zx}\frac{\partial u}{\partial z} + u\left[\frac{\partial\tau_{xx}}{\partial x} + \frac{\partial\tau_{yx}}{\partial y} + \frac{\partial\tau_{zx}}{\partial z}\right] + \tau_{xy}\frac{\partial v}{\partial x} + \tau_{yy}\frac{\partial v}{\partial y} + \tau_{zy}\frac{\partial v}{\partial z} + v\left[\frac{\partial\tau_{xy}}{\partial x} + \frac{\partial\tau_{yy}}{\partial y} + \frac{\partial\tau_{zy}}{\partial z}\right] + \tau_{xz}\frac{\partial w}{\partial x} + \tau_{yz}\frac{\partial w}{\partial y} + \tau_{zz}\frac{\partial w}{\partial z} + w\left[\frac{\partial\tau_{xz}}{\partial x} + \frac{\partial\tau_{yz}}{\partial y} + \frac{\partial\tau_{zz}}{\partial z}\right] + div(k\,grad\,T) + S_E \tag{3.26a}$$

The kinetic energy in Eq. (3.27) is subtracted from the energy Eq. (3.26a) that leaves the internal energy in the flow.

$$
\begin{aligned}
\rho\frac{Di}{Dt} =& -p\,div(\mathbf{u}) + \tau_{xx}\frac{\partial u}{\partial x} + \tau_{yx}\frac{\partial u}{\partial y} + \tau_{zx}\frac{\partial u}{\partial z} + u\left[\frac{\partial \tau_{xx}}{\partial x} + \frac{\partial \tau_{yx}}{\partial y} + \frac{\partial \tau_{zx}}{\partial z}\right] + \\
& + \tau_{xy}\frac{\partial v}{\partial x} + \tau_{yy}\frac{\partial v}{\partial y} + \tau_{zy}\frac{\partial v}{\partial z} + v\left[\frac{\partial \tau_{xy}}{\partial x} + \frac{\partial \tau_{yy}}{\partial y} + \frac{\partial \tau_{zy}}{\partial z}\right] + \\
& + \tau_{xz}\frac{\partial w}{\partial x} + \tau_{yz}\frac{\partial w}{\partial y} + \tau_{zz}\frac{\partial w}{\partial z} + w\left[\frac{\partial \tau_{xz}}{\partial x} + \frac{\partial \tau_{yz}}{\partial y} + \frac{\partial \tau_{zz}}{\partial z}\right] + div(k\ grad\ T) + S_E - \\
& \left[\begin{aligned} & -\mathbf{u}.grad\ p + u\left(\frac{\partial \tau_{xx}}{\partial x} + \frac{\partial \tau_{yx}}{\partial y} + \frac{\partial \tau_{zx}}{\partial z}\right) \\ & + v\left(\frac{\partial \tau_{xy}}{\partial x} + \frac{\partial \tau_{yy}}{\partial y} + \frac{\partial \tau_{zy}}{\partial z}\right) + w\left(\frac{\partial \tau_{xz}}{\partial x} + \frac{\partial \tau_{yz}}{\partial y} + \frac{\partial \tau_{zz}}{\partial z}\right) + \mathbf{u}.\mathbf{S}_M \end{aligned}\right] = \\
=& -p\ div\ \mathbf{u} + \left[\tau_{xx}\frac{\partial u}{\partial x} + \tau_{yx}\frac{\partial u}{\partial y} + \tau_{zx}\frac{\partial u}{\partial z} + \tau_{xy}\frac{\partial v}{\partial x}\right. \\
& \left. + \tau_{yy}\frac{\partial v}{\partial y} + \tau_{zy}\frac{\partial v}{\partial z} + \tau_{xz}\frac{\partial w}{\partial x} + \tau_{yz}\frac{\partial w}{\partial y} + \tau_{zz}\frac{\partial u}{\partial z}\right] \\
& + div(k\ grad\ T) + S_i
\end{aligned} \tag{3.28}
$$

## 3.7 Shear Stresses

The shear stresses are proportional to the linear deformations; the proportionality constant is isotropic (first) dynamic viscosity $\mu$ for the linear deformations (in this case shear). i.e.,

$$\tau_{xy} = \mu\left(\frac{\partial u}{\partial y} + \frac{\partial v}{\partial x}\right) \\ \ldots \tag{3.29}$$

For volumetric deformations, (normal stress components) a second viscosity $\lambda = -\frac{2}{3}\mu$ is used, i.e.,

$$\tau_{xx} = \mu\left(\frac{\partial u}{\partial x} + \frac{\partial u}{\partial x}\right) - \frac{2}{3}\mu\left(\frac{\partial u}{\partial x} + \frac{\partial v}{\partial y} + \frac{\partial w}{\partial z}\right) \\ \ldots \tag{3.30}$$

The stress tensor is given in (3.31) below.

$$\boldsymbol{\tau} = \begin{pmatrix} \tau_{xx} & \tau_{xy} & \tau_{xz} \\ \tau_{yx} & \tau_{yy} & \tau_{yz} \\ \tau_{zx} & \tau_{zy} & \tau_{zz} \end{pmatrix}$$
$$= \begin{pmatrix} 2\mu\frac{\partial u}{\partial x} - \frac{2}{3}\mu\, div\,\mathbf{u} & \mu\left(\frac{\partial u}{\partial y} + \frac{\partial v}{\partial x}\right) & \mu\left(\frac{\partial u}{\partial z} + \frac{\partial w}{\partial x}\right) \\ \mu\left(\frac{\partial u}{\partial y} + \frac{\partial v}{\partial x}\right) & 2\mu\frac{\partial v}{\partial y} - \frac{2}{3}\mu\, div\,\mathbf{u} & \mu\left(\frac{\partial v}{\partial z} + \frac{\partial w}{\partial y}\right) \\ \mu\left(\frac{\partial u}{\partial z} + \frac{\partial w}{\partial x}\right) & \mu\left(\frac{\partial v}{\partial z} + \frac{\partial w}{\partial y}\right) & 2\mu\frac{\partial w}{\partial z} - \frac{2}{3}\mu\, div\,\mathbf{u} \end{pmatrix} \tag{3.31}$$

Substituting for these stresses in (3.28) we get the internal energy equation as

$$\frac{\partial(\rho\, i)}{\partial t} + div(\rho\, i\,\mathbf{u}) = -p\, div\,\mathbf{u} + div(k\, grad\, T) + \Phi + S_i \tag{3.32}$$

In the above $\Phi$ is the viscous dissipation term.

$$\Phi = \mu\left\{2\left[\left(\frac{\partial u}{\partial x}\right)^2 + \left(\frac{\partial v}{\partial y}\right)^2 + \left(\frac{\partial w}{\partial z}\right)^2\right] + \left(\frac{\partial u}{\partial y} + \frac{\partial v}{\partial x}\right)^2 + \left(\frac{\partial u}{\partial z} + \frac{\partial w}{\partial x}\right)^2 + \left(\frac{\partial v}{\partial z} + \frac{\partial w}{\partial y}\right)^2\right\} - \frac{2}{3}\mu(div\,\mathbf{u})^2 \tag{3.33}$$

This term is always positive and describes the conversion of mechanical energy to heat. Note that for incompressible fluids $div\,\mathbf{u} = 0$.

## 3.8 Equations of Motion

Fluid motion is described by five partial differential equations for mass (3.9), momentum (3.18) and internal energy (3.32). Amongst the unknowns are four thermodynamic variables: $\rho$, $p$, $i$, and $T$, besides $u$, $v$ and $w$. We will assume thermodynamic equilibrium, i.e. that the time it takes for a fluid particle to adjust to new conditions is short relative to the timescale of the flow. There are seven unknowns and five equations of motion. We add two more equations of state using the two state variables $\rho$ and $T$: $p = p(\rho, T)$ and $i = i(\rho, T)$. For a perfect gas, these relations become:

$$p = \rho RT \text{ and } i = C_v T \tag{3.34}$$

At low speeds when Mach number is less than 0.2, the fluids can be considered incompressible. Then there is no linkage between the energy Eq. (3.26), and the mass and momentum Eqs. (3.9) and (3.18). In such a case we need to solve for energy equation separately if the problem involves heat transfer.

## 3.9 Summary of Fluid Flow Equations

$$\text{Mass}: \frac{\partial \rho}{\partial t} + div(\rho\,\mathbf{u}) = 0 \tag{3.9}$$

$$\begin{aligned}
x - \text{momentum}: \frac{\partial(\rho u)}{\partial t} + div(\rho u\,\mathbf{u}) &= -\frac{\partial p}{\partial x} + div(\mu\, grad\, u) + S_{Mx} \\
y - \text{momentum}: \frac{\partial(\rho v)}{\partial t} + div(\rho v\,\mathbf{u}) &= -\frac{\partial p}{\partial y} + div(\mu\, grad\, v) + S_{My} \\
z - \text{momentum}: \frac{\partial(\rho w)}{\partial t} + div(\rho w\,\mathbf{u}) &= -\frac{\partial p}{\partial z} + div(\mu\, grad\, w) + S_{Mz}
\end{aligned} \tag{3.18}$$

$$\text{Internal energy}: \frac{\partial(\rho i)}{\partial t} + div(\rho i\,\mathbf{u}) = -p\, div\mathbf{u} + div(k\, grad\, T) + \Phi + S_i \tag{3.32}$$

$$\begin{aligned}
&\text{Equations of state}: p = p(\rho, T) \text{ and } i = i(\rho, T) \\
&\text{e.g. for perfectgas}: p = \rho RT \text{ and } i = C_v T
\end{aligned} \tag{3.34}$$

We can express the above equations in integral form by using Gauss' divergence theorem that relates the flow (flux) of a vector field **a** through a surface $S$ to the behavior of the vector field inside the surface region $V$. It states that the outward flux of a vector field through a closed surface is equal to the volume integral of the divergence over the region inside the surface, i.e., the sum of all sources minus the sum of all sinks gives the net flow out of a region (Fig. 3.12).

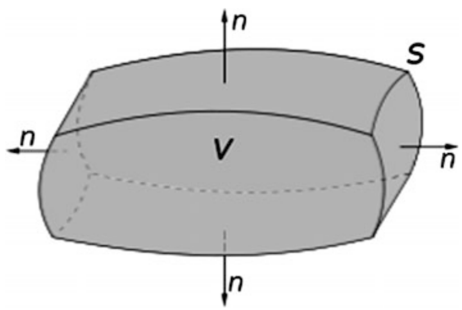


**Fig. 3.12** Region $V$ bounded by the surface $S$ with the surface normal n

If **n** is the normal

$$\int_{CV} div\,\mathbf{a}\,dV = \int_{A} \mathbf{n}\cdot\mathbf{a}\,dA \tag{3.35}$$

The above relation helps us in formulating the finite volume method by integrating the differential Eqs. (3.9), (3.18) and (3.32). This then leads to the following general conservation equation in integral form:

$$\frac{\partial}{\partial t}\left(\int_{CV}\rho\varphi\,dV\right) + \int_{A}\mathbf{n}\cdot(\rho\varphi\,\mathbf{u})\,dA = \int_{A}\mathbf{n}\cdot(\Gamma\,grad\,\varphi)\,dA + \int_{CV}S_{\varphi}\,dV \tag{3.36}$$

| Rate of Increase of $\phi$ | Net rate of Decrease of $\phi$ due To convection Across boundaries | Net rate of Increase of $\phi$ due To diffusion Across boundaries | Net rate of Creation of $\phi$ |
|---|---|---|---|

This is the actual form of the conservation equations solved by finite volume based CFD programs to calculate the flow pattern and associated scalar fields.

## Exercises 3

3.1 If the flow is non-viscous give the state quantities required to describe the flow. What do you understand by Lagrangian description of flow?

3.2 How did Euler describe the flow using a stationary control volume?

3.3 What are the state variables in a flow? Which of them are vectors and which are scalars?

3.4 What is a continuity equation for a flow? What does it give in Euler formulation? What can you solve from this equation?

3.5 Reduce the mass balance equation to a one dimensional flow and for steady state conditions show that the velocity is constant.

3.6 Derive force balance (momentum balance) equations for a three dimensional flow. What state variables in the flow are involved in these equations? Can we solve a flow problem using mass and momentum balance equations? If not why?

3.7 Discuss heat energy in a flow. What are internal and kinetic energies? Discuss the energy equation for a flow.

3.8 Euler's equations deal with the state variables: three components of velocity, pressure, density, temperature and internal energy total 7 in all. What are the seven equations to determine these quantities?

# Chapter 4
# Finite Volume Method—Diffusion Problems

**Abstract** This chapter is concerned with pure diffusion problems treated by finite volume methods, stepping stone for modern SBES and HPC approach. Only one dimensional case is considered in detail that keeps the formulation simple enabling the solutions by conventional methods.

**Keywords** One dimensional diffusion · Cell · Cramer's rule · Analytical method · Diffusion with source term · Diffusion with convection

There are five partial differential equations that define the physics of the flow besides the state equations. From (3.9), (3.18) and (3.32) we find they are all similar with several commonalities amongst them. Therefore we use a general conservative form with a variable $\phi$ representing these variables and write all these five equations in the form

$$\frac{\partial(\rho\phi)}{\partial t} + div(\rho\,\phi\,\mathbf{u}) = div(\Gamma grad\,\phi) + S_\phi \tag{4.1}$$

As we identified before, Eq. (4.1) can be stated in language: The sum of rate of increase of $\phi$ of the fluid element $\frac{\partial(\rho\phi)}{\partial t}$ and the net rate of flow of $\phi$ out of the fluid element $div(\rho\,\phi\,\mathbf{u})$ equals the sum of the rate of increase of $\phi$ due to diffusion $div(\Gamma grad\,\phi)$ and the rate of increase of $\phi$ due to sources $S_\phi$. This equation is the *transport equation* of the property $\phi$ representing the respective state variable. The first term on the left-hand side is the rate of the increase $\phi$ of the fluid element and the second term on the left-hand side is concerned with the net flow of the property $\phi$ across the boundaries and therefore a convective term. The right-hand side has two terms, the rate of the increase $\phi$ due to diffusion with the coefficient of diffusion $\Gamma$. It may be noted that terms in (3.9), (3.18) and (3.32) that do not fall in line with Eq. (4.1) are hidden in the source term, e.g., $\frac{\partial p}{\partial x}$.



J.S. Rao, *Simulation Based Engineering in Fluid Flow Design*,
DOI 10.1007/978-3-319-46382-7_4

| Rate of increase of $\phi$ of fluid element $\frac{\partial(\rho\phi)}{\partial t}$ | + | Net rate of flow of $\phi$ out of the fluid element $div(\rho\phi\mathbf{u})$ | = | Rate of increase of $\phi$ due to diffusion $div(\Gamma\ grad\ \phi)$ | + | Rate of increase of $\phi$ due to sources $S_\phi$ |
|---|---|---|---|---|---|---|

In the internal energy Eq. (3.32), $i$ can be replaced by temperature $T$ with the help of equations of state in (3.34). Equation (4.1) thus can be considered as representative equation for the mass conservation Eq. (3.9), three momentum equations in (3.18) and the internal energy Eq. (3.32). The mass conservation Eq. (3.9) is expressed in the form (4.1) as follows.

$$\begin{aligned} \frac{\partial\rho}{\partial t} + div(\rho\,\mathbf{u}) &= 0 \\ \frac{\partial(\rho\phi)}{\partial t} + div(\rho\phi\,\mathbf{u}) &= div(\Gamma grad\,\phi) + S_\varphi \\ &\Rightarrow \phi = 1; \Gamma = 0 \end{aligned} \tag{4.2}$$

Similarly $x$ momentum equation,

$$\begin{aligned} \frac{\partial(\rho u)}{\partial t} + div(\rho\,u\,\mathbf{u}) &= -\frac{\partial p}{\partial x} + div(\mu\,grad\,u) + S_{Mx} \\ \frac{\partial(\rho\phi)}{\partial t} + div(\rho\,\phi\,\mathbf{u}) &= div(\Gamma grad\,\phi) + S_\phi \\ &\Rightarrow \phi = u; \Gamma = \mu \end{aligned} \tag{4.3}$$

and the rest.

In this text we restrict ourselves for steady state flow, which means the time dependent terms are made zero. Then we have Convection Diffusion Flow equations as follows:

$$\text{Mass}: \quad div(\rho\,\mathbf{u}) = 0 \tag{4.4}$$

$$\begin{aligned} x - \text{momentum}: &\quad div(\rho u\mathbf{u}) = -\tfrac{\partial p}{\partial x} + div(\mu\,grad\,u) + S_{Mx} \\ y - \text{momentum}: &\quad div(\rho v\mathbf{u}) = -\tfrac{\partial p}{\partial y} + div(\mu\,grad\,v) + S_{My} \\ z - \text{momentum}: &\quad div(\rho w\mathbf{u}) = -\tfrac{\partial p}{\partial z} + div(\mu\,grad\,w) + S_{Mz} \end{aligned} \tag{4.5}$$

$$\text{Internal energy}: \quad div(\rho\,i\,\mathbf{u}) = -p\,div\,\mathbf{u} + div(k\,grad\,T) + \Phi + S_i \tag{4.6}$$

The general transport equation for Convection Diffusion then is

$$div(\rho\phi\mathbf{u}) = div(\Gamma\,grad\,\phi) + S_\phi \tag{4.7}$$

To explain convection and diffusion more clearly we can imagine $\phi$ to represent some dye made up of little particles suspended in the fluid. The convective term (or advective term) is transport of this dye $\phi$ due to the fluid motion; it will move around according to the velocity of the fluid around it. The diffusive term makes the dye spread out, whether or not the fluid is moving. So in fluid flow if we move along at the same velocity as the fluid we will find a small spot of dye initially becoming more and more blurred over time.

## 4.1 Diffusion Problem

Heat is the only source of energy in this universe produced by nuclear reactions in stars, e.g., our Sun. This energy from the Sun reaches the earth and is used in one form or other. Over millennia this energy is stored under earth in the form of fossil fuels. We began tapping this energy from coal first and then oil. These energy sources are used to develop reciprocating steam engines, steam turbines, internal combustion engines and then gas turbines. The heat energy is transported by fluids that can be converted to kinetic energy in steam engines or turbines and gas turbines. The fluids are restricted to flow in the designed paths as in a cylinder of an internal combustion engine or in the nozzles and diffusers of turbines. Thus all engine parts are subjected to heat and the solids transmit or conduct heat raising the temperatures and temperature gradients that lead to thermal strain and stress. The machine elements are all designed to withstand these stresses. The heat conducted within a solid body is conduction or it is called diffusion without convection. Here we will learn basic principles of one-dimensional diffusion in both closed form by direct integration and by numerical method, Finite Volume Method.

The closed form solutions in general fail for practical engineering because of intricate geometries of the flow paths. Therefore, we have developed approximate methods which now become redundant with the advent of high performance computing. Here we concentrate on finite volume method that leads to practical engineering problems.

In absence of convection, i.e., flow, pure diffusion can take place, e.g., heat conduction in a body; then Eq. (4.7) is

$$div(\Gamma grad\,\phi) + S_\phi = 0 \tag{4.8}$$

Restricting the flow to be one-dimensional in the $x$ direction, the above simplifies to

$$\frac{d}{dx}\left(\Gamma\frac{d\phi}{dx}\right) + S = 0 \tag{4.9}$$

Figure 4.1 shows a one-dimensional diffusion problem between the boundaries A to B where the property $\phi$ is kept constant at $\phi_A$ on boundary A and $\phi_B$ on boundary B. AB is divided into several finite volumes or cells along AB; a typical finite volume is at nodal point P with the boundaries placed midway between adjacent nodes as shown.

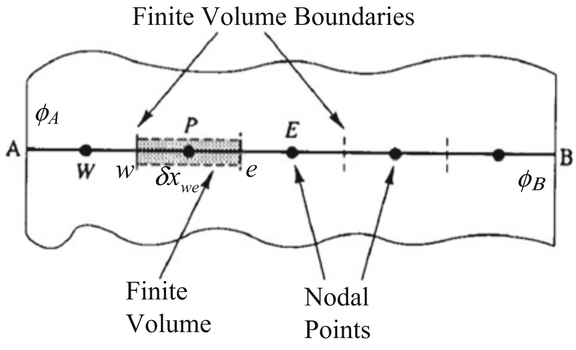


**Fig. 4.1** One-dimensional diffusion

For the cell shown at the node $P$, we have two nodes $W$ to the west and $E$ to the East. As in the notation adopted in Fig. 3.5, the west side is denoted $w$ and the east side $e$ (for one dimensional flow in $x$ direction). In a similar manner to that adopted before, the distance between $W$ and $P$ is denoted by $\delta x_{WP}$ and between $P$ and $E$ by $\delta x_{PE}$. Similarly, the distance between the face $w$ and $P$ is denoted by $\delta x_{wP}$ and between $P$ and $e$ by $\delta x_{Pe}$. The width of the cell is $\Delta x = \delta x_{we}$. Figure 4.2 gives a close-up view of the cell at nodal point $P$.

Integrating (4.9)

$$\begin{gathered}\int_{\Delta V} \frac{d}{dx}\left(\Gamma \frac{d\phi}{dx}\right) dV + \int_{\Delta V} S dV = 0 \\ \Rightarrow \\ \left(\Gamma A \frac{d\phi}{dx}\right)_e - \left(\Gamma A \frac{d\phi}{dx}\right)_w + \bar{S}\Delta V = 0\end{gathered} \tag{4.10}$$

where $A$ is the cross-sectional area of the finite volume face, $\Delta V$ is the volume and $\bar{S}$ is the average of the source over the finite volume. Equation (4.10) is essentially a balance equation stating that the diffusive flux leaving the east face minus the diffusive flux entering the west face is equal to the generation of the flux $\phi$.

If there is no source term, Eq. (4.10) reduces to

$$\left(\Gamma A \frac{d\phi}{dx}\right)_e - \left(\Gamma A \frac{d\phi}{dx}\right)_w = 0 \tag{4.11}$$

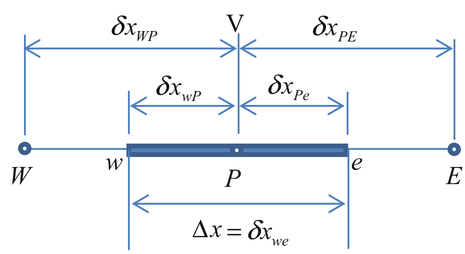


**Fig. 4.2** One-dimensional cell at node $P$

This is the simplest diffusion problem. We will introduce the Finite Volume method of solution to solve this problem. Equation (4.11) is discretized by linearization taking the diffusive coefficient $\Gamma$ at the east and west faces in terms of the nodal values as follows:

$$\begin{aligned}\Gamma_e &= \frac{1}{2}(\Gamma_P + \Gamma_E)\\ \Gamma_w &= \frac{1}{2}(\Gamma_W + \Gamma_P)\end{aligned} \tag{4.12}$$

Now the diffusive terms become

$$\begin{aligned}\left(\Gamma A \frac{d\phi}{dx}\right)_e &= \Gamma_e A_e \frac{\phi_E - \phi_P}{\delta x_{PE}}\\ \left(\Gamma A \frac{d\phi}{dx}\right)_w &= \Gamma_w A_w \frac{\phi_P - \phi_W}{\delta x_{WP}}\end{aligned} \tag{4.13}$$

Substituting (4.13) in (4.11)

$$\begin{aligned}&\Gamma_e A_e \tfrac{\phi_E - \phi_P}{\delta x_{PE}} - \Gamma_w A_w \tfrac{\phi_P - \phi_W}{\delta x_{WP}} = 0 \Rightarrow\\ &\left(\tfrac{\Gamma_e}{\delta x_{PE}} A_e + \tfrac{\Gamma_w}{\delta x_{WP}} A_w\right)\phi_P = \left(\tfrac{\Gamma_w}{\delta x_{WP}} A_w\right)\phi_W + \left(\tfrac{\Gamma_e}{\delta x_{PE}} A_e\right)\phi_E\end{aligned} \tag{4.14}$$

We can simplify the above as

$$a_P\phi_P = a_w\phi_W + a_e\phi_E \tag{4.15}$$

where

$$\begin{aligned}a_E &= \frac{\Gamma_e}{\delta x_{PE}} A_e\\ a_W &= \frac{\Gamma_w}{\delta x_{WP}} A_w\\ a_P &= a_W + a_E\end{aligned} \tag{4.16}$$

Equation (4.15) is the discretized equation for the node *P*. We can set up such equations for each of the nodes in the model. At the finite volume cells on the left and right boundaries Eq. (4.16) is modified to incorporate the boundary conditions for $\phi$. We then derive the linear algebraic equations for the problem and solve them.

If the number of elements is less in number, say 3 or 4, we can perform the solution by hand; in real life problems, these numbers may be very large, then we go to computer codes.

Worked Example 4.1:
Consider an insulated rod 80 cm long with an area of cross-section 1 $cm^2$. The thermal conductivity of the rod is 1 kW/m/K. At the left end $A$ the temperature is maintained at 0 °C and at the right end it is 100 °C.

Using Finite Volume Method and few cells to enable a hand calculation solve this problem.

To be able to carry out the solution by hand let us divide the rod into four cells with nodes 1, 2, 3 and 4 as shown in Fig. 4.3. Each cell is of length 20 cm, so also the distance between the nodes.

Equation (4.14) in this case for a node $P$ is written with the variable $\phi$ replaced by temperature $T$ and the diffusivity coefficient $\Gamma$ by thermal conductivity.

$$\begin{gathered} a_P\phi_P = a_w\phi_W + a_e\phi_E \\ \left(\frac{k_e}{\delta x_{PE}}A_e + \frac{k_w}{\delta x_{WP}}A_w\right)T_P = \left(\frac{k_w}{\delta x_{WP}}A_w\right)T_W + \left(\frac{k_e}{\delta x_{PE}}A_e\right)T_E \end{gathered} \tag{4.17}$$

Since the rod is of uniform cross-section $A_e = A_w = A = 1 \times 10^{-4}$ $m^2$. Also the thermal conductivity of the bar is same all through, therefore $k_e = k_w = k$. Further in all cells $\delta x_{PE} = \delta x_{WP} = 0.1$ m. Equation (4.17) is therefore

$$10kAT_P = 5kAT_W + 5kAT_E \tag{4.18}$$

Nodes 1 and 4 are boundary cells and therefore will be different from (4.18). Equation (4.9) is

$$\frac{d}{dx}\left(k\frac{dT}{dx}\right) = 0 \tag{4.19}$$

Integrate Eq. (4.19) over the cell surrounding node 1; we have from (4.17)

$$\begin{aligned} &\left(\frac{k_e}{\delta x_{PE}}A_e + \frac{k_w}{\delta x_{WP}}A_w\right)T_P = \left(\frac{k_w}{\delta x_{WP}}A_w\right)T_W + \left(\frac{k_e}{\delta x_{PE}}A_e\right)T_E \Rightarrow \\ &\left(\frac{k}{\delta x}A + \frac{k}{\delta x/2}A\right)T_1 = \left(\frac{k}{\delta x/2}A\right)T_A + \left(\frac{k}{\delta x}A\right)T_2 \Rightarrow \\ &kA\frac{(T_1 - T_2)}{\delta x} + kA\frac{(T_1 - T_A)}{\delta x/2} = 0 \Rightarrow \\ &5kA(T_1 - T_2) + 10kA(T_1 - T_A) = 0 \end{aligned} \tag{4.20}$$

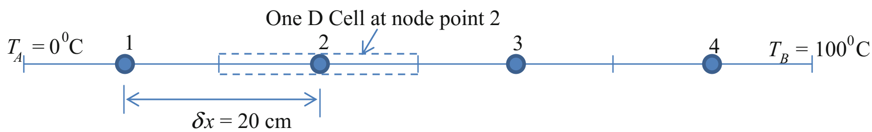


**Fig. 4.3** Four noded model with four cells

From (4.18) we can write the nodal equations for 2 and 3 as follows:

$$\begin{aligned} &\text{Node2:}\quad 10kAT_2 = 5kAT_1 + 5kAT_3 \\ &\text{Node3:}\quad 10kAT_3 = 5kAT_2 + 5kAT_4 \end{aligned} \tag{4.21}$$

For node 4

$$\begin{aligned} &\left(\frac{k_e}{\delta x_{PE}}A_e + \frac{k_w}{\delta x_{WP}}A_w\right)T_P = \left(\frac{k_w}{\delta x_{WP}}A_w\right)T_W + \left(\frac{k_e}{\delta x_{PE}}A_e\right)T_E \Rightarrow \\ &\left(\frac{k}{\delta x/2}A + \frac{k}{\delta x}A\right)T_4 = \left(\frac{k}{\delta x}A\right)T_3 + \left(\frac{k}{\delta x/2}A\right)T_B \Rightarrow \\ &kA\frac{(T_4 - T_3)}{\delta x} + kA\frac{(T_4 - T_B)}{\delta x/2} = 0 \Rightarrow \\ &5kA(T_4 - T_3) + 10kA(T_4 - T_B) = 0 \end{aligned} \tag{4.22}$$

Writing for all four nodes 1 to 4 and cancelling $kA$ we have

$$\begin{aligned} 15T_1 &= 10T_A + 5T_2 \\ 10T_2 &= 5T_1 + 5T_3 \\ 10T_3 &= 5T_2 + 5T_4 \\ 15T_4 &= 5T_3 + 10T_B \end{aligned} \tag{4.23}$$

We note that $k$ is not in the picture because the steady state solution of the rod will linearly vary from the imposed conditions, viz., $T_A = 0$ and $T_B = 100$ °C irrespective of the thermal conductivity. Here we are not concerned with the unsteady solution. Also we note that the area of cross-section does not enter because it is a uniform rod. If the rod is of variable cross-section then this will make itself present in the algebraic equations. It is also immaterial whether we convert the given boundary conditions to deg. K or not because $k$ is not involved. Besides one deg. K difference is same as one deg. C difference. Substituting for the values at both the ends $A$ and $B$, Eqs. (4.23) become

$$\begin{aligned} 15T_1 &= 5T_2 \\ 10T_2 &= 5T_1 + 5T_3 \\ 10T_3 &= 5T_2 + 5T_4 \\ 15T_4 &= 5T_3 + 1000 \end{aligned} \tag{4.24}$$

We can write the above algebraic equations in a matrix form

$$\begin{bmatrix} 15 & -5 & & \\ -5 & 10 & -5 & \\ & -5 & 10 & -5 \\ & & -5 & 15 \end{bmatrix} \begin{Bmatrix} T_1 \\ T_2 \\ T_3 \\ T_4 \end{Bmatrix} = \begin{Bmatrix} 0 \\ 0 \\ 0 \\ 1000 \end{Bmatrix} \tag{4.25}$$

The determinant value is

$$\Delta = \begin{vmatrix} 15 & -5 & & \\ -5 & 10 & -5 & \\ & -5 & 10 & -5 \\ & & -5 & 15 \end{vmatrix} = 15 \begin{vmatrix} 10 & -5 & \\ -5 & 10 & -5 \\ & -5 & 15 \end{vmatrix} + 5 \begin{vmatrix} -5 & -5 & \\ & 10 & -5 \\ & -5 & 15 \end{vmatrix}$$

$$\begin{aligned} \Delta &= 15[10(150-25)+5(-75)]+5[-5(150-25)] \\ &= 15[10\times 125-375]-25\times 125 = 13125-3125 \\ &= 10000 \end{aligned}$$

In order to apply Cramer's rule, we determine the following determinants

$$\Delta_1 = \begin{vmatrix} 0 & -5 & & \\ 0 & 10 & -5 & \\ 0 & -5 & 10 & -5 \\ 1000 & & -5 & 15 \end{vmatrix} = 5 \begin{vmatrix} 0 & -5 & 0 \\ 0 & 10 & -5 \\ 1000 & -5 & 15 \end{vmatrix} = 125000$$

$$\Delta_2 = \begin{vmatrix} 15 & 0 & & \\ -5 & 0 & -5 & \\ 0 & 0 & 10 & -5 \\ 0 & 1000 & -5 & 15 \end{vmatrix} = 15 \begin{vmatrix} 0 & -5 & 0 \\ 0 & 10 & -5 \\ 1000 & -5 & 15 \end{vmatrix} = 375000$$

$$\Delta_3 = \begin{vmatrix} 15 & -5 & 0 & \\ -5 & 10 & 0 & \\ 0 & -5 & 0 & -5 \\ 0 & & 1000 & 15 \end{vmatrix} = 15 \begin{vmatrix} 10 & 0 & 0 \\ -5 & 0 & -5 \\ 0 & 1000 & 15 \end{vmatrix} + 5 \begin{vmatrix} -5 & 0 & 0 \\ 0 & 0 & -5 \\ 0 & 1000 & 15 \end{vmatrix}$$
$$= 625000$$

$$\Delta_4 = \begin{vmatrix} 15 & -5 & 0 & 0 \\ -5 & 10 & -5 & 0 \\ 0 & -5 & 10 & 0 \\ 0 & & -5 & 1000 \end{vmatrix} = 15 \begin{vmatrix} 10 & -5 & 0 \\ -5 & 10 & 0 \\ 0 & -5 & 1000 \end{vmatrix} + 5 \begin{vmatrix} -5 & -5 & 0 \\ 0 & 10 & 0 \\ 0 & -5 & 1000 \end{vmatrix}$$
$$= 875000$$

We can now obtain the temperature field as follows:

$$
\begin{aligned}
T_A &= 0^\circ\,\mathrm{C}\,\text{given}\\
\mathrm{T}_1 &= \frac{125{,}000}{10{,}000} = 12.5^\circ\,\mathrm{C}\\
\mathrm{T}_2 &= \frac{375{,}000}{10{,}000} = 37.5^\circ\,\mathrm{C}\\
\mathrm{T}_3 &= \frac{625{,}000}{10{,}000} = 62.5^\circ\,\mathrm{C}\\
\mathrm{T}_4 &= \frac{875{,}000}{10{,}000} = 87.5^\circ\,\mathrm{C}\\
T_B &= 100^\circ\,\mathrm{C}\,\text{given}
\end{aligned}
$$

Solution of Eqs. (4.24) is given above following Cramer's rule. If the number of cells is large, we will use numerical methods and that's what commercial solvers use. In reality the solution for (4.24) can be obtained in much an easier hand calculation as given below.

$$
\begin{aligned}
&3T_1 = T_2\\
&5T_1 = T_3\\
&7T_1 = T_4\\
&21T_1 = 5T_1 + 200\\
&\Rightarrow T_1 = \tfrac{200}{16} = 12.5\\
&\ldots
\end{aligned}
$$

Worked Example 4.2:
For the problem in Worked Example 4.1, set up a second-order ordinary differential equation and verify the numerical solution using a closed form solution.

Equation (4.19) is a simple second-order ordinary differential equation and since $k$ is constant we can write it as

$$k\frac{d^2T}{dx^2} = 0 \tag{4.26}$$

Integrating twice

$$kT = c_1x + c_2 \tag{4.27}$$

At $x = 0$, $T$ is given to be 0 $\therefore c_2 = 0$. At $x = 8$ cm, $T$ is 100 °C. $\therefore c_1 = 12.5k$. This gives the exact solution

$$T = 12.5x \tag{4.28}$$

Actually we could have guessed the above solution that under steady state conditions the temperatures reached from diffusion will be linearly changing from 0 to 100 °C. The solution made agrees with the exact solution. Of course things will be different if we have the rod to be variable section (may not be even one dimensional); further the rod may be made of different materials whose thermal conductivity may be different. In that case the solution may not be easy for making a guess.

It is important to note that when the boundaries are maintained at specified temperatures, steady state conditions will reach after some elapsed time. What we have is a solution after the steady state is reached. The time to reach the steady and the manner it reaches is obtained by a transient solution with time $t$ included in the analysis, see Eq. (4.1). It is out of the scope of this text to deal with transient solution.

## 4.2 Diffusion with Source Term

Equation (4.9) gives one dimensional diffusion problem with a source term.

$$\frac{d}{dx}\left(\Gamma\frac{d\phi}{dx}\right) + S = 0 \tag{4.9}$$

Referring to Fig. 4.1 the one-dimensional diffusion problem between the boundaries A to B divided into several finite volumes or cells along AB. The close up view of the cell at nodal point $P$ is given in Fig. 4.2.

Integrating (4.9), we have written

$$\left(\Gamma A\frac{d\phi}{dx}\right)_e - \left(\Gamma A\frac{d\phi}{dx}\right)_w + \bar{S}\Delta V = 0 \tag{4.10}$$

where $A$ is the cross-sectional area of the finite volume face, $\Delta V$ is the volume and $\bar{S}$ is the average of the source over the finite volume.

When there is a source term, the area of cross-section becomes important and the problem becomes three dimensional, i.e., the temperature is not only a function of $x$ but also a function of $y$ and $z$. Here we will restrict our studies only to the one-dimensional case. This will be possible if we have a plate with infinite or sufficiently large dimensions in $y$ and $z$ directions compared to the thickness $L$ taken in the $x$ direction, see Fig. 4.4.

Worked Example 4.3:
Consider the plate in Fig. 4.4 with 80 cm thickness. The thermal conductivity is 1 kW/m/K. At the left end $A$ the temperature is maintained at 0 °C and at the right end it is 100 °C. This plate is now subjected to uniform heat generation $q$ = 1000 KW/m$^3$.

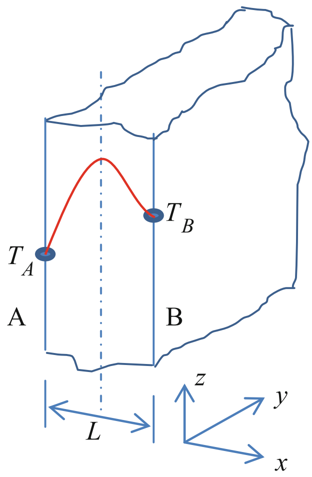


**Fig. 4.4** Plate with sufficiently long dimensions in $y$ and $z$ directions

Equation (4.9) with $k$ constant is now written as

$$k\frac{d^2T}{dx^2} + q = 0 \tag{4.29}$$

Integrating

$$\begin{aligned} k\frac{dT}{dx} + qx + C_1 &= 0 \\ kT + \frac{1}{2}qx^2 + C_1x + C_2 &= 0 \end{aligned} \tag{4.30}$$

Substituting $T = 0$ at $x = 0$, $C_2 = 0$. At $x = 0.8$ m $T = 100$, therefore

$$\begin{aligned} &100 \times 1000 + \tfrac{1}{2}1000000 \times 0.8^2 + 0.8C_1 = 0 \\ &420000 = -0.8C_1 \\ &\Rightarrow C_1 = -525000 \end{aligned} \tag{4.31}$$

Substituting in (4.30)

$$\begin{aligned} &1000T + \frac{1}{2} \times 1000000x^2 - 525000x = 0 \\ &T = 525x - 500x^2 \end{aligned} \tag{4.32}$$

The exact solution (4.28) for steady state case without any source and specified boundary conditions as in Worked Example 4.1 (the area of cross-section is immaterial in source free problem) is compared with the solution when there is a uniformly distributed heat generation source applied along the length as obtained in (4.32) with same specified boundary conditions. Being a symmetrical problem the peak temperature occurs at the middle of the plate.

Worked Example 4.4:
Solve Worked Example 4.3 by Finite Volume method.

Equation (4.10) is rewritten here

$$\int_{\Delta V} \frac{d}{dx}\left(k\frac{dT}{dx}\right)dV + \int_{\Delta V} q dV = 0 \tag{4.33}$$

The first term in the above is already dealt before. Within the control volume for the cell at $P$, see Fig. 4.2,

$$\left(kA\frac{dT}{dx}\right)_e - \left(kA\frac{dT}{dx}\right)_w + q\Delta V = 0 \tag{4.34}$$

$$\left\{k_eA\left(\frac{T_E - T_P}{\delta x}\right) - k_wA\left(\frac{T_P - T_W}{\delta x}\right)\right\} + qA\delta x = 0 \tag{4.35}$$

Now the temperature at node $P$ can be written in terms of the temperature on the east and west walls of the cell.

$$\left(\frac{k_eA}{\delta x} + \frac{k_wA}{\delta x}\right)T_P = \left(\frac{k_wA}{\delta x}\right)T_W + \left(\frac{k_eA}{\delta x}\right)T_E + qA\delta x = 0 \tag{4.36}$$

Since $k_e$ is equal to $k_w$ we can write the above as

$$\begin{aligned} 2\frac{kA}{\delta x}T_P &= \frac{kA}{\delta x}(T_W + T_E) + qA\delta x = 0 \\ 2\frac{T_P}{\delta x} &= \frac{(T_W + T_E)}{\delta x} + \frac{q}{k}\delta x = 0 \end{aligned} \tag{4.37}$$

This equation is valid for all the mid-nodes. For extreme left node 1, $T_W$ is replaced by $T_A$ and $\delta x$ is replaced by ½ $\delta x$. Then (4.35) for the extreme left node becomes

$$\left\{k_eA\left(\frac{T_E - T_P}{\delta x}\right) - k_AA\left(\frac{T_P - T_A}{\delta x/2}\right)\right\} + qA\delta x = 0 \tag{4.38}$$

Then

$$3\frac{T_P}{\delta x} = \frac{(2T_A + T_E)}{\delta x} + \frac{q}{k}\delta x \tag{4.39}$$

Similarly for the right extreme node

$$\left\{k_BA\left(\frac{T_B - T_P}{\delta x/2}\right) - k_WA\left(\frac{T_P - T_W}{\delta x}\right)\right\} + qA\delta x = 0 \tag{4.40}$$

Hence for the right end

$$3\frac{T_P}{\delta x} = \frac{(T_W + 2T_B)}{\delta x} + \frac{q}{k}\delta x \tag{4.41}$$

Writing all equations for nodes 1, 2, 3 and 4, we have

$$\begin{aligned} 3\tfrac{T_1}{\delta x} &= \tfrac{(2T_A + T_2)}{\delta x} + \tfrac{q}{k}\delta x \\ 2\tfrac{T_2}{\delta x} &= \tfrac{(T_1 + T_3)}{\delta x} + \tfrac{q}{k}\delta x = 0 \\ 2\tfrac{T_3}{\delta x} &= \tfrac{(T_2 + T_1)}{\delta x} + \tfrac{q}{k}\delta x = 0 \\ 3\tfrac{T_4}{\delta x} &= \tfrac{(T_3 + 2T_B)}{\delta x} + \tfrac{q}{k}\delta x \end{aligned} \tag{4.42}$$

When there is no heat generating source, i.e., $q = 0$, the above reduce to (4.23)

$$\begin{aligned} 3T_1 &= 2T_A + T_2 \\ 2T_2 &= T_1 + T_3 \\ 2T_3 &= T_2 + T_1 \\ 3T_4 &= T_3 + 2T_B \end{aligned} \tag{4.23a}$$

Dividing the plate into 4 one-dimensional elements similar to example 1, we first write the equation for the left extreme node from (4.39)

$$\begin{aligned} 3\tfrac{T_1}{0.2} &= \tfrac{(2T_A + T_2)}{0.2} + \tfrac{1000}{1} \times 0.2 \\ 3T_1 &= 2T_A + T_2 + 40 \end{aligned}$$

With $T_A = 0$

$$3T_1 = T_2 + 40 \tag{4.39a}$$

Then for the middle nodes 2 and 3

$$\begin{aligned} 2T_2 &= T_1 + T_3 + 40 \\ 2T_3 &= T_2 + T_4 + 40 \end{aligned} \tag{4.37a}$$

Finally for the rightmost element with node 4

$$3T_4 = T_3 + 2T_B + 40$$

Substitution for $T_B = 100$

$$3T_4 = T_3 + 240 \tag{4.41a}$$

For all the four nodes put together, we have

$$\begin{aligned} 3T_1 &= T_2 + 40 \\ 2T_2 &= T_1 + T_3 + 40 \\ 2T_3 &= T_2 + T_4 + 40 \\ 3T_4 &= T_3 + 240 \end{aligned} \tag{4.43}$$

In matrix form

$$\begin{bmatrix} 3 & -1 & & \\ -1 & 2 & -1 & \\ & -1 & 2 & -1 \\ & & -1 & 3 \end{bmatrix} \begin{Bmatrix} T_1 \\ T_2 \\ T_3 \\ T_4 \end{Bmatrix} = \begin{Bmatrix} 40 \\ 40 \\ 40 \\ 240 \end{Bmatrix} \tag{4.44}$$

The determinant value of the matrix is

$$\Delta = \begin{vmatrix} 3 & -1 & & \\ -1 & 2 & -1 & \\ & -1 & 2 & -1 \\ & & -1 & 3 \end{vmatrix} = 3\begin{vmatrix} 2 & -1 & \\ -1 & 2 & -1 \\ & -1 & 3 \end{vmatrix} + \begin{vmatrix} -1 & -1 & \\ & 2 & -1 \\ & -1 & 3 \end{vmatrix}$$

$$\begin{aligned} \Delta &= 3[2(6-1) + (-3)] + [-(5)] \\ &= 3[10-3] - 5 = 21 - 5 \\ &= 16 \end{aligned}$$

In order to apply Cramer's rule, we determine the following determinants

$$\Delta_1 = \begin{vmatrix} 40 & -1 & & \\ 40 & 2 & -1 & \\ 40 & -1 & 2 & -1 \\ 240 & & -1 & 3 \end{vmatrix} = 40\begin{vmatrix} 2 & -1 & \\ -1 & 2 & -1 \\ & -1 & 3 \end{vmatrix} + \begin{vmatrix} 40 & -1 & \\ 40 & 2 & -1 \\ 240 & -1 & 3 \end{vmatrix}$$
$$= 280 + 200 + 360 = 840$$

Therefore at $x = 0.1$, $T_1 = 840/16 = 52.5$ °C

$$\Delta_2 = \begin{vmatrix} 3 & 40 & & \\ -1 & 40 & -1 & \\ & 40 & 2 & -1 \\ & 240 & -1 & 3 \end{vmatrix} = 3\begin{vmatrix} 40 & -1 & \\ 40 & 2 & -1 \\ 240 & -1 & 3 \end{vmatrix} - 40\begin{vmatrix} -1 & -1 & \\ & 2 & -1 \\ & -1 & 3 \end{vmatrix}$$
$$= 3(200 + 360) - 40(-5) = 560 \times 3 + 200 = 1880$$

Therefore at $x = 0.3$, $T_2 = 1880/16 = 117.5$ °C

$$\Delta_3 = \begin{vmatrix} 3 & -1 & 40 & \\ -1 & 2 & 40 & \\ & -1 & 40 & -1 \\ & & 240 & 3 \end{vmatrix} = 3\begin{vmatrix} 2 & 40 & \\ -1 & 40 & -1 \\ & 240 & 3 \end{vmatrix} + \begin{vmatrix} -1 & 40 & \\ & 40 & -1 \\ & 240 & 3 \end{vmatrix} + 40\begin{vmatrix} -1 & 2 & \\ & -1 & -1 \\ & & 3 \end{vmatrix}$$
$$= 3(720 + 120) - 360 + 80 = 2520 - 360 + 80 = 2240$$

Hence at $x = 0.5$, $T_3 = 2240/16 = 140$ °C

$$\Delta_4 = \begin{vmatrix} 3 & -1 & & 40 \\ -1 & 2 & -1 & 40 \\ & -1 & 2 & 40 \\ & & -1 & 240 \end{vmatrix} = 3\begin{vmatrix} 2 & -1 & 40 \\ -1 & 2 & 40 \\ & -1 & 240 \end{vmatrix} + \begin{vmatrix} -1 & -1 & 40 \\ & 2 & 40 \\ & -1 & 240 \end{vmatrix} - 40\begin{vmatrix} -1 & 2 & -1 \\ & -1 & 2 \\ & & -1 \end{vmatrix}$$
$$= 3(1040 - 240 + 40) - 520 + 40 = 2520 - 520 + 40 = 2040$$

Therefore at $x = 0.7$, $T_4 = 2040/16 = 127.5$ °C.

This solution by FVM is also plotted in Fig. 4.5, together with exact solution given by Eq. (4.32). Table 4.1 gives the discrete values of the exact and FVM solutions.

The error at both the extreme nodes to the left and right is high compared to the middle two nodes. This is because of the approximation used in discretization at the extreme ends. If the number of elements is increased as that can be achieved in commercial codes, this error will rapidly decrease and the FVM solution converges to the exact solution.

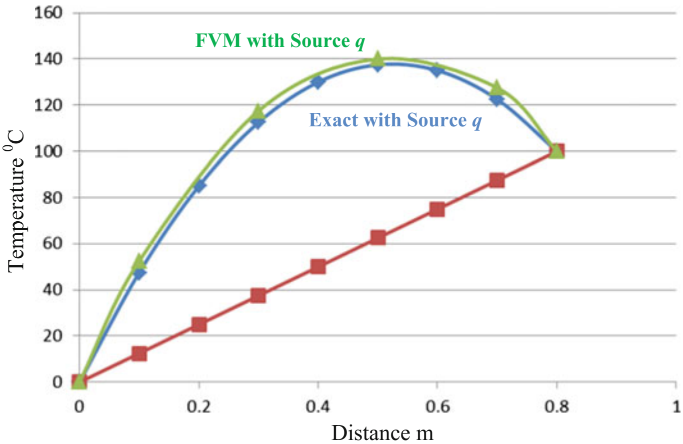


**Fig. 4.5** Diffusion with no source and with source

**Table 4.1** Exact and FVM solutions compared with source

| Distance | Exact | FVM | Error % |
|---|---|---|---|
| 0 | 0 | 0 | 0 |
| 0.1 | 47.5 | 52.5 | 10.5 |
| 0.3 | 112.5 | 117.5 | 4.44 |
| 0.5 | 137.5 | 140 | 1.82 |
| 0.7 | 122.5 | 127.5 | 4.08 |
| 0.8 | 100 | 100 | 0 |

The FVM solution is upper bound, i.e., the temperatures predicted are more than the exact solution as in Table 4.1. From Fig. 4.3 and Eq. (4.38), we note that at the left extreme end the discretization makes the left part of the cell shorter, though the heat input is taken over the full length $\delta x$. Therefore the temperature reached is more than the exact solution.

## 4.3 Diffusion with Convection

We discussed how fluids carry heat and give it to surrounding solids. The heat given to the solids is conducted within them to reach a steady state temperature condition. This problem is diffusion without considering how the heat is transferred to them from the flow. Here we will consider the diffusion problem with a source term arising out of heat transferred from flow. To facilitate this we will use a convective heat transfer coefficient. The heat can be transferred from a hot flow to the solid as in an engine/turbine or the hot body can be cooled by a cool air flow around the hot engine casing of a motor cycle (air cooled engine). We will restrict ourselves here to simple one-dimensional problem of cool air flowing around a hot body. The air-cooled engines use fins to have more surface area exposed to the cooler medium. A fin like this is a typical one dimensional problem of diffusion with a convective source term (negative in this case).

Worked Example 4.5:
Figure 4.6 shows an example of a cylindrical fin of length $L = 0.8$ m with uniform cross-sectional area $a$. The left end $A$ is maintained at 100 °C and the ambient temperature is 20 °C. The heat transfer coefficient is $h$. Determine the temperature distribution.

**Fig. 4.6** Cylindrical Fin with convective flow $T_{\text{Ambient}}$ and no heat flux

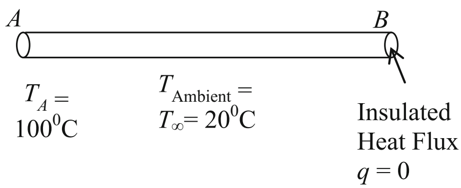

From Newton's law of cooling $q_h = h(T - T_\infty)$ and per unit length the sink source term is $S = -h \times P \times 1(T - T_\infty)$ where $P$ is the perimeter of the cross-section over which convection currents cool the fin. Substituting in Eq. (4.9)

$$\frac{d}{dx}\left(kA\frac{dT}{dx}\right) - hP(T - T_\infty) = 0 \tag{4.45}$$

Writing $n^2 = \frac{hP}{kA}$, the above equation is

$$\frac{d}{dx}\left(\frac{dT}{dx}\right) - n^2(T - T_\infty) = 0 \tag{4.46}$$

Integrating the above over a control volume

$$\int_{\Delta V} \frac{d}{dx}\left(\frac{dT}{dx}\right)dV - \int_{\Delta V} n^2(T - T_\infty)dV = 0 \tag{4.47}$$

In view of (4.11) for the first term and treating the source term is constant within the control volume, we have

$$\left[\left(A\frac{dT}{dx}\right)_e - \left(A\frac{dT}{dx}\right)_w\right] - \left[n^2(T_P - T_\infty)A\delta x\right] = 0 \tag{4.48}$$

Dividing by $A$, we have

$$\left[\left(\frac{dT}{dx}\right)_e - \left(\frac{dT}{dx}\right)_w\right] - \left[n^2(T_P - T_\infty)\delta x\right] = 0 \tag{4.49}$$

Let us adopt the same grid as in Fig. 4.3 given in Fig. 4.7.

Considering the mid nodes 2 and 3 and following linear approximation for the temperature gradient, Eq. (4.49) gives

$$\left[\left(\frac{T_E - T_P}{\delta x}\right) - \left(\frac{T_P - T_W}{\delta x}\right)\right] - \left[n^2(T_P - T_\infty)\delta x\right] = 0 \tag{4.50}$$

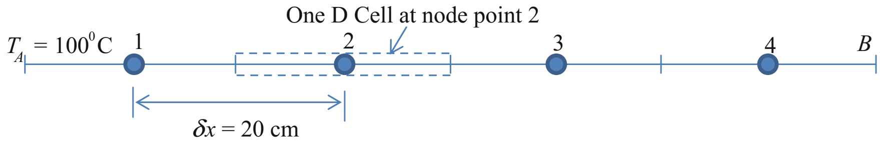


**Fig. 4.7** Diffusion with convective sink term

Separating terms and rewriting

$$\left(\frac{2}{\delta x}\right)T_P = \left(\frac{1}{\delta x}\right)T_W + \left(\frac{1}{\delta x}\right)T_E + n^2 T_\infty \delta x - n^2 T_P \delta x \tag{4.51}$$

For node 1

$$\left[\left(\frac{T_E - T_P}{\delta x}\right) - \left(\frac{T_P - T_A}{\delta x/2}\right)\right] - \left[n^2 (T_P - T_\infty)\delta x\right] = 0 \tag{4.52}$$

$$\left(\frac{3}{\delta x}\right)T_P = \left(\frac{1}{\delta x}\right)T_E + \left(\frac{2}{\delta x}\right)T_A + n^2 T_\infty \delta x - n^2 T_P \delta x \tag{4.53}$$

For node 4, the flux across the east boundary is zero

$$\left[0 - \left(\frac{T_P - T_W}{\delta x}\right)\right] - \left[n^2 (T_P - T_\infty)\delta x\right] = 0 \tag{4.54}$$

Therefore

$$\left(\frac{1}{\delta x}\right)T_P = \left(\frac{1}{\delta x}\right)T_W + n^2 T_\infty \delta x - n^2 T_P \delta x \tag{4.55}$$

Let $n^2$ = 20 $m^{-2}$, then, for node 1:

$$\begin{aligned} &\left(\frac{3}{\delta x}\right)T_1 = \left(\frac{1}{\delta x}\right)T_2 + \left(\frac{2}{\delta x}\right)T_A + 20T_\infty \delta x - 20T_1 \delta x \\ &3T_1 - T_2 = 200 + 20 \times 0.04 \times 20 - 20 \times 0.04 \times T_1 \\ &3.8T_1 - T_2 = 216 \end{aligned} \tag{4.56}$$

Node 2:

$$\begin{aligned} &\left(\frac{2}{\delta x}\right)T_2 = \left(\frac{1}{\delta x}\right)T_1 + \left(\frac{1}{\delta x}\right)T_3 + n^2 T_\infty \delta x - n^2 T_P \delta x \\ &-T_1 + 2.8T_2 - T_3 = 16 \end{aligned} \tag{4.57}$$

Node 3:

$$\begin{aligned} &\left(\frac{2}{\delta x}\right)T_3 = \left(\frac{1}{\delta x}\right)T_2 + \left(\frac{1}{\delta x}\right)T_4 + n^2 T_\infty \delta x - n^2 T_3 \delta x \\ &-T_2 + 2.8T_3 - T_4 = 16 \end{aligned} \tag{4.58}$$

Node 4:

$$\left(\frac{1}{\delta x}\right)T_4 = \left(\frac{1}{\delta x}\right)T_3 + n^2 T_\infty \delta x - n^2 T_4 \delta x$$
$$-T_3 + 1.8T_4 = 16 \tag{4.59}$$

Together for all the nodes

$$\begin{aligned} 3.8T_1 - T_2 &= 216 \\ -T_1 + 2.8T_2 - T_3 &= 16 \\ -T_2 + 2.8T_3 - T_4 &= 16 \\ -T_3 + 1.8T_4 &= 16 \end{aligned}$$

In matrix form

$$\begin{bmatrix} 3.8 & -1 & & \\ -1 & 2.8 & -1 & \\ & -1 & 2.8 & -1 \\ & & -1 & 1.8 \end{bmatrix} \begin{Bmatrix} T_1 \\ T_2 \\ T_3 \\ T_4 \end{Bmatrix} = \begin{Bmatrix} 216 \\ 16 \\ 16 \\ 16 \end{Bmatrix} \tag{4.60}$$

Solve:

$$\Delta = \begin{vmatrix} 3.8 & -1 & & \\ -1 & 2.8 & -1 & \\ & -1 & 2.8 & -1 \\ & & -1 & 1.8 \end{vmatrix} = 3.8 \begin{vmatrix} 2.8 & -1 & \\ -1 & 2.8 & -1 \\ & -1 & 1.8 \end{vmatrix} + \begin{vmatrix} -1 & -1 & \\ & 2.8 & -1 \\ & -1 & 1.8 \end{vmatrix}$$
$$= 3.8 \times 2.8(2.8 \times 1.8 - 1) + 3.8(-1.8) - (2.8 \times 1.8 - 1)$$
$$= 10.64 \times 4.04 - 6.84 - 4.04 = 42.9856 - 10.88 = 32.1056$$

$$\Delta_1 = \begin{vmatrix} 216 & -1 & & \\ 16 & 2.8 & -1 & \\ 16 & -1 & 2.8 & -1 \\ 16 & & -1 & 1.8 \end{vmatrix} = 216 \begin{vmatrix} 2.8 & -1 & \\ -1 & 2.8 & -1 \\ & -1 & 1.8 \end{vmatrix} + \begin{vmatrix} 16 & -1 & \\ 16 & 2.8 & -1 \\ 16 & -1 & 1.8 \end{vmatrix}$$
$$= 216 \times 2.8(2.8 \times 1.8 - 1) + 216(-1.8) + 16(2.8 \times 1.8 - 1) + (16 \times 1.8 + 16)$$
$$= 604.8 \times 4.04 - 388.8 - 16 \times 4.04 + 44.8 = 2443.392 - 388.8 + 64.64 + 44.8 = 2164.032$$

Therefore temperature $T_1$ = 2164.32/32.1056 = 67.4036 °C

$$\Delta_2 = \begin{vmatrix} 3.8 & 216 & & \\ -1 & 16 & -1 & \\ & 16 & 2.8 & -1 \\ & 16 & -1 & 1.8 \end{vmatrix} = 3.8\begin{vmatrix} 16 & -1 & \\ 16 & 2.8 & -1 \\ 16 & -1 & 1.8 \end{vmatrix} - 216\begin{vmatrix} -1 & -1 & \\ & 2.8 & -1 \\ & -1 & 1.8 \end{vmatrix}$$
$$= 3.8 \times 16(2.8 \times 1.8 - 1) + 3.8(16 \times 1.8 + 16) + 216(2.8 \times 1.8 - 1)$$
$$= 60.8 \times 4.04 + 318.592 + 872.64 = 1436.864$$

Therefore temperature $T_2$ = 1436.864/32.1056 = 44.7543 °C

$$\Delta_3 = \begin{vmatrix} 3.8 & -1 & 216 & \\ -1 & 2.8 & 16 & \\ & -1 & 16 & -1 \\ & & 16 & 1.8 \end{vmatrix} = 3.8\begin{vmatrix} 2.8 & 16 & \\ -1 & 16 & -1 \\ & 16 & 1.8 \end{vmatrix} + \begin{vmatrix} -1 & 16 & \\ & 16 & -1 \\ & 16 & 1.8 \end{vmatrix} + 216\begin{vmatrix} -1 & 2.8 & \\ & -1 & -1 \\ & 0 & 1.8 \end{vmatrix}$$
$$= 3.8 \times 2.8(16 \times 1.8 + 16) - 3.8 \times 16(-1.8) - (16 \times 1.8 + 16) + 216 \times 1.8$$
$$= 10.64 \times 44.8 + 109.44 - 44.8 + 388.8 = 930.112$$

Therefore temperature $T_3$ = 930.112/32.1056 = 28.9704 °C

$$\Delta_4 = \begin{vmatrix} 3.8 & -1 & & 216 \\ -1 & 2.8 & -1 & 16 \\ & -1 & 2.8 & 16 \\ & & -1 & 16 \end{vmatrix} = 3.8\begin{vmatrix} 2.8 & -1 & 16 \\ -1 & 2.8 & 16 \\ & -1 & 16 \end{vmatrix} + \begin{vmatrix} -1 & -1 & 16 \\ & 2.8 & 16 \\ & -1 & 16 \end{vmatrix} - 216\begin{vmatrix} -1 & 2.8 & -1 \\ & -1 & 2.8 \\ & 0 & -1 \end{vmatrix}$$
$$= 3.8 \times 2.8(2.8 \times 16 + 16) + 3.8(-16) - (2.8 \times 16 + 16) + 216$$
$$= 10.64 \times 60.8 - 60.8 - 60.8 + 216 = 741.312$$

Finally the temperature $T_4$ = 741.312/32.1056 = 23.0898 °C
Worked Example 4.6:
Solve Worked Example 4.5 by Exact Solution of the differential equation.:

$$\begin{aligned} &\frac{d}{dx}\left(\frac{dT}{dx}\right) - n^2(T - T_\infty) = 0 \\ &\Rightarrow \frac{d^2T}{dx^2} - n^2T = n^2T_\infty \\ &\Rightarrow \left(D^2 - n^2\right)T = n^2T_\infty \end{aligned} \tag{4.46a}$$

The auxiliary equation is

$$m^2 - n^2 = 0 \Rightarrow m = \pm n$$

The complimentary function is $Ae^{nx} + Be^{-nx}$ and particular integral is $T_\infty$, therefore the total solution is

$$\begin{aligned} T &= Ae^{nx} + Be^{-nx} + T_\infty \\ \frac{dT}{dx} &= n(Ae^{nx} + Be^{-nx}) \end{aligned} \tag{4.61}$$

At $x = 0$, $T = 100$ °C, therefore

$$\begin{aligned} T_A &= A + B + T_\infty \\ A + B &= T_A - T_\infty \end{aligned} \tag{4.62}$$

At $x = L$, $\frac{dT}{dx} = 0$ gives

$$\begin{aligned} &\frac{dT}{dx} = n(Ae^{nx} + Be^{-nx}) = 0 \Rightarrow \\ &n\left(Ae^{nL} - Be^{-nL}\right) = 0 \Rightarrow \\ &A = B\frac{e^{-nL}}{e^{nL}} \end{aligned} \tag{4.63}$$

Substituting for $A$ in (4.62) we get

$$\begin{aligned} &B\frac{e^{-nL}}{e^{nL}} + B = T_A - T_\infty \\ &\Rightarrow B\left(e^{-2nL} + 1\right) = T_A - T_\infty \\ &\Rightarrow B = \frac{T_A - T_\infty}{1 + e^{-2nL}} \end{aligned} \tag{4.64}$$

Therefore,

$$A = \frac{T_A - T_\infty}{1 + e^{-2nL}} e^{-2nL}$$

The solution can now be written as

$$T = \frac{T_A - T_\infty}{1 + e^{-2nL}} e^{-2nL} e^{nx} + \frac{T_A - T_\infty}{1 + e^{-2nL}} e^{-nx} + T_\infty \tag{4.65}$$

Using further $1 + e^{-2x} = \frac{e^x + e^{-x}}{e^x}$ and $\cosh x = \frac{1}{2}(e^x + e^{-x})$

$$T = \frac{T_A - T_\infty}{\frac{2\cosh nL}{e^{nL}}} e^{-2nL} e^{nx} + \frac{T_A - T_\infty}{\frac{2\cosh nL}{e^{nL}}} e^{-nx} + T_\infty \tag{4.66}$$

Simplifying, the exact solution

$$T = T_\infty + (T_A - T_\infty)\frac{\cosh[n(L-x)]}{\cosh(nL)} \tag{4.67}$$

In this case,

$$\begin{aligned} T &= 20 + 80\frac{\cosh[4.4721(0.8-x)]}{\cosh(3.577)} \\ &= 20 + \frac{80}{17.9097}\cosh[4.4721(0.8-x)] \\ &= 20 + 4.669\cosh[4.4721(0.8-x)] \end{aligned} \tag{4.68}$$

The Finite Volume Solution is compared with the above exact solution in Table 4.2 and Fig. 4.8. Within the approximation of discretization into four cells, we find that the agreement is good. By increasing the number of cells, the FV solution will converge to an exact solution.

**Table 4.2** Comparison of finite volume solution with exact solution 1-D diffusion with convection problem

| Distance | Exact | FVM | % Error |
|---|---|---|---|
| 0 | 100 | 100 | |
| 0.1 | 73.52642006 | 67.4036 | 8.33 |
| 0.3 | 42.09179525 | 44.7543 | −6.33 |
| 0.5 | 29.54038441 | 28.9704 | 1.93 |
| 0.7 | 25.14372597 | 23.0898 | 4.59 |
| 0.8 | 24.669 | | |

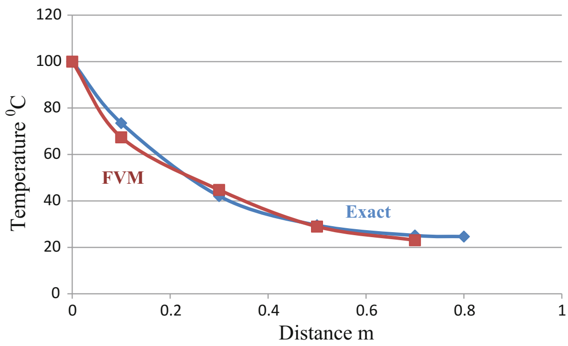


**Fig. 4.8** Comparison of finite volume solution with exact solution 1-D diffusion with convection problem

**Exercises 4**

[In problems 4.7–4.10 use finite volume method with number of one-dimensional cells that can solve by hand; say 2 to 4. Verify the numerical solution by closed form solutions where possible. Also where possible develop a computer program using any commercial codes available in your school.]

4.1 Show that all Euler's equations can be expressed by one transport equation for each thermodynamic variable.

4.2 What is a diffusion problem? Illustrate with an example.

4.3 For a steady state one dimensional heat conduction show that the temperature varies linearly along the chosen independent coordinate.

4.4 How does a source term affect the diffusion problem? Cite an example.

4.5 Illustrate a problem of diffusion in convective flow.

4.6 What are the advantages of finite volume method over closed form solution?

4.7 Determine the steady state rate of heat transfer per unit area through a 5.0 cm thick homogeneous slab with its faces maintained at uniform temperatures of 300 °C and $20^0$ C. $k$ for the material is 0.19 W/m/K.

4.8 The forced convective heat transfer coefficient for a hot fluid flowing over a cool surface at 15 °C is 250 W/m$^2$ °C. The fluid temperature upstream of the cool surface is 85 °C. What is the heat transfer rate per unit surface area from the fluid to the surface?

4.9 A home wall consists of 15 cm thick fiberglass whose $k = 0.004$ Wm$^2$-K between two sheets each 0.75 cm thick. The inner wall is exposed to 20 °C air and the fiberglass is covered by a sheetrock whose $k = 0.4$ Wm$^2$-K. On the outside the sheathing and shingles with $k = 0.15$ Wm$^2$-K cover the fiberglass as shown in figure. The air outside is −5 °C. Determine the temperature distribution in the wall with the assumption that the wall is semi-infinite in the height.

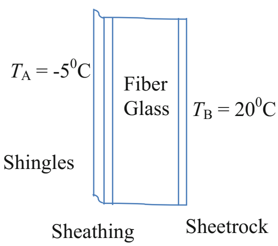


4.10 An aluminium rod 2.5 cm diameter and 8 cm long having $k$ equal to 200 W/m/K projects out from a wall maintained at 150 °C. Air at 30 °C flows by this rod with $h$ = 120 W/m$^2$K. Determine the tip temperature.

4.11 The rod in problem 4.10 has a variable cross-section with the diameter varying linearly from 2.5 to 4 cm over its length 8 cm. The temperatures at the left end and right end are specified at 150 and 250 °C. Determine the temperature distribution under adiabatic conditions. You can split the rod into a convenient number of uniform dia sections.

4.12 A 0.001 m thick conductive plane wall ($k$ = 120 W/m-K) separates two fluids left side $A$ and right side $B$. Fluid $A$ is at 100 °C and the heat transfer coefficient between the fluid and the wall is $h$ = 10 W/m$^2$-K, while fluid $B$ is at 0 °C with $h$ = 100 W/m$^2$-K. Determine the temperature distribution in the wall.

4.13 A freezer wall is similar to that of the problem 4.9 above. The wall separates the freezer air at $T_B = -10$ °C from air within the room at $T_A$ = 20 °C. The heat transfer coefficient between the freezer air and the inner wall of the freezer is $h_B$ = 10 W/m$^2$-K and the heat transfer coefficient between the room air and the outer wall of the freezer is $h_A$ = 10 W/m$^2$-K. The wall is composed of a 1.0 cm thick layer of fiberglass blanket sandwiched between two 5.0 mm sheets of stainless steel. The thermal conductivity of fiberglass and stainless steel are 0.06 and 15 W/m-K, respectively. The cross-sectional area of the wall can be taken as 1 m$^2$. Determine the net heat transfer rate of the freezer.

4.14 A composite wall is made of two materials ($A$ with $k_A$ = 0.8 W/m-K and $B$ with $k_B$ = 4 W/m-K), each has thickness $L$ = 10 mm. The surface of the wall $A$ at $x = 0$ is perfectly insulated. A very thin heater is placed between the insulation and material $A$; the heating element provides 4500 W/m$^2$ of heat. The surface of the wall at $x = 2L$ is exposed to a fluid at 300 K with heat transfer coefficient 100 W/m$^2$-K. Determine the temperature of the heating element and the temperature distribution through the wall.

# Chapter 5
# Finite Volume Method—Convection-Diffusion Problems

**Abstract** This chapter is an extension of the previous one on diffusion-convection. The treatment is again using one dimensional finite volume method and closed form solutions.

**Keywords** Convection-diffusion · Finite volume method

Fluid flow plays significant role in transporting heat and diffusing the same in the flow (also to the surrounding solid—heat transfer in both the liquid and solid simultaneously, called conjugate heat transfer; not considered here). The steady convection-diffusion problem (neglecting time dependent terms) can be obtained from the transport equation (4.7) for a general property $\phi$

$$div(\rho\phi\mathbf{u}) = div(\Gamma\ grad\ \phi) + S_{\varphi} \tag{5.1}$$

## 5.1 Steady State One-Dimensional Convection and Diffusion

Let us consider the case with no source terms and confining to one-dimensional problems as in Chap. 4, Eq. (5.1) is

$$\frac{d}{dx}(\rho u\phi) = \frac{d}{dx}(\Gamma\frac{d\phi}{dx}) \tag{5.2}$$

The continuity equation from (3.8) should also be satisfied, which for the one-dimensional steady flow reduces to

$$\frac{d(\rho u)}{dx} = 0 \tag{5.3}$$



J.S. Rao, *Simulation Based Engineering in Fluid Flow Design*,
DOI 10.1007/978-3-319-46382-7_5

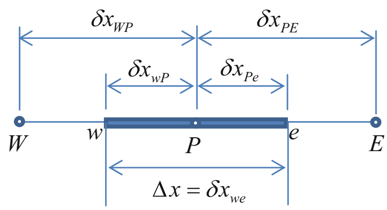


**Fig. 5.1** One dimensional control volume around node *P*

Figure 4.2 gives the one-dimensional control volume around node *P*, with the neighboring nodes *W* to the west and *E* to the east as shown in Fig. 5.1.

The right-hand side of Eq. (5.2) represents diffusive terms and the left-hand side the convective terms. Upon integration over the control volume, Eqs. (5.2) and (5.3) give

$$(\rho u A\phi)_e - (\rho u A\phi)_w = \left(\Gamma A\frac{d\phi}{dx}\right)_e - \left(\Gamma A\frac{d\phi}{dx}\right)_w \tag{5.4}$$

$$(\rho u A)_e - (\rho u A)_w = 0 \tag{5.5}$$

In the above $\rho u$ is the convective mass flux per unit area $F$ and $\frac{\Gamma}{\delta x}$ is the diffusion conductance $D$ at the faces of the cell, i.e.,

$$\begin{aligned} F &= \rho u \\ D &= \frac{\Gamma}{\delta x} \end{aligned} \tag{5.6}$$

The values of $F$ and $D$ at the west face $w$ and east face $e$ are

$$\begin{aligned} F_w &= (\rho u)_w \\ D_w &= \left(\frac{\Gamma}{\delta x}\right)_w \\ F_e &= (\rho u)_e \\ D_e &= \left(\frac{\Gamma}{\delta x}\right)_e \end{aligned} \tag{5.7}$$

For a uniform cell along the length, $A_e = A_w = A$, Eqs. (5.4) and (5.5) reduce to

$$\begin{aligned} (\rho u\phi)_e - (\rho u\phi)_w &= \left(\Gamma\frac{d\phi}{dx}\right)_e - \left(\Gamma\frac{d\phi}{dx}\right)_w \Rightarrow \\ F_e\phi_e - F_w\phi_w &= D_e(\phi_E - \phi_P) - D_W(\phi_P - \phi_W) \end{aligned} \tag{5.8}$$

$$\begin{aligned}(\rho u)_e - (\rho u)_w &= 0 \Rightarrow \\ F_e - F_w &= 0\end{aligned} \tag{5.9}$$

The diffusion problem in Eq. (4.9) for a uniform bar is given by an ordinary second order differential equation and is solvable to determine the two constants of integration by using the boundary values. In the case of convection it is a coupled problem with the velocity $u$ and the transport property $\phi$ as given in Eqs. (5.2) and (5.3). If we are able to determine $u$ in some manner we still need to calculate the transport property $\phi_e$ and $\phi_w$ at the faces $e$ and $w$, as required in (5.8). The simplest thing is to adapt a linear variation of the transport property between $W$ and $E$ of the cell in Fig. 5.1. We can then write the transport property values at $e$ and $w$ in terms of the nodal values at $W$, $P$ and $E$ as

$$\begin{aligned}\phi_e &= \frac{1}{2}(\phi_P + \phi_E) \\ \phi_w &= \frac{1}{2}(\phi_W + \phi_P)\end{aligned} \tag{5.10}$$

Equation (5.8) is now written for the nodal values of the transport property as

$$\frac{1}{2}F_e(\phi_P + \phi_E) - \frac{1}{2}F_w(\phi_W + \phi_P) = D_e(\phi_E - \phi_P) - D_W(\phi_P - \phi_W) \tag{5.11}$$

Rearranging the above in terms of nodal values of transport property

$$\begin{aligned}&\phi_p\left[\left(D_w - \tfrac{1}{2}F_w\right) + \left(D_e + \tfrac{1}{2}F_e\right)\right] = \phi_w\left(D_w + \tfrac{1}{2}F_w\right) + \phi_E\left(D_e - \tfrac{1}{2}F_e\right) \Rightarrow \\ &\phi_p\left[\left(D_w + \tfrac{1}{2}F_w\right) + \left(D_e - \tfrac{1}{2}F_e\right) + (F_e - F_w)\right] = \phi_w\left(D_w + \tfrac{1}{2}F_w\right) + \phi_E\left(D_e - \tfrac{1}{2}F_e\right)\end{aligned} \tag{5.12}$$

Rewriting

$$\begin{aligned}&a_P\phi_p = a_W\phi_W + a_E\phi_E \\ &\text{where} \\ &a_W = \left(D_w + \tfrac{1}{2}F_w\right) \\ &a_E = \left(D_e - \tfrac{1}{2}F_e\right) \\ &a_P = a_W + a_E + (F_e - F_w)\end{aligned} \tag{5.13}$$

The difference between the pure diffusion problem given in (4.17) and the above convection-diffusion problem of (5.13) is the presence of additional terms containing the convective mass flux per unit area $F = \rho u$.

### *5.1.1 Exact Solution for Convection-Diffusion Problem*

To satisfy Eq. (5.3), we notice $u$ is constant, therefore Eq. (5.2) becomes

$$\begin{gathered} \frac{d}{dx}(\rho u\phi) = \frac{d}{dx}\left(\Gamma\frac{d\phi}{dx}\right) \Rightarrow \\ \frac{d^2\phi}{dx^2} - \frac{\rho u}{\Gamma}\frac{d\phi}{dx} = 0 \end{gathered} \tag{5.14}$$

The auxiliary equation is

$$\left(D^2 - \frac{\rho u}{\Gamma}D\right)\phi = 0 \tag{5.15}$$

Then

$$\begin{gathered} \left(m^2 - \frac{\rho u}{\Gamma}m\right) = 0 \Rightarrow \\ m = 0 \quad \text{and} \quad m = \frac{\rho u}{\Gamma} \end{gathered} \tag{5.16}$$

$$\therefore \phi = A + Be^{\frac{\rho u}{\Gamma}x} \tag{5.17}$$

Let $\phi_0$ and $\phi_L$ be prescribed at $x = 0$ and $x = L$, then

$$\begin{gathered} A + B = \phi_0 \\ A + Be^{\frac{\rho u}{\Gamma}L} = \phi_L \end{gathered} \tag{5.18}$$

i.e.,

$$\begin{gathered} A + (\phi_0 - A)e^{\frac{\rho u}{\Gamma}L} = \phi_L \Rightarrow A\left(1 - e^{\frac{\rho u}{\Gamma}L}\right) = \phi_L - \phi_0 e^{\frac{\rho u}{\Gamma}L} \\ \therefore A = \frac{\phi_L - \phi_0 e^{\frac{\rho u}{\Gamma}L}}{\left(1 - e^{\frac{\rho u}{\Gamma}L}\right)} \end{gathered} \tag{5.19}$$

$$B = \phi_0 - \frac{\phi_L - \phi_0 e^{\frac{\rho u}{\Gamma}L}}{\left(1 - e^{\frac{\rho u}{\Gamma}L}\right)} \Rightarrow \frac{\phi_0 - \phi_L}{\left(1 - e^{\frac{\rho u}{\Gamma}L}\right)} \tag{5.20}$$

Therefore

$$\begin{gathered} \phi = \frac{\phi_L - \phi_0 e^{\frac{\rho u}{\Gamma}L}}{\left(1 - e^{\frac{\rho u}{\Gamma}L}\right)} + \frac{\phi_0 - \phi_L}{\left(1 - e^{\frac{\rho u}{\Gamma}L}\right)} e^{\frac{\rho u}{\Gamma}x} \Rightarrow \\ \phi\left(1 - e^{\frac{\rho u}{\Gamma}L}\right) = \phi_0\left(-e^{\frac{\rho u}{\Gamma}L} + e^{\frac{\rho u}{\Gamma}x}\right) + \phi_L\left(1 - e^{\frac{\rho u}{\Gamma}x}\right) \end{gathered} \tag{5.21}$$

$$\begin{gathered} \phi\left(1 - e^{\frac{\rho u}{\Gamma}L}\right) = \phi_0\left(-e^{\frac{\rho u}{\Gamma}L} - 1 + 1 + e^{\frac{\rho u}{\Gamma}x}\right) + \phi_L\left(1 - e^{\frac{\rho u}{\Gamma}x}\right) \\ \frac{(\phi - \phi_0)}{(\phi_L - \phi_0)} = \frac{\left(e^{\frac{\rho u}{\Gamma}x} - 1\right)}{\left(e^{\frac{\rho u}{\Gamma}L} - 1\right)} \end{gathered} \tag{5.22}$$

### *5.1.2 Finite Volume Method for Convection-Diffusion Problem*

Consider the one dimensional domain in Fig. 5.2 80 cm long in which the property $\phi$ is transported. $\phi_0 = 1$ at $x = 0$ and $\phi_L = 0$ at $x = 0.8$ m. $\rho = 1$ kg/m$^3$, $u = 0.1$ m/s and $\Gamma = 0.1$ kg/m/s; i.e., $\frac{\rho u}{\Gamma} = 1\,\text{m}^{-1}$.

The domain is discretized into 4 cells as shown with 4 nodes 1, 2, 3 and 4 with $\delta x = 0.2$ m. From Eq. (5.7)

$$F = \rho u = 0.1$$
$$D = \left(\frac{\Gamma}{\delta x}\right) = \frac{0.1}{0.2} = 0.5$$

First, we notice that Eq. (5.13) is valid for mid nodes, 2 and 3. Therefore

$$\begin{aligned} a_{W2,3} &= \left(D + \frac{1}{2}F\right) = 0.55 \\ a_{E2,3} &= \left(D - \frac{1}{2}F\right) = 0.45 \\ a_{P2,3} &= a_W + a_E + (F_e - F_w) = 1.0 \end{aligned} \tag{5.23}$$

Therefore for cells 2 and 3

$$\begin{aligned} a_P\phi_p &= a_W\phi_W + a_E\phi_E \\ \phi_2 &= 0.55\phi_1 + 0.45\phi_3 \\ \phi_3 &= 0.55\phi_2 + 0.45\phi_4 \end{aligned} \tag{5.24}$$

For end nodes 1 and 4, we have to develop appropriate relations. For cell 1, $\phi_w = \phi_A = 1$, we make an approximation in the convective flux term with $D_A = \frac{2\Gamma}{\delta x} = 2D$ at this boundary in Eq. (5.11) as

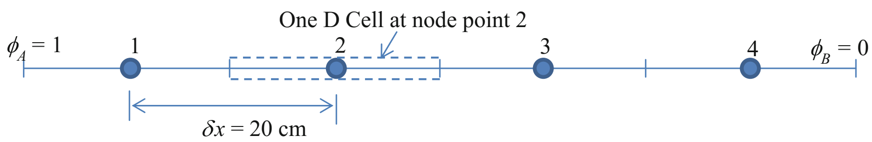


**Fig. 5.2** One dimensional convection-diffusion problem

$$\begin{aligned}
&\frac{1}{2}F_e(\phi_P + \phi_E) - \frac{1}{2}F_w(\phi_W + \phi_P) = D_e(\phi_E - \phi_P) - D_W(\phi_P - \phi_W) \Rightarrow \\
&\frac{1}{2}F_e(\phi_P + \phi_E) - F_A\phi_A = D_e(\phi_E - \phi_P) - D_A(\phi_P - \phi_A) \\
&0.05(\phi_1 + \phi_2) - 0.1 = 0.5(\phi_2 - \phi_1) - (\phi_1 - 1) = 0.5\phi_2 - 1.5\phi_1 + 1 \\
&1.55\phi_1 = 0.45\phi_2 + 1.1
\end{aligned} \tag{5.25}$$

Similarly for cell 4 with $D_B = \frac{2\Gamma}{\delta x} = 2D$

$$\begin{aligned}
&\frac{1}{2}F_e(\phi_P + \phi_E) - \frac{1}{2}F_w(\phi_W + \phi_P) = D_e(\phi_E - \phi_P) - D_w(\phi_P - \phi_W) \Rightarrow \\
&F_B\phi_B - \tfrac{1}{2}F_w(\phi_W + \phi_P) = D_B(\phi_B - \phi_P) - D_w(\phi_P - \phi_W) \\
&0 - 0.05(\phi_3 + \phi_4) = -\phi_4 - 0.5(\phi_4 - \phi_3) = -1.5\phi_4 + 0.5\phi_3 \\
&1.45\phi_4 = 0.55\phi_3 \Rightarrow \phi_4 = 0.37931\phi_3
\end{aligned} \tag{5.26}$$

Using the above result in the third equation of (5.24)

$$\phi_3 = 0.6632\phi_2$$

Substituting the above in the second equation of (5.24)

$$\phi_2 = 0.784\phi_1$$

Now substitute the above in (5.25)

$$1.55\phi_1 = 0.45\phi_2 + 1.1 \Rightarrow \phi_1 = 0.9188$$

Then

$$\begin{aligned}
\phi_1 &= 0.9188 \\
\phi_2 &= 0.7203 \\
\phi_3 &= 0.4777 \\
\phi_4 &= 0.1812
\end{aligned} \tag{5.27}$$

The exact solution in (5.22) is

$$\phi = 1 - \frac{(e^x - 1)}{(e^{0.8} - 1)} \Rightarrow 1.815966 - 0.815966e^x \tag{5.28}$$

Finite Volume Method solution Eq. (5.27) is compared with the Exact Solution in (5.28) in Table 5.1 and Fig. 5.3. We note that the finite volume method agrees closely with the exact solution.

**Table 5.1** Comparison of finite volume solution with exact values

| Distance m | FV solution | Exact |
|---|---|---|
| 0 | 1 | 1 |
| 0.1 | 0.9188 | 0.9141841 |
| 0.3 | 0.7203 | 0.7145271 |
| 0.5 | 0.4777 | 0.4706655 |
| 0.7 | 0.1812 | 0.1728123 |
| 0.8 | 0 | 0 |

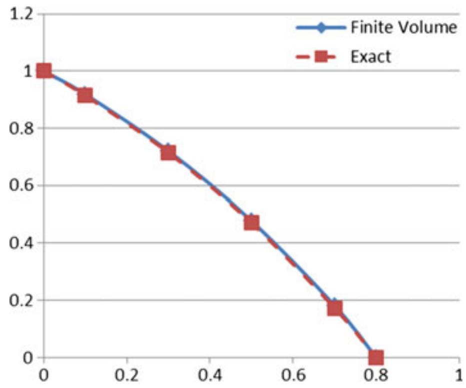


**Fig. 5.3** Comparison of finite volume method with exact solution

## Exercises 5

5.1 Consider Eqs. (4.5) and (4.6) to derive a single general transport equation.

5.2 Simplify the general transport equation for the steady state case without any viscous effects and without any source.

5.3 Explain convection and diffusion by imagining a $\phi$ to represent some dye made up of little particles suspended in the fluid. Discuss the convective term as transport of this $\phi$, say temperature, due to the fluid motion and derive the corresponding governing Eq.

5.4 Derive a numerical solution using one dimensional finite volume method for the problem of diffusion (temperature) in a flow. You can also give a closed for solution for a problem with just one cell.

5.5 In the diffusion equation if $\phi$ represents a dye that is transported while diffusing show that the coefficient of diffusion $\Gamma$ is $\frac{\text{kg}}{\text{ms}}$. A 1 m long pipe carries water at 10 cm/s. One unit of dye at $x = 0$ that vanishes at the end of 1 m. The coefficient of diffusivity can be taken as 0.1 kg/m/s. Make a plot of the transported dye as a function of length using three cells of the pipe.

5.6 Compare the result obtained in 5.5 from an exact solution.

# Chapter 6
# Pressure—Velocity Coupling in Steady Flows

**Abstract** This chapter considers pressure-velocity coupling by finite volume method for steady flows both incompressible and compressible cases. Pitot and Venturi tubes for measurement of velocity are given that use Bernoulli principles. For adiabatic flows stagnation conditions are derived. For isentropic flows, sonic and supersonic conditions are obtained. Supersonic flows with a normal shock in divergent portion of a nozzle are obtained by considering quasi one-dimensional flow with area changing in nozzles. Different forms of energy equations for adiabatic flows are presented. Mach number and characteristic Mach number in a given flow are derived. Quasi one-dimensional flow through converging diverging nozzles is discussed. Nozzle performance for various back pressures is explained for isentropic flow with a normal shock forming in the divergent portion. The flows through a diffuser are also presented. The modeling of converging-diverging nozzles using finite volume method by computational fluid dynamics is explained leading to SBES with HPC for designs.

**Keywords** Pressure-velocity coupling · Stagnation conditions · Converging-diverging nozzles · Diffusers · Pitot and Venturi tubes · Quasi one dimensional flow · Area-velocity relation · Sonic and super-sonic flows · Shock · Normal shock · Mach number · CFD · SBES · HPC

In the previous chapters we assumed the velocity field to be given; however the velocity in a flow is a part of the fluid mechanics problem—the simplest being the velocity and pressure are coupled. Considering one dimensional steady flow in $x$ direction Eq. (3.18), we have

$$u\frac{du}{dx} = -\frac{1}{\rho}\frac{dp}{dx} \tag{6.1}$$

This is Euler's equation for one dimensional flow that couples pressure and velocity. For incompressible flows, the density $\rho$ is constant. This is also a statement of conservation of energy. The kinetic energy of the flow by virtue of the velocity it has and the pressure energy is conserved.



J.S. Rao, *Simulation Based Engineering in Fluid Flow Design*,
DOI 10.1007/978-3-319-46382-7_6

## 6.1 Steady State One-Dimensional Incompressible Problem

Integrating Eq. (6.1) we get

$$\frac{u^2}{2} + \frac{p}{\rho} = \text{constant} \Rightarrow \\ \frac{\rho u^2}{2} + p = \text{constant} \tag{6.2}$$

$\frac{\rho u^2}{2}$ is the dynamic pressure and $p$ is the static pressure sometimes written for convenience as $p_s$. The sum of these pressures $p_t$ is called *total pressure* or stagnation *pressure*. From (6.2)

$$\frac{\rho u^2}{2} + p_s = p_t \tag{6.3}$$

The static pressure in a flow can be determined by drilling a small hole on the wall surface parallel to the flow, see Fig. 6.1.

Equation (6.3) is applicable to one dimensional flow in a pipe line as shown in Fig. 6.2. The pipe cross-sectional area $a_1$ changes to $a_2$ as a result the dynamic and static pressures change; however, the stagnation pressure or total pressure remains the same. We can obtain the following relative equation.

$$\frac{\rho u_1^2}{2} + p_1 = \frac{\rho u_2^2}{2} + p_2 \tag{6.4}$$

Besides the continuity equation should be satisfied in the pipe shown in Fig. 6.2, i.e.

$$u_1 a_1 = u_2 a_2 \tag{6.5}$$

Consequently, the velocity is higher in the narrower cross-section and is lower in larger cross-sectional pipe sections.

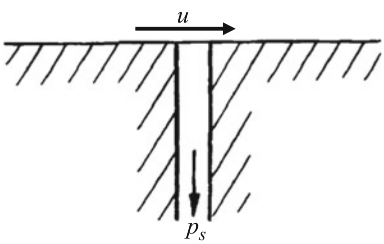


**Fig. 6.1** Determination of static pressure

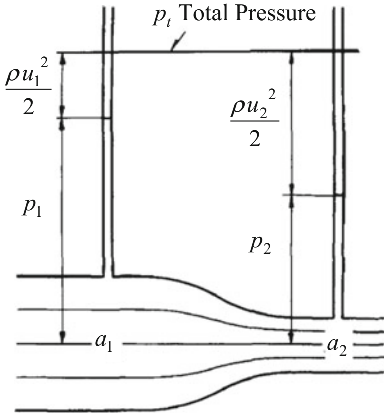


**Fig. 6.2** One dimensional pipe flow

## *6.1.1 Streamline Flow*

When the flow is not confined to $x$ direction such as a horizontal pipe, for example the oil pipe in Fig. 3.2 or the penstock in Fig. 3.3, we can have one dimensional streamline flow as shown in Fig. 6.3. Here a streamline is chosen with a cylindrical element of fluid of cross-sectional area $da$ and length $ds$ as shown. As adopted before, let $p$ be the pressure on the left-hand face, then the pressure on the right-hand face is given by $p + \frac{\partial p}{\partial s} ds$ as shown in Fig. 6.3. Since the flow is not confined to horizontal plane, we have to account for the gravity forces of the weight of this element, which is $\rho gdads$. The velocity $u$ is a function of time $t$ as well as distance $s$ or $u = u(s, t)$. Therefore the net change in velocity is represented by $Du$ and we can now apply Newton's II law.

$$\begin{aligned} \rho dads \frac{Du}{Dt} &= -da \frac{\partial p}{\partial s} ds - \rho gdads \cos\theta \Rightarrow \\ \frac{Du}{Dt} &= -\frac{1}{\rho} \frac{\partial p}{\partial s} - g \cos\theta \end{aligned} \tag{6.6}$$

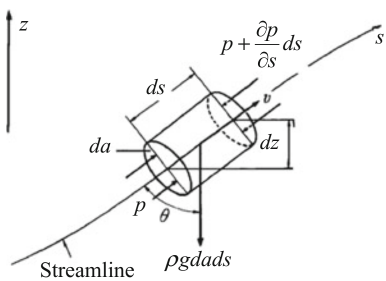


**Fig. 6.3** Streamline flow

Taking the total derivative of $u$ is $\frac{Du}{Dt} = \frac{\partial u}{\partial t} + \frac{\partial u}{\partial s}\frac{ds}{dt} = \frac{\partial u}{\partial t} + u\frac{\partial u}{\partial s}$. Also $\cos\theta = \frac{dz}{ds}$, therefore (6.6) above becomes

$$\frac{\partial u}{\partial t} + u\frac{\partial u}{\partial s} = -\frac{1}{\rho}\frac{\partial p}{\partial s} - g\frac{dz}{ds} \tag{6.7}$$

For steady state, the above reduces to Euler's equation for one-dimensional flow.

$$u\frac{\partial u}{\partial s} = -\frac{1}{\rho}\frac{\partial p}{\partial s} - g\frac{dz}{ds} \tag{6.8}$$

Note that the continuity equation should also be satisfied along with the above Euler's equation. If the flow is compressible, the gas Eq. (2.21) should also be included.

Integrating (6.8) along the stream line, we have

$$\frac{u^2}{2} + \int \frac{dp}{\rho} + gz = \text{constant} \tag{6.9}$$

For an incompressible fluid with density constant, the above can be simplified further

$$\frac{u^2}{2} + \frac{p}{\rho} + gz = \text{constant} \tag{6.10}$$

The units in (6.10) are $m^2/s^2$, they can be expressed as kg $m^2/(s^2$ kg). Noting that the energy in Joules J is kg $m^2/s^2$, $\frac{u^2}{2}, \frac{p}{\rho}$ and $gz$ represent kinetic energy, pressure energy and potential energy respectively. Dividing Eq. (6.10) by $g$ it can be expressed in terms of head (m), $\frac{u^2}{2}, \frac{p}{\rho}$ and $gz$, being velocity head, pressure head and potential head respectively. $H$ is the total head which is constant.

$$\frac{u^2}{2g} + \frac{p}{\rho g} + z = H = \text{constant} \tag{6.11}$$

Multiplying (6.10) by the density $\rho$, we have

$$\frac{\rho u^2}{2} + p + \rho gz = \text{constant} \tag{6.12}$$

The units in the above are $N/m^2$, i.e., $kg/(s^2m)$ and express energy per unit volume. When the streamline is horizontal, the above reduces to Eq. (6.2). The penstock in Fig. 3.3 can be modeled as a one-dimensional flow problem of Fig. 6.3.

## 6.2 Pitot and Venturi Tubes

Henri Pitot in 1732 discovered that the height of a fluid column is proportional to the square of the velocity, while measuring the flow in the river Seine in France. Pitot tube faces a streamlined flow with a hole opened to face the flow and another hole in a vertical direction to pick up separate pressures. Let the static pressure be $p$ and velocity $u$ in the undisturbed streamlined flow. In the first opening of the Pitot tube 1 a stagnation point, the flow gets stopped making the velocity $u$ zero and the pressure there is $p_1$ (Fig. 6.4).

From (6.2), we get

$$\frac{\rho u^2}{2} + p = p_1 \tag{6.2a}$$

At the second hole, the pressure $p_2$ is $p$ again, substituting for $p$ in the above

$$u = \sqrt{\frac{2(p_1 - p_2)}{\rho}} \tag{6.13}$$

The difference in the head $H$ of the flow can be measured from the Pitot tube which is given by $H = \frac{p_1 - p_2}{\rho g}$. Therefore

$$u = \sqrt{2gH} \tag{6.14}$$

Giovanni Battista Venturi (1746–1822) is an Italian physicist, who used Bernoulli's principle to measure the velocity in a flow in 1797; his apparatus is shown in Fig. 6.5.

In the narrowed part, Sect. 6.2 of the Venturi Tube in a flow, the velocity increases and pressure decreases. The decrease in the pressure from $p_1$ to $p_2$ is a measure of the velocity $u_1$. The difference in the head $H$ of the fluid (or water) is $H = \frac{p_1 - p_2}{\rho g}$. When the flow is a gas (or air), we use a U-tube as shown. If the pipe is horizontal, from Eq. (6.4)

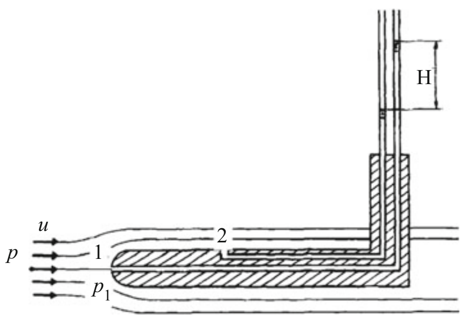


**Fig. 6.4** Pitot tube

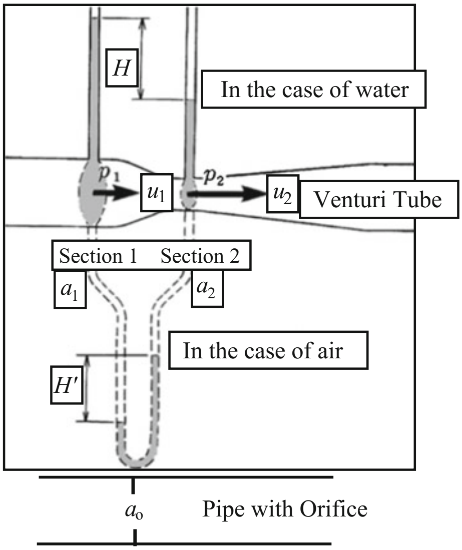


**Fig. 6.5** Venturi meter/orifice meter

$$\frac{\rho u_1^2}{2} + p_1 = \frac{\rho u_2^2}{2} + p_2 \tag{6.4a}$$

or

$$\frac{p_1 - p_2}{\rho} = \frac{u_2^2 - u_1^2}{2} \tag{6.4b}$$

Substituting $u_1 = \dfrac{u_2 a_2}{a_1}$

$$u_2 = \frac{1}{\sqrt{1 - \left(\dfrac{a_2}{a_1}\right)^2}} \sqrt{\frac{2(p_1 - p_2)}{\rho}} = \frac{\sqrt{2gH}}{\sqrt{1 - \left(\dfrac{a_2}{a_1}\right)^2}} \tag{6.15}$$

The flow rate then is

$$Q = a_2 u_2 = \frac{a_2\sqrt{2gH}}{\sqrt{1 - \left(\dfrac{a_2}{a_1}\right)^2}} \tag{6.16}$$

In practice there is some loss of energy between the two sections $a_1$ and $a_2$ and therefore the actual flow rate will be less than what is given in Eq. (6.16). Therefore we can modify the above as

$$Q = C_d \frac{a_2\sqrt{2gH}}{\sqrt{1 - \left(\frac{a_2}{a_1}\right)^2}} \tag{6.17}$$

$C_d$ is the coefficient of discharge determined through the test from Eq. (6.17).

An alternative arrangement is introducing an obstruction or orifice in the pipe with a diameter $d$ and area $a_o$ as shown in the lower part of Fig. 6.5. In this case the flow rate becomes

$$Q = C_d \frac{a_o\sqrt{2gH}}{\sqrt{1 - \left(\frac{a_o}{a}\right)^2}} \tag{6.17a}$$

Worked Example 6.1:
Orifice method is adopted to measure the flow rate of methanol through a 4 cm dia pipe. The orifice meter is equipped with 3 cm dia orifice plate and a mercury manometer across the orifice. The methanol density is 800 kg/m$^3$. If the manometer reads 10 cm what is the flow rate? The discharge coefficient is 0.6. The density of mercury is 13,600 kg/m$^3$.

Since methane and mercury have different densities, the pressure difference is

$$\Delta p = p_1 - p_2 = \left(\rho_{\mathrm{Hg}} - \rho_{\mathrm{methane}}\right) gH$$

From (6.15)

$$u_o = \sqrt{\frac{2\left(\rho_{\mathrm{Hg}} - \rho_{\mathrm{methane}}\right) gH}{\rho_{\mathrm{methane}}\left\{1 - \left(\frac{a_o}{a}\right)^2\right\}}} \quad \therefore Q = C_d a_o u_o = C_d \frac{a_o\sqrt{2\left(\frac{\rho_{\mathrm{Hg}}}{\rho_{\mathrm{methane}}} - 1\right) gH}}{\sqrt{1 - \left(\frac{a_o}{a}\right)^2}}$$

Now

$a_0 = \frac{9\pi}{4} \times 10^{-4}\ \mathrm{m}^2,\quad \left(\frac{a_0}{a}\right)^2 = \frac{81}{256} \Rightarrow \sqrt{1 - \left(\frac{a_0}{a}\right)^2} = \sqrt{1 - \frac{81}{256}} = \sqrt{\frac{175}{256}} = 0.8268;$
$\frac{\rho_{\mathrm{Hg}}}{\rho_{\mathrm{methane}}} = \frac{13600}{800} = 17$

$$Q = C_d \frac{a_o\sqrt{2\left(\frac{\rho_{\mathrm{Hg}}}{\rho_{\mathrm{methane}}} - 1\right) gH}}{\sqrt{1 - \left(\frac{a_o}{a}\right)^2}} = 0.6 \times 7.06858 \times 10^{-4} \frac{\sqrt{2 \times 16 \times 9.81 \times 0.1}}{0.8268}$$

$$= 4.2411 \times 10^{-4} \times \frac{5.6028}{0.8268} = 0.00287\ \mathrm{m}^3/\mathrm{s}$$

## 6.3 Stagnation Conditions in Adiabatic Flow

In Eq. (6.3) we defined stagnation pressure and static pressures for an incompressible flow. Now consider an element passing through a given point in an inviscid compressible adiabatic flow with velocity $V$. Here $p$, $\rho$ and $T$ are the local quantities, also called *static* quantities. In a specific process, let us imagine that the element under question is brought to rest adiabatically. The resulting temperature of the gas element is denoted as *stagnation temperature* $T_0$ (also called *total temperature*).

The corresponding enthalpy of the element is *stagnation enthalpy* (also called *total enthalpy*) denoted by $h_0$ which for a calorically perfect gas is given by Eq. (2.27)

$$h_0 = c_p T_0 \tag{6.18}$$

Energy equation given in (3.26) for this simplified flow reduces to

$$\begin{aligned} \rho \frac{DE}{Dt} &= -div(p\mathbf{u}) \Rightarrow \\ \rho \frac{D\left(e + \frac{1}{2}V^2\right)}{Dt} &= -\nabla \cdot pV \end{aligned} \tag{6.19}$$

Let us add $\frac{p}{\rho}$ inside the substantial derivative term on the left hand side and a corresponding term to the right hand side, then

$$\begin{aligned} \rho \frac{D\left(e + \frac{p}{\rho} + \frac{1}{2}V^2\right)}{Dt} &= -p\nabla \cdot V - V\nabla \cdot p + \rho \frac{D\left(\frac{p}{\rho}\right)}{Dt} \Rightarrow \\ \rho \frac{D\left(h + \frac{1}{2}V^2\right)}{Dt} &= \frac{\partial p}{\partial t} \end{aligned} \tag{6.20}$$

For steady adiabatic case, the above reduces to

$$h + \frac{1}{2}V^2 = \text{constant} \tag{6.21}$$

Therefore for a steady adiabatic inviscid flow, $h + \frac{1}{2}V^2$ is a constant along a streamline. If we imagine that such a flow is brought to rest, the fluid element will have zero velocity and according to the definition of stagnation enthalpy, $h$ in this case becomes $h_0$. Hence the constant in Eq. (6.21) is $h_0$.

$$h + \frac{1}{2}V^2 = h_0 \tag{6.21a}$$

The flow in most cases originates from a uniform free stream, and then $h_0$ is same for each streamline. Therefore for such a flow originating from a uniform free stream

$$h_0 = \text{constant} \tag{6.22}$$

For such an adiabatic flow, Eq. (6.22) represents the energy equation. For a calorically perfect gas, the stagnation enthalpy $h_0$ and stagnation temperature $T_0$ are related through Eq. (2.27) $h_0 = c_p T_0$. Hence for a calorically perfect gas, stagnation temperature is constant throughout a steady inviscid adiabatic flow, given by

$$h_0 = \text{constant} \tag{6.23}$$

For an adiabatic flow considering two different points 1 and 2 in the flow, we obtain

$$\begin{aligned} h_1 + \frac{1}{2}V_1^2 &= h_0 \\ h_2 + \frac{1}{2}V_2^2 &= h_0 \\ \therefore h_1 + \frac{1}{2}V_1^2 &= h_2 + \frac{1}{2}V_2^2 \end{aligned} \tag{6.24}$$

## 6.4 Isentropic Flow

Consider the element in the flow considered above in Sect. 6.3 is now brought to rest not only adiabatically but also reversibly. That is the element is brought to rest slowly in an isentropic manner. Then the resulting pressure $p_0$ and the density $\rho_0$ are called stagnation pressure and density respectively. Note that the stagnation temperature will be still same since isentropic flow is also an adiabatic flow.

Let the local pressure and temperature at a given point 1 in an isentropic flow be $p_1$ and $T_1$ respectively. If the stagnation temperature is $T_0$ then we can use Eq. (2.60)

$$\begin{aligned} \frac{p_2}{p_1} &= \left(\frac{\rho_2}{\rho_1}\right)^{\gamma} = \left(\frac{T_2}{T_1}\right)^{\frac{\gamma}{\gamma-1}} \Rightarrow \\ p_0 &= p_1 \left(\frac{T_0}{T_1}\right)^{\frac{\gamma}{\gamma-1}} \\ \rho_0 &= \rho_1 \left(\frac{T_0}{T_1}\right)^{\frac{1}{\gamma-1}} \end{aligned} \tag{6.25}$$

## 6.5 Speed of Sound

A typical example of compressible flow is the sound travel in a given medium. The speed of sound is an extremely important quantity in the solution of compressible flow problems. We know that sound travels with a finite velocity in air. When we speak for example, a pressure front is generated; the energy released is transferred to the molecules of neighboring air. The energized molecules move about in a random way, and eventually collide with other close-by molecules. A kind of domino effect takes place and the energy is transferred from one set of molecules to another. Thus a wave is generated which progresses in the air medium. This microscopic molecular motion generates macroscopically average values of temperature, pressure and density. Therefore, slight variations of $T$, $p$ and $\rho$ occur locally, when the wave passes through a given location. The speed at which the wave passes through a given location is the *speed of sound* in the medium at the existing local conditions.

According to Kinetic Theory of Gases (Maxwell-Boltzmann equation) the molecules of a gas move with an average velocity $\sqrt{\frac{8RT}{\pi}}$ m/s where $R$ $(\frac{\mathrm{J}}{\mathrm{kgK}})$ is the gas constant and $T$ (K) is the temperature. Since the molecular collisions cause the propagation of wave front and transfer the energy, the speed of sound can be expected to be in the region of the speed at which the molecules move. For a given gas the average velocity of molecular motion is dependent only on the temperature. Therefore, the speed of sound in a given gas can also expected to be a function of its temperature alone.

Now let us assume that a sound wave moving with a velocity $a$ from right to left into a stagnant gas as shown in Fig. 6.6. Let the temperature, pressure and density in the stagnant gas on left side 1 be $T$, $p$ and $\rho$ respectively. Let the passing wave disturb the medium by generating slight variations and let the local values in region be $T + dT$, $p + dp$ and $\rho + d\rho$ respectively. For the application compressible flow equations, let us consider the propagating wave in Fig. 6.6 to be stationary, so that the stagnation gas has now a relative motion from the left to right as shown in Fig. 6.7.

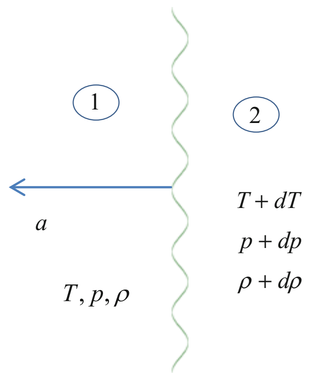


**Fig. 6.6** Propagation of sound wave moving from right to left

**Fig. 6.7** Stationary sound wave in a moving gas

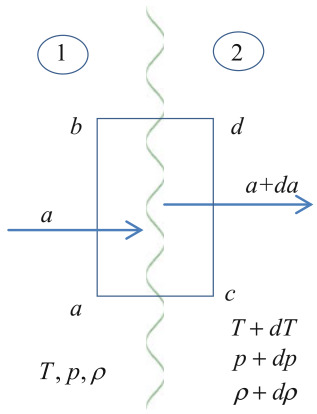


The relative flow to the sound wave in Fig. 6.7 can be considered as steady flow and it is adiabatic, since heat is neither added nor taken away from the system. There are no body forces, therefore it is a reversible flow and hence it is isentropic.

Considering the flow through side *ab* of unit width perpendicular to the figure into the stationary wave and the flow out correspondingly through *cd*, the continuity equation gives

$$\rho a = (\rho + d\rho)(a + da)$$

Neglecting higher-order terms,

$$\begin{aligned} a &= -\rho \tfrac{da}{d\rho} \\ da &= -\tfrac{a d\rho}{\rho} \end{aligned} \tag{6.26}$$

This can also be obtained directly from Eq. (3.9) for the steady case. The momentum equation in (3.18) for this one-dimensional adiabatic flow (inviscid flow and no source terms) is

$$\begin{aligned} div\left(\rho a^2\right) &= -\frac{dp}{dx} \Rightarrow \\ \frac{d\rho}{dx}a^2 + 2\rho a \frac{da}{dx} &= -\frac{dp}{dx} \Rightarrow \\ a^2 d\rho + 2\rho a da &= -dp \Rightarrow \\ dp &= -a^2 d\rho - 2\rho a da \Rightarrow \\ da &= -\frac{dp + a^2 d\rho}{2a\rho} \end{aligned} \tag{6.27}$$

Using (6.26), we get

$$-\frac{ad\rho}{\rho} = -\frac{dp + a^2 d\rho}{2a\rho} \Rightarrow \\ a^2 = \frac{dp}{d\rho} \tag{6.28}$$

Since the process is isentropic, the rate of change of pressure with density is also isentropic and hence the velocity of sound in the gas is

$$a = \sqrt{\left(\frac{dp}{d\rho}\right)_s} \tag{6.29}$$

From (6.20)

$$\frac{p_2}{p_1} = \left(\frac{\rho_2}{\rho_1}\right)^\gamma$$

i.e., $\frac{p}{\rho^\gamma} =$ constant = $c$.

$$\frac{p}{\rho^\gamma} = c \tag{6.30}$$

Differentiating with respect to $\rho$.

$$\left(\frac{\partial p}{\partial \rho}\right)_s = c\gamma\rho^{\gamma-1} \Rightarrow \\ = \gamma\frac{p}{\rho} \tag{6.31}$$

Substituting in Eq. (6.29)

$$a = \sqrt{\frac{\gamma p}{\rho}} \\ = \sqrt{\gamma RT} \tag{6.32}$$

Thus the speed of sound in a calorically perfect gas is a function of only the temperature. The speed of sound in air for $\gamma$ = 1.4 is about $\sqrt{\frac{1.4\pi}{8}} \approx \frac{3}{4}$ times the average speed at which the molecules move. The speed of the sound at 20 °C is $\sqrt{1.4 \times 287.1 \times 293} = 343.17$ m/s.

*Mach number M* is defined by the ratio of local velocity to the speed of sound under the given local conditions, i.e.,

$$\begin{aligned} M &= \frac{V}{a} \\ &= \frac{V}{\sqrt{\gamma RT}} \end{aligned} \tag{6.33}$$

## 6.6 Shocks in Supersonic Flow

We recall here that any disturbance at some point in a flow generates a wave and is transmitted at the local speed of sound. This is like transmitting information in the flow, e.g., the presence of a body in the flow.

Consider first the presence of a body in a subsonic flow $M < 1$ as in Fig. 6.8. The gas molecules which impact on the body surface experience a change in the momentum, which in turn is transmitted to the neighboring molecules by random molecular motion. The speed at which the transmission takes place is at the local velocity of the sound in the flow. Since the speed of flow is subsonic, the transmission signal can work upstream easily and warn the flow the presence of the obstacle in the path. The flow moves out of the way of the obstacle and form a well-organized pattern, i.e., a streamlined flow.

Now consider the flow to be supersonic, i.e., $M > 1$ as in Fig. 6.9. Here too the disturbance due to the body is propagated at the sonic velocity via the molecular collision, but unfortunately it cannot work upstream as the incoming flow is at a speed more than sonic velocity, i.e., more than the propagating wave velocity. The disturbance waves pile up and coalesce with the incoming flow, thus forming a standing wave in front of the body.

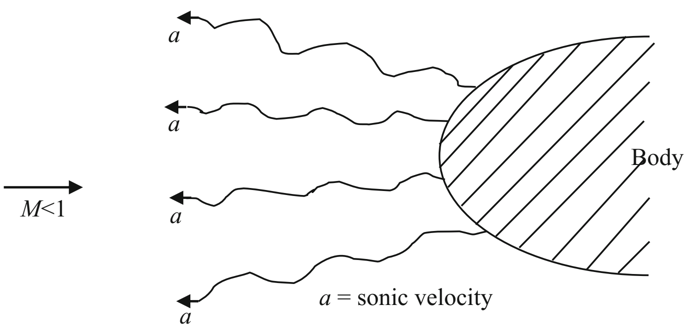


**Fig. 6.8** Disturbance from molecular collisions propagated upstream in subsonic flow

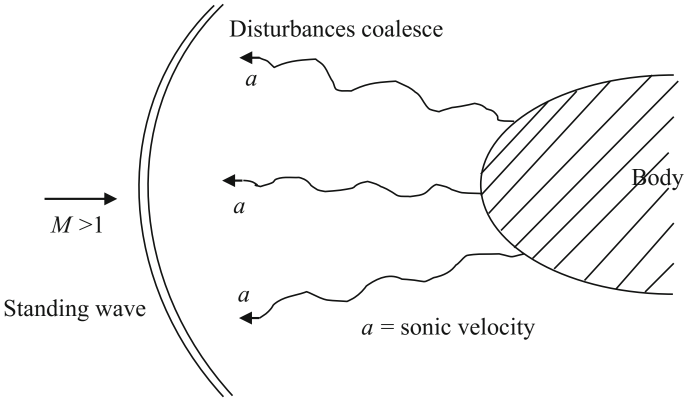


**Fig. 6.9** Formation of a standing wave (shock) in supersonic flow

**Fig. 6.10** Supersonic flow over blunt object

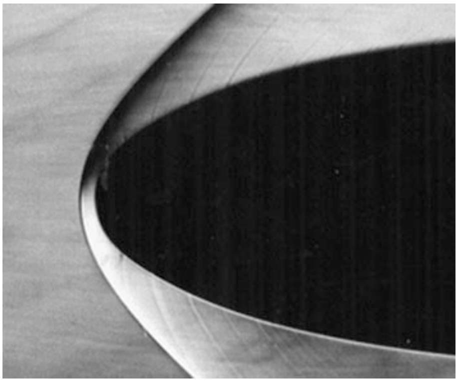

A Schlieren photograph of supersonic flow over a blunt object, see Fig. 6.10, demonstrates the formation of shock in supersonic flows.

The above flows are considered when they are external to the body, e.g., the flow over an automobile, over an aircraft wing etc. Many compressible practical flows are internal, e.g., those of nozzles in turbo machinery. Rocket propulsion is also achieved by internal compressible flow through nozzles that are converging or diverging or combined converging and diverging. As an example the nozzle of a liquid propulsion Vikas engine is shown in Fig. 6.11 used in Polar Satellite Launch Vehicle.

**Fig. 6.11** PSLV second stage Vikas engine nozzle

## 6.7 Other Forms of Energy Equation for Adiabatic Flow

We will first express energy Eq. (6.24) in useful forms for application to nozzle flows. Using the enthalpy Eq. (2.27) in (6.24)

$$c_p T_1 + \frac{1}{2} V_1^2 = c_p T_2 + \frac{1}{2} V_2^2 \tag{6.34}$$

With the help of (2.30a) $c_p = \frac{\gamma R}{\gamma - 1}$ is substituted in the above

$$\frac{\gamma R}{\gamma - 1} T_1 + \frac{1}{2} V_1^2 = \frac{\gamma R}{\gamma - 1} T_2 + \frac{1}{2} V_2^2 \tag{6.31}$$

From (6.32) we use $a = \sqrt{\gamma RT}$ in the above to get

$$\frac{a^2}{\gamma - 1} + \frac{1}{2} V_1^2 = \frac{a_2^2}{\gamma - 1} + \frac{1}{2} V_2^2 \tag{6.32}$$

Let the region 2 correspond to stagnation conditions, where the total speed of sound is $a_0$ with $V_2 = 0$. Considering region 1 to be any given location in the flow with $a$ and $V$ representing the speed of sound and velocity, then

$$\frac{a^2}{\gamma - 1} + \frac{1}{2} V^2 = \frac{a_0^2}{\gamma - 1} \tag{6.33}$$

Now, let us define $a^*$ as the speed of sound associated with a condition in the flow where the fluid element is speeded up (if the flow is subsonic) or slowed down (if the flow is supersonic) adiabatically to sonic velocity.

Let region 2 in Eq. (6.32) correspond to such $a^*$ condition, where the speed of sound is $a^*$ with $V_2 = a^*$, $M_2 = M^* = 1$, and region 1 as before with $a$ and $V$ representing the speed of sound and velocity, then

$$\begin{aligned} \frac{a^2}{\gamma - 1} + \frac{1}{2} V^2 &= \frac{a^2}{\gamma - 1} + \frac{1}{2} a^{*2} \\ \frac{a^2}{\gamma - 1} + \frac{1}{2} V^2 &= \frac{\gamma + 1}{2(\gamma - 1)} a^{*2} \end{aligned} \tag{6.34}$$

In the above $a$ and $V$ represent the speed of sound and velocity at any given location in the flow and that $a^*$ is a characteristic value associated with the same location. We can write this equation for any two points along a streamline as

$$\frac{a^2}{\gamma - 1} + \frac{1}{2} V_1^2 = \frac{a_2^2}{\gamma - 1} + \frac{1}{2} V_2^2 = \frac{\gamma + 1}{2(\gamma - 1)} a^{*2} = \text{constant} \tag{6.35}$$

Comparing the above with (6.33), we have

$$\frac{\gamma + 1}{2(\gamma - 1)} a^{*2} = \frac{a_0^2}{\gamma - 1} \tag{6.36}$$

For steady adiabatic and inviscid flow, the above equation tells us that the two quantities, stagnation speed of sound $a_0$ and value of speed of the sound at sonic conditions $a^*$ are continuous along a given streamline. If all the streamlines emanate from the same uniform free field conditions, then $a_0$ and $a^*$ are constants throughout the flow field.

Now, let us use the definition of stagnation temperature $T_0$ from (2.27) and (6.21a) with $h_0 = c_p T_0$. Then Eq. (6.34) for given conditions of $T$ and $V$ and substituting for $c_p$ from (2.34) and using (6.32) becomes

$$\begin{aligned} c_p T + \frac{1}{2}V^2 &= h_0 = c_p T_0 \Rightarrow \\ \frac{T_0}{T} &= 1 + \frac{V^2}{2c_p T} \Rightarrow \\ &= 1 + \frac{V^2}{2\frac{\gamma R}{\lambda - 1}T} \Rightarrow \\ &= 1 + \frac{V^2}{\frac{2a^2}{\gamma - 1}} \Rightarrow \\ &= 1 + \frac{\gamma - 1}{2}M^2 \end{aligned} \tag{6.37}$$

For any two positions

$$c_p T_1 + \frac{1}{2}V_1^2 = c_p T_2 + \frac{1}{2}V_2^2 = c_p T_0 \tag{6.38}$$

Equation (6.37) tells us that the local temperature is related to stagnation temperature through local Mach number only for a given adiabatic compressible inviscid flow. We can further write using Eq. (2.60) for isentropic flow, the relations for local values of pressure and density as

$$\frac{p_0}{p} = \left(1 + \frac{\gamma - 1}{2}M^2\right)^{\frac{\gamma}{\gamma - 1}} \tag{6.39}$$

$$\frac{\rho_0}{\rho} = \left(1 + \frac{\gamma - 1}{2}M^2\right)^{\frac{1}{\gamma - 1}} \tag{6.40}$$

### *6.7.1 Mach Number for Which the Flow Can Be Considered Incompressible*

Equation (6.40) defines the density in an isentropic compressible flow for a given gas at a point where the Mach number is defined, in terms of stagnation density. Let us consider air with specific heat ratio $\gamma = 1.4$, the stagnation density when it is stationary is $\rho_0$. Let a fluid element in this stationary air be accelerated to a Mach number $M$ by means of an expansion through a nozzle, and then the density is given by

$$\frac{\rho_0}{\rho} = \left(1 + \frac{1.4-1}{2}\,M^2\right)^{\frac{1}{1.4-1}} = \left(1 + 0.2\,M^2\right)^{-2.5}$$

For Mach number 0.32,

$$\frac{\rho_0}{\rho} = (1 + 0.2 \times 0.1024)^{-2.5} \Rightarrow$$
$$\frac{\rho}{\rho_0} = \frac{1}{(1 + 0.2 \times 0.1024)^{2.5}} = 0.95$$

This shows that the variation in density is only 5 % for Mach numbers even up to 0.3. Since the compressible flow is essentially an outcome of the changes in density property of the medium, we can for all practical purposes of engineering accuracy consider subsonic flows with Mach number $M < 0.3$ to be incompressible.

If we consider the location in the general flow, where the velocity is exactly sonic ($M = 1$) with temperature, pressure and density marked as * quantities, $T^*$, $p^*$ and $\rho^*$ respectively are given by

$$\begin{aligned} \frac{T_0}{T^*} &= 1 + \frac{\gamma-1}{2} \\ \frac{p_0}{p^*} &= \left(1 + \frac{\gamma-1}{2}\right)^{\frac{\gamma}{\gamma-1}} \\ \frac{\rho_0}{\rho^*} &= \left(1 + \frac{\gamma-1}{2}\right)^{\frac{1}{\gamma-1}} \end{aligned} \tag{6.41}$$

i.e.,

$$\begin{aligned} \frac{T^*}{T_0} &= \frac{2}{\gamma+1} \\ \frac{p^*}{p_0} &= \left(\frac{2}{\gamma+1}\right)^{\frac{\gamma}{\gamma-1}} \\ \frac{\rho^*}{\rho_0} &= \left(\frac{2}{\gamma+1}\right)^{\frac{1}{\gamma-1}} \end{aligned} \tag{6.42}$$

### 6.7.2 *Characteristic Mach Number*

According to definition of Mach number, if $a = \sqrt{\gamma RT}$ is the local speed of sound and $V$ is the local velocity, $M = \frac{V}{a}$. We can define another Mach number called *Characteristic Mach number* $M^*$ which is the ratio of local velocity $V$ and speed of sound at sonic conditions $a^* = \sqrt{\gamma RT^*}$, i.e., $M^* = \frac{V}{a^*} = \frac{V}{\sqrt{\gamma RT^*}}$. The relation between $M$ and $M^*$ can be obtained as follows. Dividing Eq. (6.34) by $V^2$

$$\begin{aligned} \frac{\left(\frac{a}{V}\right)^2}{\gamma - 1} + \frac{1}{2} &= \frac{\gamma + 1}{2(\gamma - 1)}\left(\frac{a^*}{V}\right)^2 \Rightarrow \\ \frac{1}{(\gamma - 1)M^2} &= \frac{\gamma + 1}{2(\gamma - 1)}\left(\frac{1}{M^*}\right)^2 - \frac{1}{2} \Rightarrow \\ M^2 &= \frac{2}{\frac{(\gamma + 1)}{M^{*2}} - (\gamma - 1)} \end{aligned} \tag{6.43}$$

We can rewrite the above as

$$M^{*2} = \frac{(\gamma + 1)M^2}{2 + (\gamma - 1)M^2} \tag{6.43a}$$

The characteristic Mach number $M^*$ behaves qualitatively in the same way as the Mach number $M$, i.e., $M = 1$ if $M^* = 1$, $M < 1$ if $M^* < 1$ and $M > 1$ if $M^* > 1$. When $M \to \infty$, however the characteristic Mach number $M^*$ tends to a finite value which from the La Hopital' rule $\lim_{x\to\infty} \frac{f(x)}{g(x)} = \lim \frac{f'(x)}{g'(x)}$, i.e.,

$$M \to \infty \, M^* \to \sqrt{\frac{\gamma + 1}{\gamma - 1}} \tag{6.44}$$

## 6.8 Quasi-One Dimensional Flow

Important examples of compressible flow are the flow through nozzles and diffusers. Nozzles and diffusers are mechanically similar, though they may be applied for different purpose. They consist of a converging portion, throat and a diverging portion, and for this reason they are also called converging-diverging nozzles or diffusers. They are symmetrical about the direction of flow and conical in nature. The surface of the cone may be formed by either inclined straight line or a curve revolving about the axial direction of flow.

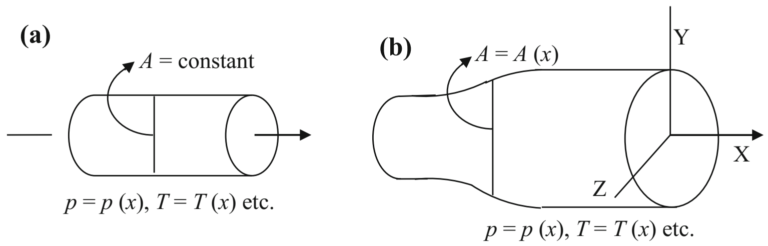


**Fig. 6.12** One dimensional and quasi-one-dimensional flows

The flow is one dimensional, when all the state quantities are functions of $x$ alone, e.g., $T = T(x)$. If the area of cross-section $A$ is constant we have a stream tube as shown in Fig. 6.12a. If area of cross-section is also a function of $x$, i.e., $A = A(x)$ as in Fig. 6.12b, the flow is essentially three dimensional in nature, i.e., the flow field variables are functions of $x$, $y$, and $z$. This is because the flow remains tangential to the wall at the boundary.

If the area $A = A(x)$ varies moderately along the length, then the flow field variable components in the $y$, and $z$ directions will be small in comparison to the variation in the $x$ direction. In such a case with $A = A(x)$, it can be assumed that $p = p(x)$, $V = V(x)$ etc., and the flow is termed Quasi-one-dimensional flow.

Figure 6.13 shows a Quasi-one-dimensional flow with the control volume in a variable cross-section duct. The continuity Eq. (4.4) for the steady one-dimensional flow is

$$\frac{d}{dx}(\rho V) = 0 \tag{6.45}$$

Integrating over the volume between $x = x_1$, where area $A = A_1$ to $x = x_2$, where area $A = A_2$ we have

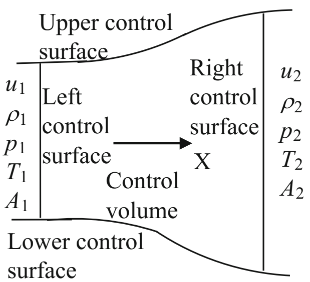


**Fig. 6.13** Quasi-one-dimensional flow control volume

$$\int_{A_1}^{A_2} \left( \frac{d}{dx}(\rho V) \right) dx dA = 0 \Rightarrow$$
$$\rho_1 V_1 A_1 = \rho_2 V_2 A_2 \tag{6.46}$$

The $x$ momentum equation in (3.18) can be written as

$$div(\rho V^2) = -\frac{dp}{dx} \tag{6.47}$$

Integrating the above in the control volume,

$$\int_{cv} div(\rho V^2) dA dx + \int_{cv} \frac{dp}{dx} dA dx = 0 \tag{6.48}$$

Using Gauss divergence theorem $\int_{CV} div\, \mathbf{a}\, dV = \int_{A} \mathbf{n} \cdot \mathbf{a}\, dA$ from Eq. (3.35) for the first integral and integrating the second integral with respect $x$ Eq. (6.48) becomes

$$\int_{A} \rho V^2 dA + \int_{A} p dA = 0 \tag{6.49}$$

On the upper and lower surfaces, the first integral is zero and taking the left and right surfaces of the control volume into account, it yields $-\rho_1 V_1^2 A_1 + \rho_2 V_2^2 A_2$. The second integral for the left and right surfaces is $-p_1 A_1 + p_2 A_2$, for the upper and lower surfaces it is $\int_{A_1}^{A_2} -pdA$. Therefore

$$-\rho_1 V_1^2 A_1 + \rho_2 V_2^2 A_2 - p_1 A_1 + p_2 A_2 - \int_{A_1}^{A_2} p dA = 0 \Rightarrow$$
$$p_1 A_1 + \rho_1 V_1^2 A_1 + \int_{A_1}^{A_2} p dA = p_2 A_2 + \rho_2 V_2^2 A_2 \tag{6.50}$$

The energy equation for the present from (3.32) is given by

$$div(\rho \mathbf{u}) \left( e + \frac{1}{2} V^2 \right) = -p\, div\, \mathbf{u}$$

Integrating over the control volume and using Gauss's theorem

$$\begin{aligned}
\int_A (\rho V)\left(e+\frac{1}{2}V^2\right)dA &= -\int_A pV dA \Rightarrow \\
&-\rho_1\left(e_1+\frac{1}{2}V_1^2\right)V_1A_1+\rho_2\left(e_2+\frac{1}{2}V_2^2\right)V_2A_2 \\
&= -(-p_1V_1A_1+p_2V_2A_2) \Rightarrow \\
&p_1V_1A_1+\rho_1\left(e_1+\frac{1}{2}V_1^2\right)V_1A_1 = p_2V_2A_2+\rho_2\left(e_2+\frac{1}{2}V_2^2\right)V_2A_2
\end{aligned} \tag{6.51}$$

Using the continuity Eq. (6.46), $\rho_1V_1A_1=\rho_2V_2A_2$, divide the left hand side by $\rho_1V_1A_1$ and the right-hand side by $\rho_2V_2A_2$ Eq. (6.51) can be recast as

$$\frac{p_1}{\rho_1}+e_1+\frac{1}{2}V_1^2=\frac{p_2}{\rho_2}+e_2+\frac{1}{2}V_2^2 \tag{6.52}$$

For a perfect gas with the help of Eqs. (2.21) and (2.22), the above reduces to

$$h_1+\frac{1}{2}V_1^2=h_2+\frac{1}{2}V_2^2 \tag{6.53}$$

Further for adiabatic flow, we can deduce that

$$h_{01}=h_{02}=h_0 \tag{6.54}$$

The Eqs. (6.46), (6.50) and (6.53) together with enthalpy Eq. (2.27) and the equation of state (2.21) form the required five governing differential equations for the five unknowns $V_2$, $\rho_2$, $p_2$, $T_2$ and $h_2$.

## 6.9 Area-Velocity Relation

An important characteristic of the quasi-one-dimensional flow is that the change in velocity is directly dependent on the change in the area of cross-section and local Mach number. This area velocity relation is derived as follows.

### *6.9.1 Continuity Equation in Differential Form*

From the continuity relation that $\rho VA$ is constant, we have $d\,(\rho VA)=0$. Note that we cannot set $\frac{\partial}{\partial y}=\frac{\partial}{\partial z}=0$ and make $\frac{\partial}{\partial x}=\frac{d}{dx}$ in Eq. (3.9) for steady flow which gives simply $d\ (\rho V) = 0$. This equation is valid for truly one-dimensional flow and for quasi-one-dimensional flow $d\ (\rho VA) = 0$ should be employed to take into account the variable cross-sectional area of flow. Therefore

$$d(\rho VA) = d\rho VA + \rho dVA + \rho VdA = 0 \tag{6.55a}$$

i.e.,

$$\frac{d\rho}{\rho} + \frac{dV}{V} + \frac{dA}{A} = 0 \tag{6.55b}$$

### 6.9.2 Momentum Equation in Differential Form

Let us take two areas close to each other with $A_1 = A$ and $A_2 = A + dA$. We can then write $p_1 = p$ and $p_2 = p + dp$, $\rho_1 = \rho$ and $\rho_2 = \rho + d\rho$ etc. Equation (6.50) then becomes

$$pA + \rho V^2 A + pdA = (p + dp)(A + dA) + (\rho + d\rho)(V + dV)^2(A + dA) \tag{6.56}$$

Neglecting higher order terms

$$Adp + AV^2 d\rho + \rho V^2 dA + 2\rho VAdV = 0 \tag{6.57}$$

Multiplying (6.55a) by $V$

$$d\rho V^2 A + \rho VdVA + \rho V^2 dA = 0$$

and subtracting from 6.57) we get

$$\begin{aligned} &dp = -\rho VdV \Rightarrow \\ &\frac{dp}{\rho} = -VdV \end{aligned} \tag{6.58}$$

Multiplying and dividing the left hand-side by $d\rho$, we can rewrite the above as

$$\frac{dp}{\rho} = \frac{dp}{d\rho}\frac{d\rho}{\rho} = -VdV \tag{6.59}$$

### 6.9.3 Energy Equation in Differential Form

Equation (6.53) can be directly written as an energy equation in differential form

$$dh + VdV = 0 \tag{6.60}$$

Now in (6.59) we use $\frac{dp}{d\rho} = a^2$ from (6.29)

$$\begin{aligned} a^2 \frac{d\rho}{\rho} &= -VdV \\ \frac{d\rho}{\rho} &= -\frac{V^2}{a^2}\frac{dV}{V} = -M^2\frac{dV}{V} \end{aligned} \tag{6.61}$$

Substituting the above in (6.55b)

$$\begin{aligned} \frac{d\rho}{\rho} + \frac{dV}{V} + \frac{dA}{A} &= 0 \Rightarrow \\ \frac{dV}{V}\left(1 - M^2\right) + \frac{dA}{A} &= 0 \end{aligned}$$

or

$$\frac{dA}{A} = \left(M^2 - 1\right)\frac{dV}{V} \tag{6.62}$$

The above is the Area-Velocity relation for a quasi-one-dimensional flow. Let us consider the following cases to understand converging-diverging nozzles that are commonly employed in all sorts of nozzles, ever since De Laval used it in his steam turbine.

*Case*1: Converging Duct in Subsonic Flow

A converging duct in subsonic flow, $M < 1$, with area decreasing, i.e., $\frac{dA}{A}$ is negative, Eq. (6.62) tells us that $\frac{dV}{V}$ is positive, i.e., the velocity increases. Hence we need a converging nozzle to accelerate a given subsonic flow. Figure 6.14a illustrates this.

*Case*2: Diverging Duct in Subsonic Flow (Diffuser)

Obviously we need a diverging duct with a positive $\frac{dA}{A}$ to decelerate a given subsonic flow, i,e., $\frac{dV}{V}$ becomes negative. This is illustrated in Fig. 6.14b. This is also called a *Diffuser*.

Diffusers are used to slow the fluid's velocity, say from an axial or centrifugal flow compressor to enhance mixing into the surrounding fluid, e.g., in a combustion chamber.

*Case*3: Consider a supersonic flow and if we wish to accelerate this flow further, i.e., $\frac{dV}{V}$ to be positive, $\frac{dA}{A}$ should be positive since $M^2 - 1$ is now positive. Therefore

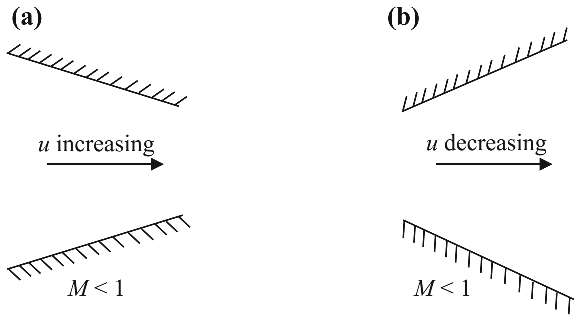


**Fig. 6.14** Converging duct accelerates subsonic flow

we need a diverging duct to accelerate a supersonic flow, see Fig. 6.15b. This is what we do in the case of rocket nozzles to give high thrust, see Fig. 6.11.

*Case*4: The reverse of case 3 is true in the case of a converging nozzle under supersonic flow, see Fig. 6.15a. For $M > 1$, with $\frac{dA}{A}$ decreasing $\frac{dV}{V}$ also decreases. This is illustrated in Fig. 6.15a and is the case of a supersonic diffuser.

*Case*5: If we have sonic flow, i.e., $M = 1$, then $\frac{dA}{A} = 0$, or $dA = 0$. This means, we should have a local minimum for the varying area. In practice this turns out to be a minimum area of cross-section in the duct to obtain sonic conditions. This principle is used in supersonic nozzles and diffusers. A supersonic nozzle is shown in Fig. 6.16a. The converging part accelerates the subsonic flow that reaches sonic condition represented by * as defined in Sect. 6.7, where Mach number becomes 1. In the diverging part the flow continues to be accelerated further beyond Mach number 1.

*Case*6: In this case we have a supersonic diffuser which is similar to the geometry of the nozzle of Case 5, only the entry conditions are supersonic instead of being subsonic in the supersonic nozzle. The converging flow decelerates the flow from high Mach number to sonic or * conditions at the minimum area of cross-section or the throat; in the diverging portion, the flow is further decelerated from Mach number 1 at the throat. This is illustrated in Fig. 6.16b.

Because of the versatility of the converging-diverging nozzles for supersonic and subsonic flows, they are extensively used in all steam and gas turbines, compressors, aircraft engines, rockets, space launch vehicles and torpedoes.

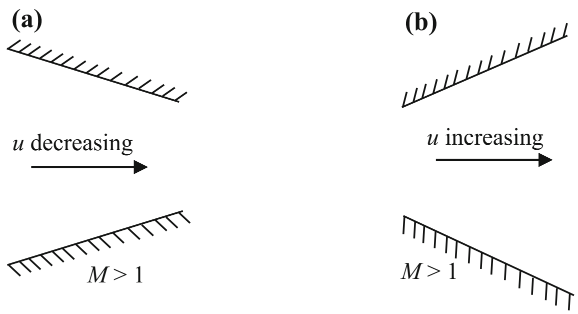


**Fig. 6.15** Converging duct decelerates supersonic flow

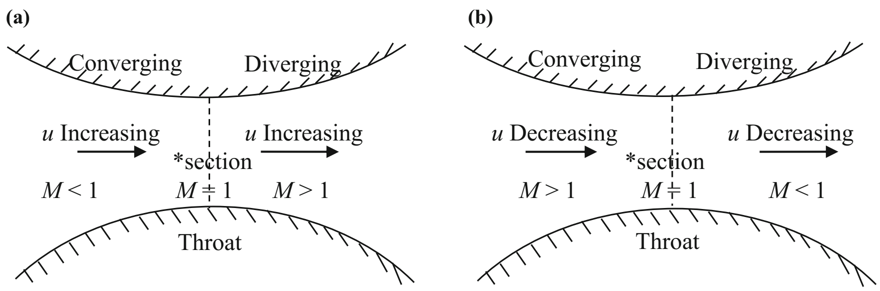


**Fig. 6.16** Throat* section **a** Supersonic nozzle. **b** Supersonic diffuser

Though CFD codes are developed with high performance computing for today's applications and used in the nozzle flows considering turbulence, boundary layers, mixing etc., the basic flow happens to be predominantly quasi-one-dimensional flow.

## 6.10 Example of Nozzle Flow—Subsonic Flow Throughout

We will first derive an important relation between area $A$ and Mach number $M$ for a supersonic nozzle in terms of specific heat ratio $\gamma$ for the gas and a characteristic area $A^*$ in accordance with the definition of * quantities defined before.

For the nozzle to accelerate subsonic flows ($M < 1$), we have seen that a converging duct is necessary to increase the velocity. We have also seen that a diverging portion is necessary to accelerate further a supersonic flow. Therefore we may conclude that the throat section of a nozzle can achieve the maximum possible subsonic velocity. Hence the nozzle throat can at best be under sonic conditions. If sonic flow exists at the throat, we then have a * section there. Therefore at the throat of a nozzle under sonic conditions, $A = A^*$, we have $M^* = 1$ and $V^* = a^*$. Let at any other section, converging or diverging portion, the area be $A$, Mach number be $M$ and the velocity $V$.

From continuity Eq. (6.46)

$$\rho^* V^* A^* = \rho V A \tag{6.63}$$

Since $V^* = a^*$, the above can be written as

$$\frac{A}{A^*} = \frac{\rho^*}{\rho} \frac{a^*}{V} \tag{6.64}$$

Multiplying and dividing the right-hand side by stagnation density $\rho_0$

$$\frac{A}{A^*} = \frac{\rho^*}{\rho_0}\frac{\rho_0}{\rho}\frac{a^*}{V} \tag{6.64a}$$

The stagnation density can be defined in terms of density where the Mach number is 1, which at present is the throat section of the nozzle, using Eq. (6.42) $\frac{\rho*}{\rho_0} = \left(\frac{2}{\gamma+1}\right)^{\frac{1}{\gamma-1}}$.

Equation (6.40) gives $\frac{\rho_0}{\rho} = \left(1 + \frac{\gamma-1}{2}M^2\right)^{\frac{1}{\gamma-1}}$ and (6.43a) gives $M^{*2} = \frac{(\gamma+1)M^2}{2+(\gamma-1)M^2}$.

Squaring equation (6.64a) on both sides, we can substitute the required quantities from (6.42), (6.40) and (6.43a) to give

$$\left(\frac{A}{A^*}\right)^2 = \left(\frac{2}{\gamma+1}\right)^{\frac{2}{\gamma-1}}\left(1 + \frac{\gamma-1}{2}M^2\right)^{\frac{2}{\gamma-1}}\left(\frac{2+(\gamma-1)M^2}{(\gamma+1)M^2}\right) \tag{6.65}$$

Simplifying, we get

$$\frac{A}{A^*} = \frac{1}{M}\left[\left(\frac{2}{\gamma+1}\right)\left(1 + \frac{\gamma-1}{2}M^2\right)\right]^{\frac{\gamma+1}{2(\gamma-1)}} \tag{6.66}$$

The above is an important and significant result that the Mach number at any location is simply a function of the ratio of the local duct area to the duct area where sonic conditions exist. For a nozzle with supersonic flow in the diverging portion, the throat itself is the location where sonic conditions exist. The difficulty in solving for Mach number at a given location is because Eq. (6.66) is nonlinear; therefore we need an iteration procedure to be adopted. For this purpose, we can rewrite (6.66) in the following form

$$M\frac{A}{A^*}\left[\left(\frac{\gamma+1}{2+(\gamma-1)M^2}\right)\right]^{\frac{\gamma+1}{2(\gamma-1)}} - 1 = \Delta \tag{6.66a}$$

Assume a value for $M = M_1$ for a given area $\frac{A}{A^*}$ and $\gamma$ and find the remainder $\Delta = \Delta_1$. Increment the value of $M_1$ by $\Delta M$ to $M_2$ and determine $\Delta_2$. Using the remainders $\Delta_1$ and $\Delta_2$ interpolate a new value $M$. Repeat the iteration process until $\Delta = 0$ or until no change takes place in the value of $M$ to a desired accuracy. You can write a small program on your computer or calculator to get the required solutions. Note that we will get two roots, one for subsonic case with sonic conditions at the throat and another for perfect supersonic expansion case.

### *6.10.1 Example of Axisymmetric Nozzle Flow*

Consider the rocket nozzle given in Fig. 6.17, whose inlet wall is made of two circles, both 3.937 cm radius, the first once centered at (−5.08, 0). The second circle forms the throat section of the nozzle, with its center on the vertical line passing through the throat section. The nozzle exit wall is a cone with an angle 15° as shown. The total length of the nozzle is 12.192 cm. Mathematically the geometry is expressed as:

Inlet Circle:

$$(x+5.08)^2+y^2=3.937^2 \tag{a}$$

Slope at any point on the wall of the inlet circle:

$$\frac{dy}{dx}=-\frac{x+5.08}{y} \tag{b}$$

Equation for the throat circle:

$$x^2+(y-y_1)^2=3.937^2 \tag{c}$$

In the above $y_1$ is determined in such a way that the inlet and throat circles meet at a point with a common tangent, thus forming the inlet wall of the nozzle.

Slope at any point on the wall of the throat circle:

$$\frac{dy}{dx}=-\frac{x}{y-y_1} \tag{d}$$

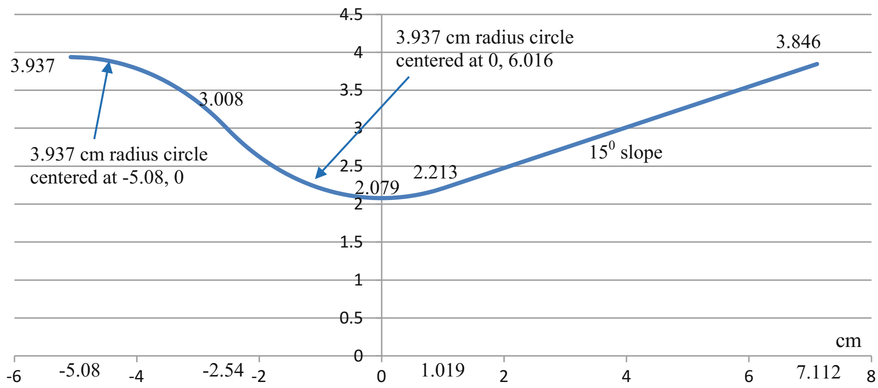


**Fig. 6.17** Rocket nozzle geometry

For a common tangent between the inlet and throat circles from (b) and (d), we have

$$\frac{x+5.08}{y} = \frac{x}{y-y_1} \Rightarrow \qquad \text{(e)}$$
$$y_1 = \frac{5.08y}{x+5.08}$$

Substituting for $y_1$ from (e) the equation for throat circle in (c) can now be written as

$$x^2(x+5.08)^2 + x^2y^2 = 3.937^2(x+5.08)^2 \qquad \text{(f)}$$

Substituting for $y^2 = 3.937^2 - (x+5.08)^2$ from (a), we get

$$x^2(x+5.08)^2 + x^2\left(3.937^2 - (x+5.08)^2\right) = 3.937^2(x+5.08)^2 \Rightarrow$$
$$x^2 = (x+5.08)^2 \Rightarrow 2 \times 5.08x = -5.08^2 \qquad \text{(g)}$$
$$\therefore x = -2.54$$

This gives from (a), $y = 3.008$, giving the common point at $x = -2.54$ and $y = 3.008$ as shown in Fig. 6.17.

From (e) we get $y_1 = 6.016$ and the throat circle is

$$x^2 + (y - 6.016)^2 = 3.937^2 \qquad \text{(h)}$$

The slope of the throat circle wall is then given from (d) as

$$\frac{dy}{dx} = -\frac{x}{y-6.016} \qquad \text{(i)}$$

Exhaust Nozzle Shape:

$$y = \tan 15^0 x + c$$
$$= 0.267949x + c \qquad \text{(j)}$$

The slope of the exhaust nozzle from the above is

$$\frac{dy}{dx} = 0.267949 \qquad \text{(k)}$$

where the throat circle meets the exhaust nozzle, they should have a common tangent, therefore, equating (i) and (k) and substituting for $y$ from (j),

$$
\begin{aligned}
-\frac{x}{y-6.016} &= 0.267949 \Rightarrow \\
-\frac{x}{0.267949x+c-6.016} &= 0.267949 \Rightarrow \\
c &= \frac{6.016\times 0.267949-(1+0.267949^2)x}{0.267949}
\end{aligned}
\tag{l}
$$

For a common point between the throat circle and the exhaust wall of the nozzle we substitute equation (h) in (j)

$$x^2+(0.267949x+c-6.016)^2=3.937^2 \tag{m}$$

Substituting for $c$ from (l), and then with the help of (h), we get

$$
\begin{aligned}
x &= 1.019 \\
y &= 2.21325
\end{aligned}
\tag{n}
$$

The value of constant $c$ is then obtained from (j),

$$c = 1.940 \tag{o}$$

The exhaust nozzle is then given by

$$y = 0.267949x+1.940 \tag{p}$$

The entire nozzle is then given by (a), (h) and (p) above

$$
\begin{aligned}
y &= \sqrt{3.937^2-(x+5.08)^2} & -5.08<x<-2.54 \\
y &= 6.016-\sqrt{3.937^2-x^2} & -2.54<x<1.019 \\
y &= 1.94+0.267949x & 1.019<x<7.112 \text{ cm}
\end{aligned}
\tag{6.67}
$$

The nozzle is shown in Fig. 6.17 and Table 6.1.

**Table 6.1** Rocket nozzle data for eight sections

| Stn. | $x$ (cm) | $y$ (cm) | $A$ (sq cm) |
|---|---|---|---|
| 1 | −5.0800 | 3.9370 | 48.6946 |
| 2 | −3.8100 | 3.7264 | 43.6243 |
| 3 | −2.5400 | 3.0081 | 28.4272 |
| 4 | 0.0000 | 2.0790 | 13.5787 |
| 5 | 1.0185 | 2.2131 | 15.3869 |
| 6 | 2.5400 | 2.6280 | 21.5783 |
| 7 | 5.0800 | 3.3015 | 34.3431 |
| 8 | 7.1120 | 3.8458 | 46.4647 |

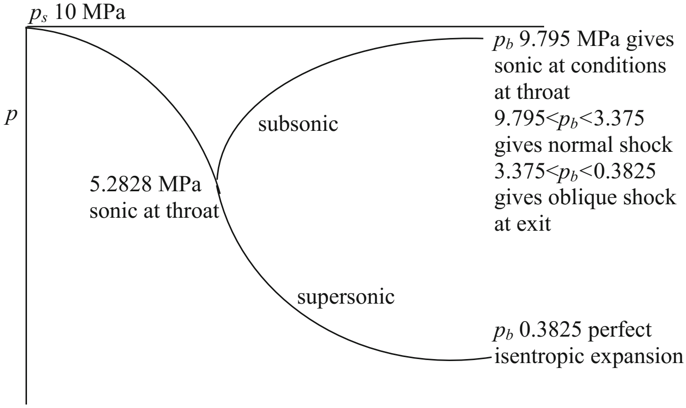


**Fig. 6.18** Nozzle performance for various back pressures

The performance of the nozzle depends on the ratio of the back pressure at the exit to supply pressure of the reservoir from which the nozzle is fed. First of all we don't expect any flow if the back pressure at the exit is same as supply pressure, see Fig. 6.18. We need a pressure differential to have the flow through the nozzle.

If the back pressure is lowered slightly from the reservoir pressure, we first have isentropic flow throughout the nozzle. Subsequently if the back pressure is reduced further, the nozzle gets choked with the Mach number equal to unity at the throat. As soon as the throat Mach number becomes unity, the divergence duct will still continue to have subsonic isentropic flow.

With a further decrease in the back pressure, a normal shock appears in the diverging portion and travels to the exit. When the back pressure is further reduced, the normal shock that has travelled to the exit portion of the nozzle splits into oblique shocks at the nozzle exit. These shocks that occur in the diverging portion of the nozzle and at the exit are not isentropic. They are not studied in this introductory course.

When the back pressure is further reduced, perfect isentropic expansion takes place followed by Prandtl-Meyer waves. These are not studied here.

### 6.10.2 Subsonic Flow

Let the stagnation pressure of air with $\gamma = 1.4$ in the reservoir be $p_0 = 10$ MPa from which the nozzle of Fig. 6.17 is fed. The back pressure at exit, station 8 is assumed to be slightly lower than reservoir pressure, $p_b = 9.805$ MPa so that a small quantity of flow can take place. Using (6.39) for station 8

$$\frac{p_0}{p} = \left(1 + \frac{\gamma - 1}{2} M^2\right)^{\frac{\gamma}{\gamma-1}} \Rightarrow$$
$$10 = 9.805\left(1 + 0.2M_8^2\right)^{3.5} \tag{6.39'}$$

Therefore $M_8 = 0.168$. We can now use (6.66) to determine $A^*$ for this flow, where sonic flow will occur. Note that for subsonic flow, the throat is not the * area with $M < 1$.

$$\frac{A}{A^*} = \frac{1}{M}\left[\left(\frac{2}{\gamma+1}\right)\left(1 + \frac{\gamma - 1}{2} M^2\right)\right]^{\frac{\gamma+1}{2(\gamma-1)}} \Rightarrow$$
$$\frac{46.4647}{A^*} = \frac{1}{0.168}\left[\frac{1}{1.2}\left(1 + 0.2 \times 0.168^2\right)\right]^3 \Rightarrow \tag{6.66'}$$
$$A^* = 13.226 \text{ cm}^2$$

$A^*$ obtained above for this subsonic flow is less than the throat area $13.5787 \text{ cm}^2$, so it does not exist in the nozzle. It is a hypothetical cross-section, where the flow would have become sonic. Now we can calculate $\frac{A}{A^*}$ for each of the 8 cross-sections and given in Table 6.2.

Now, Eq. (6.66a) can be used to determine Mach numbers at all the sections.

$$M\frac{A}{A^*}\left[\left(\frac{\gamma+1}{2 + (\gamma - 1)M^2}\right)\right]^{\frac{\gamma+1}{2(\gamma-1)}} - 1 = \Delta \Rightarrow$$
$$M\frac{A}{A^*}\left[\left(\frac{1.2}{1 + 0.2\,M^2}\right)\right]^3 - 1 = \Delta \tag{6.66a'}$$

Mach numbers determined by an iteration process described earlier are given in Table 6.2. Note that we get two roots, one for subsonic case and the other for a supersonic perfect expansion case, we pick the subsonic value.

**Table 6.2** Subsonic flow through the nozzle

| Stn. | $\frac{A}{A^*}$ | $M$ | $\frac{p}{p_4}$ | $\frac{T}{T_4}$ | $\frac{\rho}{\rho_4}$ |
|---|---|---|---|---|---|
| 1 | 3.6708 | 0.1601 | 1.5591 | 1.1353 | 1.3733 |
| 2 | 3.2888 | 0.1794 | 1.5521 | 1.1338 | 1.3689 |
| 3 | 2.1429 | 0.2833 | 1.5013 | 1.1231 | 1.3367 |
| 4 | 1.0237 | 0.8400 | 1.0000 | 1.0000 | 1.0000 |
| 5 | 1.1600 | 0.6253 | 1.2196 | 1.0583 | 1.1523 |
| 6 | 1.6267 | 0.3890 | 1.4300 | 1.1076 | 1.2911 |
| 7 | 2.5812 | 0.2315 | 1.5292 | 1.1290 | 1.3544 |
| 8 | 3.5028 | 0.1680 | 1.5563 | 1.1347 | 1.3716 |

The pressure at the throat Sect. 6.4 is given by Eq. (6.39), which for Sect. 6.4 is

$$\begin{aligned} \frac{p_0}{p} &= \left(1+\frac{\gamma-1}{2}M^2\right)^{\frac{\gamma}{\gamma-1}} \Rightarrow \\ 10 &= p_4\left(1+0.2\times 0.84^2\right)^{3.5} \Rightarrow \\ p_4 &= 6.3\ \text{MPa} \end{aligned} \tag{6.39''}$$

We can determine the pressure ratios at each of the eight sections in terms of any chosen value, say $p_4$ by writing

$$\begin{aligned} \frac{p}{p_4} &= \frac{p_0}{p_4}\frac{p}{p_0} \\ &= \frac{10}{6.3}\frac{1}{\left(1+0.2M^2\right)^{3.5}} \\ &= \frac{1.5873}{\left(1+0.2M^2\right)^{3.5}} \end{aligned}$$

The values thus obtained are given in Table 6.2. Note that the pressure at nozzle entry has dropped from the stagnation pressure 10 MPa to 1.5591 × 6.83 = 9.822 MPa.

We can determine the temperature ratio at any section; say 4, with stagnation temperature from (6.37)

$$\frac{T_0}{T_4} = 1+\frac{\gamma-1}{2}M_4^2 = 1+0.2\times 0.84^2 = 1.1411$$

The temperature ratio of any section with that of the throat can be obtained from

$$\begin{aligned} \frac{T}{T_4} &= \frac{T_0}{T_4}\frac{T}{T_0} \\ &= \frac{1.1411}{\left(1+0.2M^2\right)^{3.5}} \end{aligned}$$

The temperature ratios are also given in Table 6.2. Finally we can find the density ratio from (6.40) as

$$\frac{\rho_0}{\rho_4} = \left(1+0.2\times 0.84^2\right)^{2.5} = 1.391$$

The density ratio of any section with that of the throat can be obtained from

**Table 6.3** Subsonic flow with sonic condition at the throat

| Stn. | $\frac{A}{A^*}$ | $M$ | $\frac{p}{p_4}$ | $\frac{T}{T_4}$ | $\frac{\rho}{\rho_4}$ |
|---|---|---|---|---|---|
| 1 | 3.5857 | 0.1640 | 1.8577 | 1.1936 | 1.5564 |
| 2 | 3.3126 | 0.1838 | 1.8488 | 1.1919 | 1.5511 |
| 3 | 2.0932 | 0.2907 | 1.7851 | 1.1801 | 1.5126 |
| 4 | 1.0000 | 1.0000 | 1.0000 | 1.0000 | 1.0000 |
| 5 | 1.1331 | 0.6526 | 1.4219 | 1.1058 | 1.2858 |
| 6 | 1.5890 | 0.4003 | 1.6950 | 1.1627 | 1.4578 |
| 7 | 2.5214 | 0.2374 | 1.8201 | 1.1866 | 1.5338 |
| 8 | 3.4217 | 0.1721 | 1.8542 | 1.1929 | 1.5542 |

$$\frac{\rho}{\rho_4} = \frac{\rho_0}{\rho_4}\frac{\rho}{\rho_0} = \frac{1.391}{\left(1 + 0.2M^2\right)^{2.5}}$$

The density ratios are also given in Table 6.2. The pressure variation over the nozzle length is depicted in Fig. 6.18.

## 6.11 Nozzle Flow—Subsonic Flow with Sonic Conditions at the Throat

In this case $\frac{A}{A^*} = 1$, i.e., $A_4 = A^* = 13.5787\ \text{cm}^2$. Therefore we can calculate $\frac{A}{A^*}$ for all the eight sections of the nozzle. They are given Table 6.3.

For the values of $\frac{A}{A^*}$, we can determine the Mach numbers from (6.66a) (pick the subsonic values). They are also given in Table 6.3. The pressure at the throat can be determined from (6.39) as

$$\frac{p_0}{p} = \left(1 + \frac{\gamma - 1}{2}M^2\right)^{\frac{\gamma}{\gamma-1}} \Rightarrow$$
$$10 = p_4\left(1 + 0.2 \times 1^2\right)^{3.5} \Rightarrow$$
$$p_4 = 5.2828\ \text{MPa}$$

We can now determine the pressure ratios in each of the eight sections in terms of $p_4$ by writing

$$\frac{p}{p_4} = \frac{p_0}{p_4}\frac{p}{p_0}$$
$$= \frac{10}{5.2828}\frac{1}{(1+0.2M^2)^{3.5}}$$
$$= \frac{1.8929}{(1+0.2\,M^2)^{3.5}}$$

The pressure at the nozzle exit $p_b$ is $\frac{p_8}{p_4} = 1.8542 \Rightarrow p_8 = 1.8542 \times 5.2828 =$ 9.795 MPa. Thus a very small pressure differential (10–9.795 = 0.205 MPa) is sufficient to create sonic conditions at the throat. This pressure differential maintained subsonic flow throughout the nozzle as given in Table 6.3. Note that the pressure at the nozzle entry is $\frac{p_1}{p_4} p_4 = 1.8577 \times 5.2828 = 9.795$ MPa slightly less than the value compared to 9.822 MPa of the subsonic flow considered before with Mach number less than 1 at the throat. The pressure at the throat, however, dropped to 5.2828 MPa from the previous value of 6.3 MPa.

We can next determine the temperature ratio at any section; say 4, with stagnation temperature from (6.37)

$$\frac{T_0}{T_4} = 1 + \frac{\gamma - 1}{2} M_4^2 = 1 + 0.2 \times 1^2 = 1.2$$

The temperature ratio of any section with that of the throat can be obtained from

$$\frac{T}{T_4} = \frac{T_0}{T_4}\frac{T}{T_0}$$
$$= \frac{1.2}{(1+0.2\,M^2)^{3.5}}$$

The temperature ratios are also given in Table 6.3. Finally we can find density ratio from (6.40) as

$$\frac{\rho_0}{\rho_4} = \left(1 + 0.2 \times 1^2\right)^{2.5} = 1.5774$$

The density ratio of any section with that of the throat can be obtained from

$$\frac{\rho}{\rho_4} = \frac{\rho_0}{\rho_4}\frac{\rho}{\rho_0}$$
$$= \frac{1.5774}{(1+0.2M^2)^{2.5}}$$

The density ratios are also given in Table 6.3. The pressure variation over the nozzle length for this subsonic flow with *condition at the throat is also depicted in Fig. 6.18.

## 6.12 Nozzle Flow—Supersonic Flow with Perfect Expansion

As in the previous case, sonic conditions exist at the throat section, i.e., $\frac{A}{A^*} = 1$ and $A_4 = A^* = 13.5787\ \text{cm}^2$. Values of $\frac{A}{A^*}$ therefore are same as in the previous case of Sect. 6.11 of subsonic isentropic flow with sonic condition at the throat given in Table 6.3. However, in the present case, we should pick the supersonic Mach number solutions for the diverging portion of the nozzle from the solution of (6.66a). These are given in Table 6.4.

The pressure at the throat section for perfect supersonic expansion remains the same as in the previous case of Sect. 6.11 with sonic conditions at the throat, which is 5.2828 MPa. We can determine the pressure ratios at each of the eight sections in terms of $p_4$, using the same formula of the previous section but with different Mach numbers in the diverging portion.

$$\frac{p}{p_4} = \frac{1.8929}{(1 + 0.2\,M^2)^{3.5}}$$

This gives the same pressure ratios as in the previous Sect. 6.11 for the nozzle inlet sections up to the throat, however, the Mach numbers are supersonic in the nozzle diverging portion and hence the pressure ratios here are different. These pressure ratios are given in Table 6.4. The pressure in the nozzle exit is $p_b = p_8 = 0.0724 \times 5.2828 = 0.3825$ MPa.

Thus a very large pressure differential (10 – 0.3825 = 9.6175 MPa) is necessary to produce perfect expansion. Hence when we reduce the back pressure from 9.795 MPa the throat remains sonic, supersonic expansion takes place in the diverging portion of the nozzle from the throat up to a location where normal shock is formed. Subsequent to the normal shock, subsonic flow prevails until the exit, to match with the back pressure that may be present for such conditions. When the back pressure is further lowered, the normal shock at the exit splits into oblique shocks and when the back pressure is lowered to 0.3825 MPa, perfect expansion takes place. Thus for a back pressure anywhere between 0.3825 and 9.795 MPa,

**Table 6.4** Perfect expansion solution

| Stn. | $\frac{A}{A^*}$ | $M$ | $\frac{p}{p_4}$ | $\frac{T}{T_4}$ | $\frac{\rho}{\rho_4}$ |
|---|---|---|---|---|---|
| 1 | 3.5857 | 0.1640 | 1.8577 | 1.1936 | 1.5564 |
| 2 | 3.3126 | 0.1838 | 1.8488 | 1.1919 | 1.5511 |
| 3 | 2.0932 | 0.2907 | 1.7851 | 1.1801 | 1.5126 |
| 4 | 1.0000 | 1.0000 | 1.0000 | 1.0000 | 1.0000 |
| 5 | 1.1331 | 1.4319 | 0.5686 | 0.8510 | 0.6681 |
| 6 | 1.5890 | 1.9267 | 0.2711 | 0.6887 | 0.3936 |
| 7 | 2.5214 | 2.4520 | 0.1194 | 0.5448 | 0.2191 |
| 8 | 3.4217 | 2.7760 | 0.0724 | 0.4722 | 0.1532 |

isentropic flow does not exist, either a normal shock in the diverging portion of the nozzle or oblique shock at the nozzle exit will be present.

The case of the normal shock or oblique shock is out of this basic course and we limit ourselves only to isentropic flows.

The pressure ratios for all the 8 sections for perfect expansion are given in Table 6.4. Figure 6.18 gives the pressure along the length of the nozzle. Note that the pressure at the nozzle entry also remains the same as in previous case in Sect. 6.11

The temperature ratios also remain same up to Sect. 6.4, at sections in the diverging portion, the supersonic solution of the Mach number should be used in the formula given in Sect. 6.11, as

$$\frac{T}{T_4} = \frac{1.2}{(1 + 0.2\,M^2)^{3.5}}$$

The temperature ratios are also given in Table 6.4.

The density ratio of any section with that of the throat can be obtained from

$$\frac{\rho}{\rho_4} = \frac{1.5774}{(1 + 0.2\,M^2)^{2.5}}$$

Once again the density ratios of the converging duct remain the same as in the previous case and those in the diverging duct will have to be determined with the supersonic solution for the Mach number. These density ratios are also given in Table 6.4.

Let us recollect the flow conditions for the two isentropic solutions, the first one where sonic conditions were reached in the nozzle throat with subsonic flow everywhere else, Table 6.3, and the second one where the flow is entirely supersonic in the diverging portion of the nozzle with the throat remaining under sonic conditions, the perfect expansion case in Table 6.4.

The back pressure for the sonic flow at the throat and subsonic flow in the whole nozzle was 9.795 MPa. The next fully isentropic solution, the perfect expansion case occurred at the back pressure as low as 0.3825 MPa. For $0.3825 \leq p_b \leq 9.795$ MPa, the flow is not isentropic and shock occurs in the diverging portion of the nozzle.

Since the inlet flow properties from Sects. 6.1–6.4 remain unchanged for the two cases considered in Tables 6.3 and 6.4, the mass flow across the nozzle is the same for both these isentropic solutions. In fact the inlet flow properties will remain unchanged for back pressure $0.3825 \leq p_b \leq 9.795$ MPa. In this entire range of the back pressure, the flow across the nozzle is therefore constant.

Continuing, when the back pressure is lowered further from the 0.3825 MPa, the flow properties will continue to remain the same in the entry of the nozzle as in Tables 6.3 and 6.4, and in addition the flow properties in the exit portion of the nozzle will also be same as in Table 6.4. Expansion waves will appear in the nozzle exit for $p_b < 0.3825$ MPa. The flow across the nozzle remains unchanged once the back pressure is brought to 9.795 MPa from the stagnation pressure of 10 MPa. Any reduction in the back pressure from 9.795 MPa fails to increase the mass flow across the nozzle.

The maximum flow condition is obtained when the nozzle flow reaches sonic conditions. Therefore the nozzle is said to be choked at this condition of subsonic isentropic flow with sonic conditions at the throat. This is in agreement with our discussion on the formation of the shock in Sect. 6.6 that once a weak shock is formed at the throat, the flow ahead of the shock cannot be warned of the changes in flow behind the shock and therefore the nozzle gets choked once the sonic conditions are reached at the throat.

## 6.13 CFD Solution of Isentropic Flow in Converging-Diverging Nozzles

Let us consider the nozzle given in Fig. 6.17 and Table 6.1. We will consider perfect expansion case with supersonic flow in the diverging portion as given in Fig. 6.18 with reservoir pressure 10 MPa and back pressure 0.3825 MPa. The actual flow is three-dimensional in nature; however, we determined closed form solutions using quasi-one dimensional flow analyses. Here we will consider the three-dimensional flow. The first step is to make the CAD model of the geometry given in Fig. 6.17 as shown in Fig. 6.19 (Fig. 6.20).

We have limited ourselves to one-dimensional analysis both analytical and numerical (CFD) in this first course. The numerical CFD in general is to adopt a three-dimensional geometry so that accurate simulation can be carried out of a real life three-dimensional problem. The three dimensional analysis follows the one-dimensional analysis and is not explained here. However, we will illustrate a three-dimensional analysis of the nozzle treated as a quasi-one-dimensional flow.

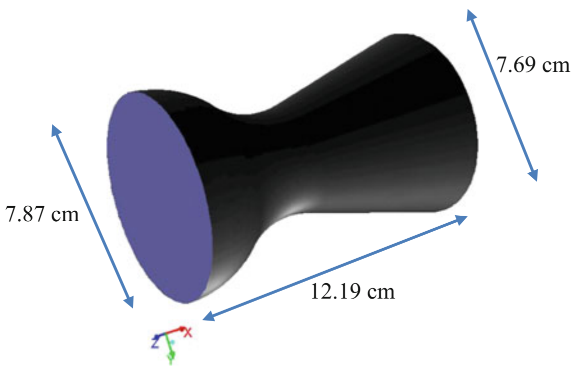


**Fig. 6.19** CAD model of the nozzle

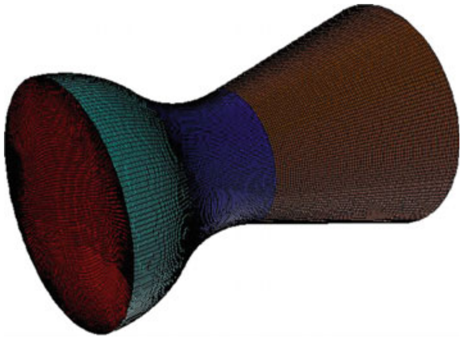

**Fig. 6.20** Flow medium mesh

The reader is advised to adopt any commercial code and study the brochures and arrive at the following procedure and solutions. The purpose of this exercise is to illustrate the modern practice in industry and how the students are expected to carry out the work.

Hexahedral elements are used with average skewness 0.3; the total number of elements is 1.42 million. The dense mesh at the entry of the nozzle is shown in Fig. 6.21. You may learn this process in any code such as Hyper Mesh.

Appropriate numerical process is to be adopted (by studying the manuals), say 2nd order upwind scheme. We will not consider turbulence (introduced in next chapter) and restrict to Euler's equations and solved for the purpose of known results from quasi-one dimensional flow discussed before.

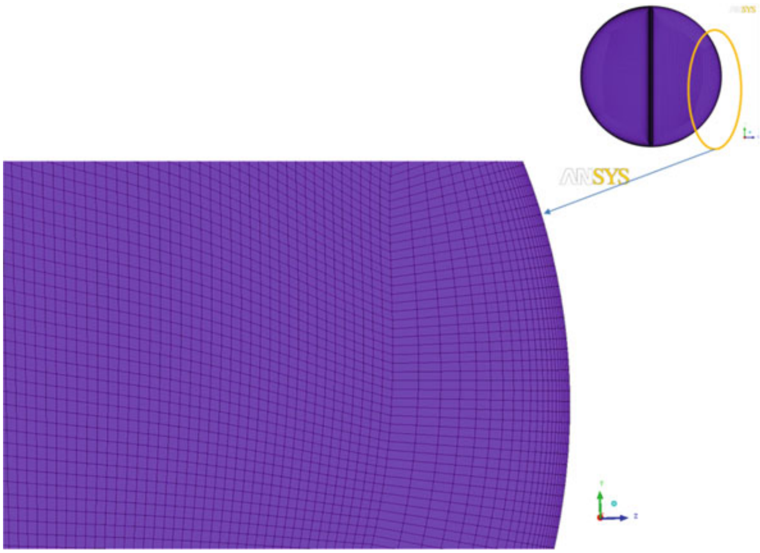


**Fig. 6.21** Mesh details at the nozzle entry

Air with a total pressure of 10 MPa and 2500 K is introduced at the inlet of the convergent-divergent nozzle. Pressure drop of 9.6175 MPa was assumed at the outlet and the flow pattern for the given condition of supersonic perfect expansion flow without any shock in the divergent portion is studied.

The results obtained are given for Static Pressure, Total Pressure, Velocity Contours at the Mid-plane, Mach Number Contours at the Mid-plane, Temperature (K) Contours at the Mid-plane and Velocity Vectors at the Mid-plane in the Nozzle in Figs. 6.22, 6.23, 6.24, 6.25, 6.26 and 6.27 respectively.

The static pressure at the entry is practically same as the stagnation pressure, since the velocity is very small at the entry. There is very little kinetic energy and thermal energy is also same. As the flow accelerates, the velocity increases and therefore the static pressure decreases keeping the total energy in the system constant.

The total pressure should be constant in an idealized one dimensional flow. In the converging flow portion with subsonic flow, there is no boundary layer that sticks to the walls and therefore the total pressure here is constant. In the diverging portion with supersonic flow, there is a boundary layer (this discussion is beyond the present scope) and slight reduction of the total pressure on the walls. Actually we should adopt the solution with a turbulence model rather than turbulence free model in the numerical analysis here.

The velocity contours in three dimensional analysis at the mid-plane in the nozzle are given in Fig. 6.24. The velocity gradually increases from the entry

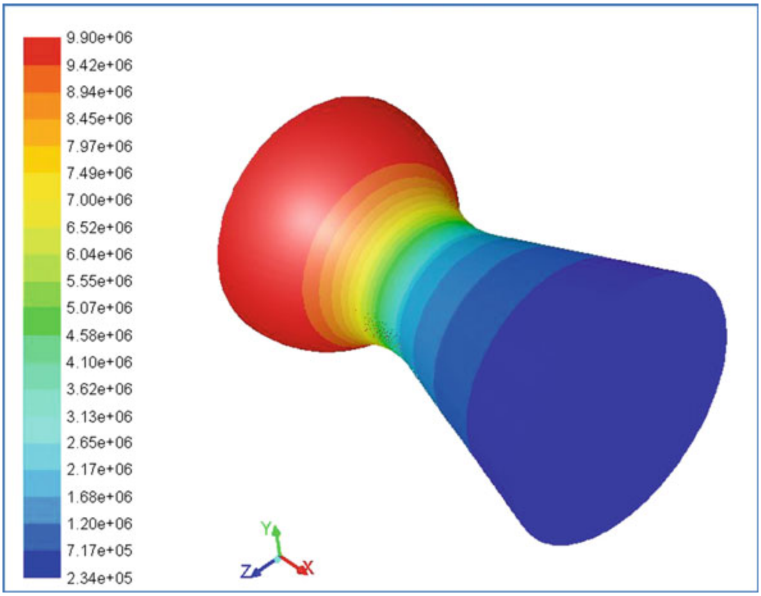


**Fig. 6.22** Static pressure distribution in the nozzle

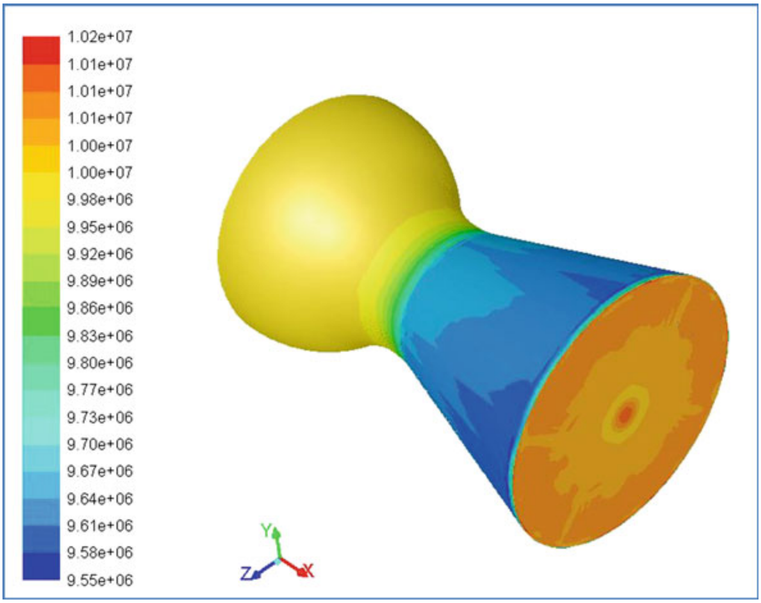


**Fig. 6.23** Total pressure distribution in the nozzle

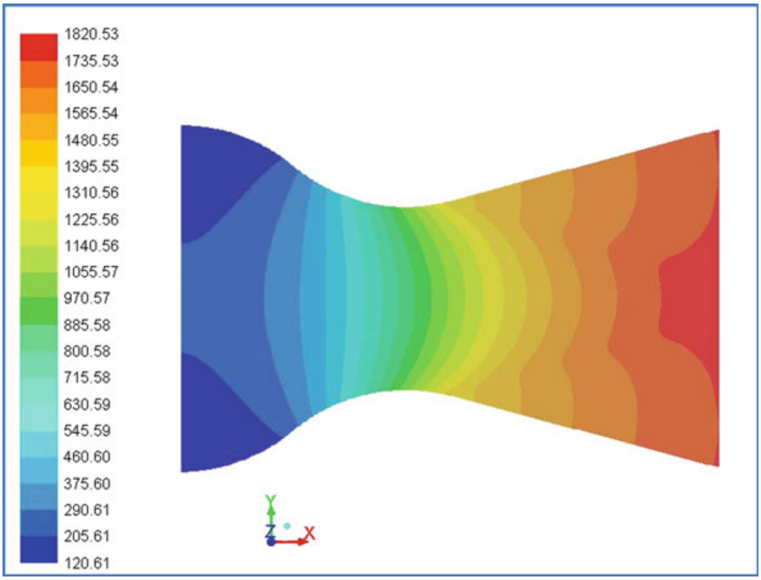


**Fig. 6.24** Velocity contours at the mid-plane in the nozzle

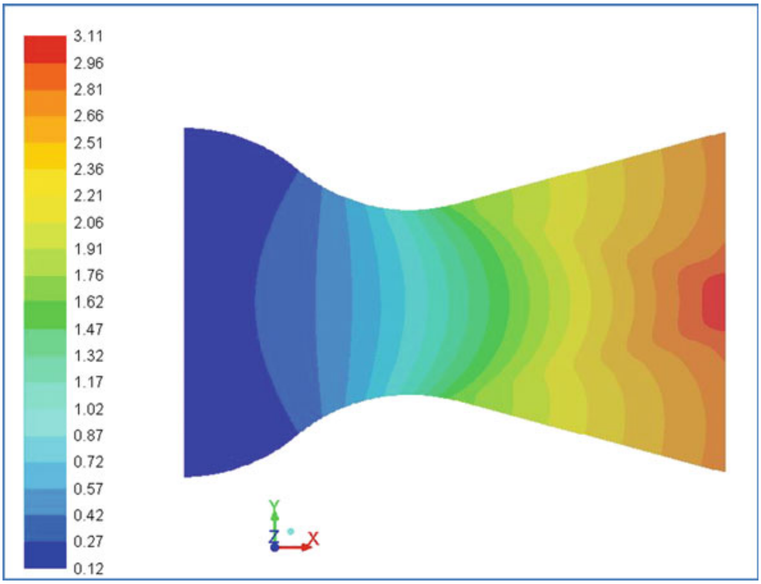


**Fig. 6.25** Mach number contours at the mid-plane in the nozzle

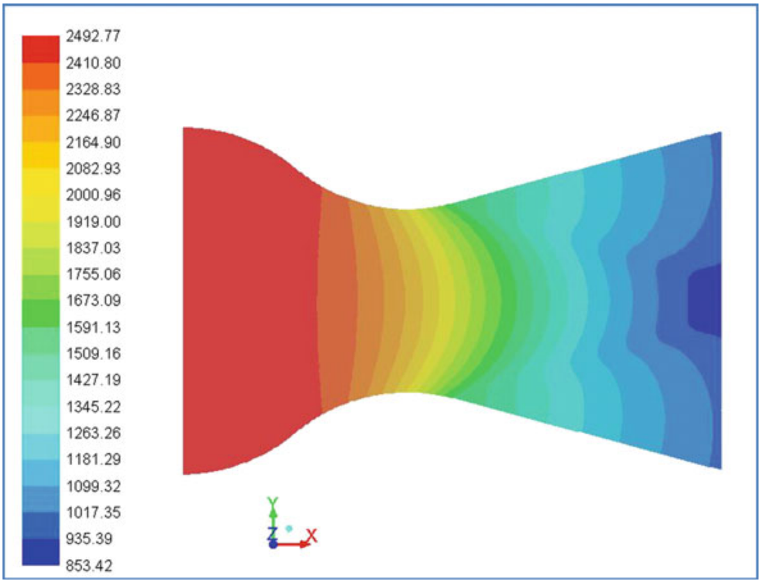


**Fig. 6.26** Temperature (K) contours at the mid-plane in the nozzle

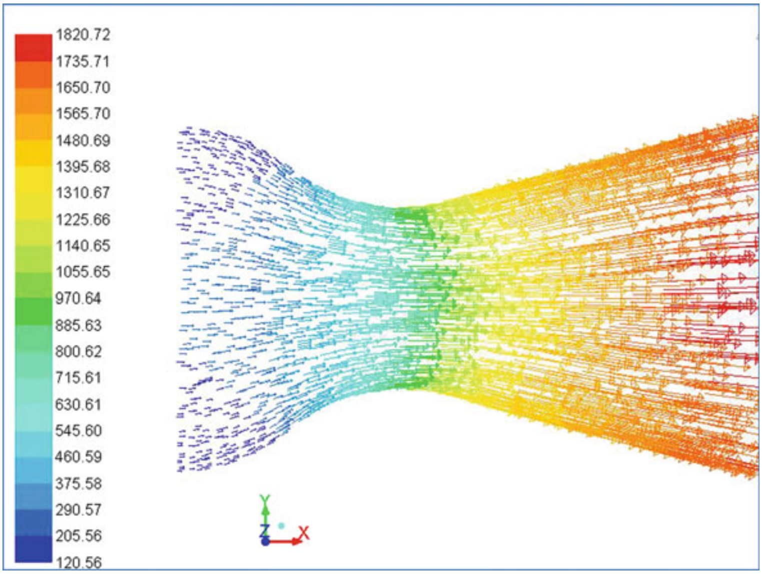


**Fig. 6.27** Velocity vectors at the mid-plane in the nozzle

region 120 m/s to sonic conditions around 800 m/s at the throat and finally to 1820 m/s at the exit with supersonic velocity in all the diverging nozzle. In idealized one-dimensional flow, the velocity will be constant in any cross-section.

As the velocity increases, the static pressure falls as shown in Fig. 6.22, the total pressure remaining almost constant in Fig. 6.23.

Figure 6.25 shows the corresponding Mach number Contours at the Mid-plane in the Nozzle.

The temperature contours are given in Fig. 6.26. The temperature decreases from stagnation temperature 2500 K to around 2000 K at the throat to 850 K at the exit. As the velocity increases, the temperature falls keeping the enthalpy constant.

Finally the velocity vectors at the mid-plane in the nozzle are shown in Fig. 6.27. The magnitudes vary from 120 to 1820 m/s as with Fig. 6.24. The directions of these vectors are parallel to the walls gradually straightening out to the central axis at the middle. In pure one-dimensional flow, the direction of the vectors is constant normal to the cross-section.

The flow is perfect expansion isentropic flow with Mach number >3 at the exit.

Table 6.5 below gives a comparison of analytical results with the CFD numerical results. They are in good agreement.

The results obtained are compared in Figs. 6.28, 6.29, 6.30 and 6.31 for Mach number, pressure ratio, temperature ratio and density ratio taken with throat section and they are in good agreement.

**Table 6.5** Comparison of analytical solution with numerical results

| Section no. | | 1 | 2 | 3 | 4 | 5 | 6 | 7 | 8 |
|---|---|---|---|---|---|---|---|---|---|
| A/A* | | 3.5857 | 3.3126 | 2.0932 | 1.0000 | 1.1331 | 1.5890 | 2.5214 | 3.4217 |
| M | *Analytical* | 0.1640 | 0.1838 | 0.2907 | 1.0000 | 1.4319 | 1.9267 | 2.4520 | 2.7760 |
| | *Numerical* | 0.1637 | 0.1894 | 0.3180 | 1.0025 | 1.4040 | 1.9004 | 2.4334 | 2.7705 |
| $p/p_4$ | *Analytical* | 1.8577 | 1.8488 | 1.7851 | 1.0000 | 0.5686 | 0.2711 | 0.1194 | 0.0724 |
| | *Numerical* | 1.8587 | 1.8466 | 1.7657 | 1.0000 | 0.6016 | 0.2845 | 0.1233 | 0.0738 |
| $T/T_4$ | *Analytical* | 1.1936 | 1.1919 | 1.1801 | 1.0000 | 0.8510 | 0.6887 | 0.5448 | 0.4722 |
| | *Numerical* | 1.1943 | 1.1921 | 1.1769 | 1.0000 | 0.8623 | 0.6982 | 0.5507 | 0.4746 |
| $\rho/\rho_4$ | *Analytical* | 1.5564 | 1.5511 | 1.5126 | 1.0000 | 0.6681 | 0.3936 | 0.2191 | 0.1532 |
| | *Numerical* | 1.5588 | 1.5515 | 1.5026 | 1.0000 | 0.6935 | 0.4069 | 0.2241 | 0.1555 |

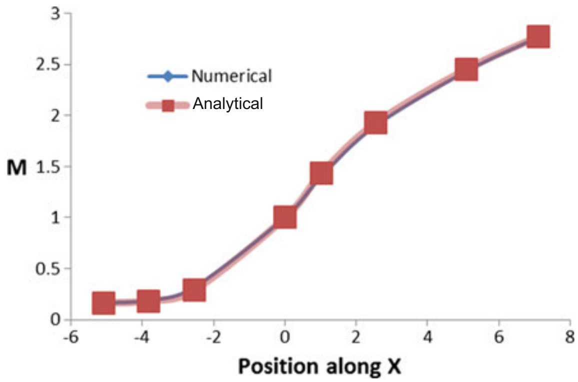


**Fig. 6.28** Comparison of numerical and analytical results for mach number

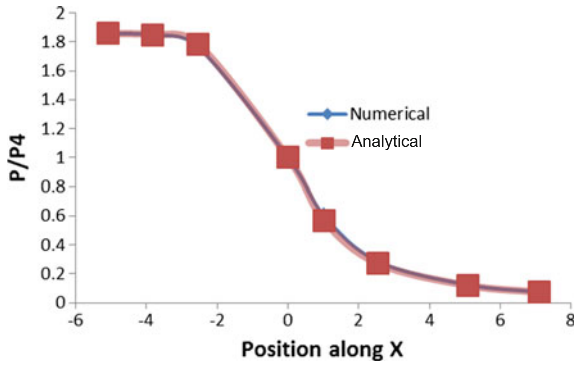


**Fig. 6.29** Comparison of numerical and analytical results for pressure ratio

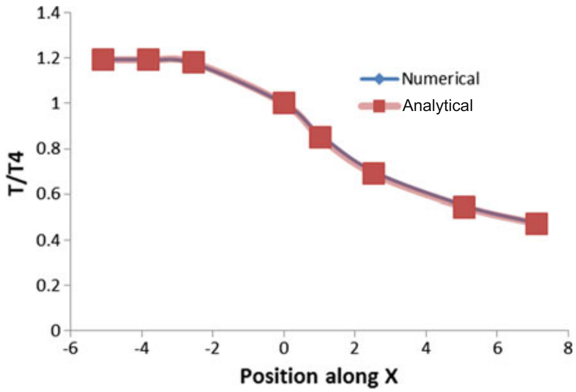


**Fig. 6.30** Comparison of numerical and analytical results for temperature ratio

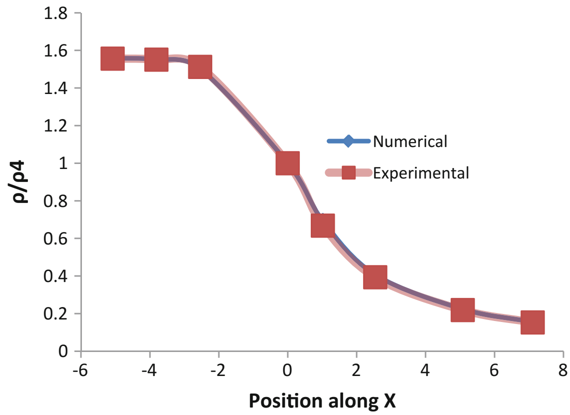


**Fig. 6.31** Comparison of numerical and analytical results for density ratio

## Exercises 6

6.1 Considering an incompressible steady flow, reduce the Euler's equations to one dimensional flow with velocity, pressure coupling and show that the pressure and kinetic energies are conserved. Define total pressure. Is total pressure same as stagnation pressure? Show how you can use this principle of conservation of energy to measure static pressure in a flow.

6.2 For an incompressible steady flow, show that the product of velocity and area of cross-section is a constant. Derive a relation for relative static pressures between two locations of a pipe with cross-sectional area $a_1$ changing to $a_2$. What are the stagnation pressures at these locations?

6.3 What is a streamline flow as opposed to flow in a straight pipe? What is total head in a streamline flow? Show that the sum of pressure and kinetic energies and the total head together is a constant in streamline flow.

6.4 Describe a Pitot tube and illustrate how the velocity can be measured in an open channel. Which is the stagnation point in the Pitot tube and explain why it is a stagnation point? What are the pressure and velocity values at this stagnation point?

6.5 Describe a Venturi meter and explain how you can determine the flow rate. Derive any relations from Bernoulli principle. A Venturi meter is used to measure the flow rate of water through a 6 cm dia pipe. The Venturi meter measures 3 cm dia and the manometer read 20 cm. What is the flow rate?

6.6 What is adiabatic flow? How are stagnation enthalpy and temperature related? For a steady adiabatic inviscid flow, show from the energy equation that $h + \frac{1}{2}V^2$ is a constant along a streamline and that this constant is stagnation enthalpy.

6.7 For an isentropic flow with pressure, temperature and density given at a specific location, derive relations for stagnation pressure and density in terms of stagnation temperature and specific heat ratio.

6.8 From fundamental principles show that the speed of sound at 20 °C is 343.17 m/s. The specific heat ratio is 1.4 and gas constant $R$ = 287.1 Pa m$^3$/kg °K

6.9 What are subsonic and supersonic flows? How does a shock form in supersonic flows?

6.10 For an isentropic flow given a Mach number at a point, derive the pressure in terms of stagnation pressure, likewise derive the density in terms of stagnation density. Based on the variations in density with a Mach number show that an isentropic flow can be considered as incompressible if the Mach number is lower than 0.3.

6.11 Explain what Characteristic Mach number is in an isentropic flow and derive a relation connecting it to the Mach number for a given location.

6.12 Show that

(a) converging nozzle accelerates a given subsonic flow; give typical applications
(b) a diverging nozzle (or a diffuser) decelerates a given subsonic flow; give typical applications

6.13 Show that

(a) converging nozzle or supersonic diffuser decelerates a given supersonic flow
(b) a diverging duct accelerates a supersonic flow

6.14 Show that a converging-diverging Laval nozzle accelerates the subsonic flow throughout the length. In such a nozzle can supersonic flow occur in the converging duct? What maximum value of Mach number can be attained at the throat?

6.15 Show that a converging-diverging nozzle can also act as a supersonic diffuser when the entry conditions are supersonic instead of being subsonic in the supersonic nozzle. Show that the throat is either sonic or * conditions.

6.16 Show that the Mach number at any location in a nozzle is a function of the ratio of the local duct area to the duct area where sonic conditions exist and derive a relation for this. How do you solve this equation?

6.17 A converging-diverging nozzle is given by 7 cm dia entry becoming 4 cm at the throat in a distance of 10 cm. From this throat, the nozzle diverges to 8 cm dia at exit over a distance of 15 cm. Both the converging and diverging nozzles have straight edges. Choose two intermediate sections equally placed in the converging and diverging ducts and make a total number of 7 stations including the entry, throat and exit locations. The nozzle is fed by a stagnation pressure 2450 Pa and the outlet pressure is 30 Pa. Determine the velocity, Mach number, pressure and temperature.

6.18 The inlet pressure is from a reservoir with 10 MPa. Discuss the performance of the nozzle as the back pressure at the exit is gradually reduced from 10 MPa starting the flow through the nozzle. Determine

(a) The back pressure when the nozzle gets choked.
(b) The back pressure when isentropic shock-free flow is regained.

# Chapter 7
# Turbulence

**Abstract** In this chapter, Reynolds turbulence phenomenon and viscous flows are considered. Navier-Stokes equations are derived by including Reynolds viscous forces in Euler equations. Reynolds Averaging technique of Navier-Stokes equation is presented with Boussinesq hypothesis that Reynolds stresses could be linked to the mean rate of deformation leading to and Turbulence viscosity. Turbulence models are explained that go with RANS approach for CFD. The example of Chap. 6 is continued here for CFD analysis of turbulent flow in nozzles.

**Keywords** Turbulence · Turbulent viscosity · Boussinesq hypothesis · Turbulence models · RANS approach

In 1883 Professor Osborne Reynolds in Manchester discovered the instability of water flow down a pipe in an experiment shown in Figs. 7.1 and 7.2.

He found the laminar flow in the pipe transits to instability and turbulence as the flow velocity is gradually increased when it reaches a critical velocity. This phenomenon is primarily a function of the pipe diameter $d$, the fluid density $\rho$, and the fluid dynamic viscosity $\mu$.

The velocity $V$ at which this transition takes place is called *critical velocity*, $V = V\ (d,\ \rho,\ \mu)$. By dimensional reasoning we find a dimensionless parameter, $R$ named *Reynolds number* given by

$$R = \frac{\rho V d}{\mu} \tag{7.1}$$

In the above, $\rho Vd$ is inertial force that destabilizes the flow and $\mu$ is the viscous damping that stabilizes the flow. As $R$ increases the inertial forces grow relatively larger and the flow becomes destabilized. Instead of a dimensional critical velocity



J.S. Rao, *Simulation Based Engineering in Fluid Flow Design*,
DOI 10.1007/978-3-319-46382-7_7

**Fig. 7.1** Professor Osborne Reynolds with his apparatus, Courtesy Professor Gibson, Head Mechanical Department Manchester University

**Fig. 7.2** Flow transition from laminar to turbulent flow

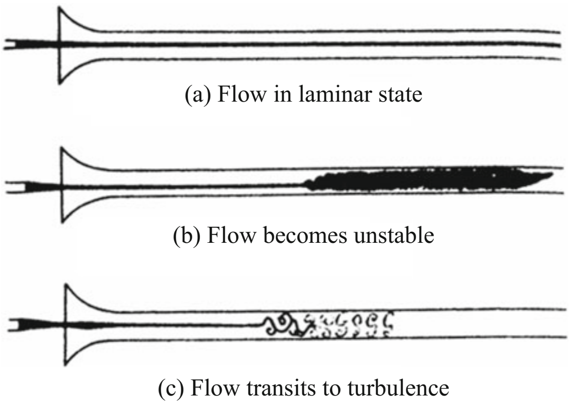


for each experimental condition, we use nondimensional velocity, i.e., Reynolds number $R$ that becomes applicable to all Newtonian fluid flows in round pipes of all diameters.

For water the flow is laminar when $R < 2300$, transient when $2300 < R < 4000$ and turbulent when $R > 4000$.

## 7.1 What Is Turbulence?

We notice turbulent flow in everyday life. The flow of water in a small canal appears smooth and stream lined, in a river even it appears smooth in summer season, whereas in rainy season it is more turbulent. It is particularly visibly if one observes the flow around a pier while looking down a road bridge.

It is an unsteady, aperiodic motion in which all three velocity components fluctuate, mixing matter, momentum, and energy. The $x$ component of velocity $U_i(t)$ can be decomposed into mean component $U_i$ and fluctuating part $u_i(t)$ (Fig. 7.3)

$$U_i(t) = U_i + u_i(t) \tag{7.2}$$

Similarly other velocity components, pressure and temperature also fluctuate over a mean part. Let us consider the flow around a cylinder with velocity gradually increased, see Fig. 7.4. The flow starts separating at $R = 5$. Figure 7.4a shows the flow streamlined, though separated with $R = 9.6$. As $R$ is increased, say to 13.1, the separation point slightly goes further in the downstream, as shown in Fig. 7.4b. In Fig. 7.4c as the Reynolds number is increased further to 26, the separation point is seen to be further ahead.

For $R$ below 30, the flow is stable. Beyond this value say $R = 30.2$, oscillations appear and the flow becomes unstable.

The separation point moves upstream, increasing drag up to $R = 2000$. Figure 7.4d shows the separation point further downstream.

As the velocity is further increased with Reynolds number reaching 10,000, one can see eddies formed and convected into the flow. Figure 7.4e shows the eddies formed and being convected in the turbulent flow.

When a fluid (air) flows over and around objects in its path, spiraling eddies are formed, these eddies are called Von Karman vortices. Figure 7.5 shows the formation of vortex while an airfoil is subjected to external flow. These vortices form eddies and are transported in the flow with the kinetic energy associated with them dissipating gradually leaving the flow to be streamlined and steady.

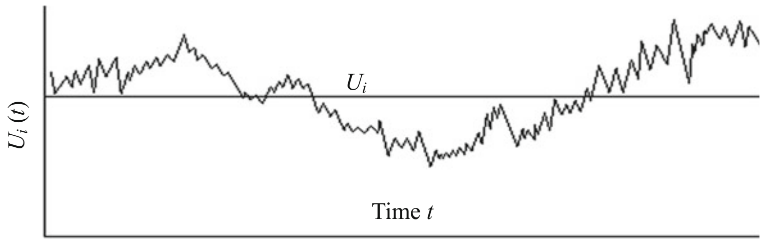


**Fig. 7.3** Unsteady velocity decomposed to steady and unsteady parts

**Fig. 7.4** Flow around a cylinder with increasing Reynolds number

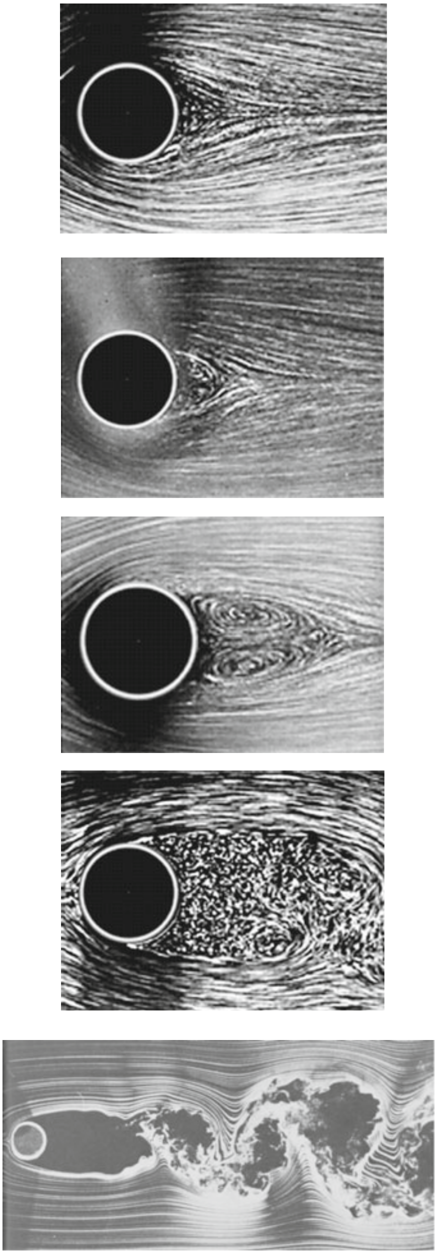

(a) $R = \mathbf{9.6}$

(b) $R = 13.1$

(c) $R = 26$

(d) $R = 2000$

(e) $R = 10000$

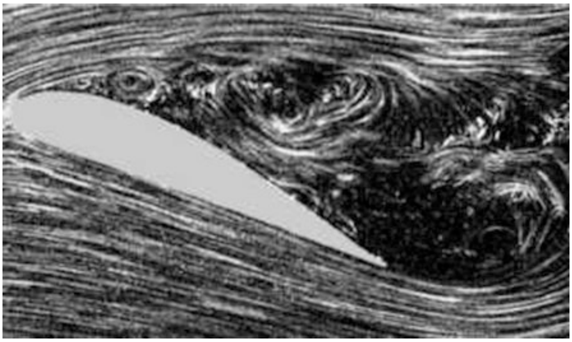

**Fig. 7.5** Formation of a vortex for flow over an airfoil

The characteristics of turbulent flows can be summarized as:

1. Turbulent flows always occur at high Reynolds numbers. They are caused by the complex interaction between the viscous terms and the inertia terms in the momentum equations.
2. Turbulence is a feature of fluid flow, not of the fluid. When the Reynolds number is high enough, most of the dynamics of turbulence are the same whether the fluid is an actual fluid or a gas. Most of the dynamics are then independent of the properties of the fluid.
3. Turbulent flows are characterized by their irregularity or randomness. A full deterministic approach is very difficult, usually they are described statistically. Turbulent flows are always chaotic. But not all chaotic flows are turbulent. Waves in the ocean, for example, can be chaotic but are not necessarily turbulent. If a flow is chaotic, but not diffusive, it is not turbulent.
4. The diffusivity of turbulence causes rapid mixing and increased rates of momentum, heat, and mass transfer. A flow that looks random but does not exhibit the spreading of velocity fluctuations through the surrounding fluid is not turbulent, e.g., the trail left behind a jet plane that seems chaotic, but does not diffuse for miles is then not turbulent.
5. Turbulent flows are dissipative. Kinetic energy gets converted into heat due to viscous shear stresses. Turbulent flows die out quickly when no energy is supplied.

Turbulence is a continuum phenomenon. Even the smallest eddies are significantly larger than the molecular scales. Turbulence is therefore governed by the equations of fluid mechanics.

## 7.2 Reynolds Equations

Under turbulent conditions, we first decompose velocity and pressure following Eq. (7.2) as

$$\begin{aligned} &\text{Velocity: } \mathbf{u} = \mathbf{U} + \mathbf{u}' \\ &\text{Pressure: } p = P + p' \end{aligned} \tag{7.3}$$

Turbulent kinetic energy $k$ (per unit mass) is defined as (with bar above a quantity denoting averaged value):

$$\begin{aligned} &k = \frac{1}{2}\left(\overline{u'^2} + \overline{v'^2} + \overline{w'^2}\right) \\ &\text{Turbulence intensity: } T_i = \frac{\left(\frac{2}{3}k\right)^{1/2}}{U_{ref}} \end{aligned} \tag{7.4}$$

The continuity equation given in (3.9) is written as

$$\begin{aligned} &\frac{\partial \rho}{\partial t} + div(\rho \mathbf{u}) = 0 \\ &\text{Time average: } \frac{\partial \rho}{\partial t} + \overline{div\, \rho \mathbf{u}} = \frac{\partial \rho}{\partial t} + div(\rho \mathbf{U}) = 0 \end{aligned} \tag{7.5}$$

Time averaging the momentum equations in (3.19) results in the following Reynolds equations without source terms.

$$\begin{aligned} &\frac{\partial(\rho u)}{\partial t} + div(\rho u \mathbf{u}) = -\frac{\partial p}{\partial x} + div(\mu\, grad\, u) \Rightarrow \\ &\frac{\partial(\rho U)}{\partial t} + div(\rho U \mathbf{U}) = -\frac{\partial P}{\partial x} + div(\mu\, grad\, U) + \left[-\frac{\partial\left(\rho\overline{u'^2}\right)}{\partial x} - \frac{\partial\left(\rho\overline{u'v'}\right)}{\partial y} - \frac{\partial\left(\rho\overline{u'w'}\right)}{\partial z}\right] \end{aligned} \tag{7.6a}$$

$$\begin{aligned} &\frac{\partial(\rho v)}{\partial t} + div(\rho v \mathbf{u}) = -\frac{\partial p}{\partial y} + div(\mu\, grad\, v) \Rightarrow \\ &\frac{\partial(\rho V)}{\partial t} + div(\rho V \mathbf{U}) = -\frac{\partial P}{\partial y} + div(\mu\, grad\, V) + \left[-\frac{\partial\left(\rho\overline{u'v'}\right)}{\partial x} - \frac{\partial\left(\rho\overline{v'^2}\right)}{\partial y} - \frac{\partial\left(\rho\overline{v'w'^v}\right)}{\partial z}\right] \end{aligned} \tag{7.6b}$$

$$\begin{aligned} &\frac{\partial(\rho w)}{\partial t} + div(\rho w \mathbf{u}) = -\frac{\partial p}{\partial z} + div(\mu\, grad\, w) \Rightarrow \\ &\frac{\partial(\rho W)}{\partial t} + div(\rho W \mathbf{U}) = -\frac{\partial P}{\partial z} + div(\mu\, grad\, W) + \left[-\frac{\partial\left(\rho\overline{u'w'}\right)}{\partial x} - \frac{\partial\left(\rho\overline{v'w'}\right)}{\partial y} - \frac{\partial\left(\rho\overline{w'^2}\right)}{\partial z}\right] \end{aligned} \tag{7.6c}$$

These Eqs. (7.6a)–(7.6c) contain an additional stress tensor from the last terms in each equation. These are called the Reynolds stresses given below in Eq. (7.7).

$$\boldsymbol{\tau} = \begin{pmatrix} \tau_{xx} & \tau_{xy} & \tau_{xz} \\ \tau_{yx} & \tau_{yy} & \tau_{yz} \\ \tau_{zx} & \tau_{zy} & \tau_{zz} \end{pmatrix} = \begin{pmatrix} -\rho\overline{u'^2} & -\rho\overline{u'v'} & -\rho\overline{u'w'} \\ -\rho\overline{u'v'} & -\rho\overline{v'^2} & -\rho\overline{v'w'} \\ -\rho\overline{u'w'} & -\rho\overline{v'w'} & -\rho\overline{w'^2} \end{pmatrix} \tag{7.7}$$

In turbulent flow, the above Reynolds stresses are usually large compared to the viscous stresses. The normal stresses $\tau_{xx}$, $\tau_{yy}$, $\tau_{zz}$ are always non-zero because they contain squared velocity fluctuations. The shear stresses would also be non-zero since the fluctuations are statistically not independent.

Note that $\rho$ is the mean density and the above equations are suitable for flows where changes in the mean density are important, but the effect of density fluctuations on the mean flow is negligible.

### 7.2.1 Reynolds Averaged Navier-Stokes Equations, RANS

The momentum equations without source terms are

$$\begin{aligned} \frac{\partial(\rho u)}{\partial t} + div(\rho u \mathbf{u}) &= -\frac{\partial p}{\partial x} + div(\mu\, grad\, u) + S_{Mx} \\ \frac{\partial(\rho v)}{\partial t} + div(\rho v \mathbf{u}) &= -\frac{\partial p}{\partial y} + div(\mu\, grad\, v) + S_{My} \\ \frac{\partial(\rho w)}{\partial t} + div(\rho w \mathbf{u}) &= -\frac{\partial p}{\partial z} + div(\mu\, grad\, w) + S_{Mz} \end{aligned} \tag{3.18}$$

Equations (7.6a)–(7.6c) above without the variable pressure and velocity components are

$$\begin{aligned} \frac{\partial(\rho U)}{\partial t} + div(\rho U \mathbf{U}) &= -\frac{\partial P}{\partial x} + div(\mu\, grad\, U) \\ \frac{\partial(\rho V)}{\partial t} + div(\rho V \mathbf{U}) &= -\frac{\partial P}{\partial y} + div(\mu\, grad\, V) \\ \frac{\partial(\rho W)}{\partial t} + div(\rho W \mathbf{U}) &= -\frac{\partial P}{\partial z} + div(\mu\, grad\, W) \end{aligned} \tag{7.8}$$

Equations (7.8) are the same as Eqs. (3.18) if we consider the averaged values of pressure and velocity. As mentioned before, we consider the mean density in these equations as the density fluctuations on the mean flow is negligible. Equations (7.8) are Reynolds Averaged Navier-Stokes equations, popularly called RANS equations. Their solution is the same as Euler's equations. For most engineering applications it is unnecessary to resolve the details of the turbulent fluctuations.

To accomplish the solution of Navier-Stokes equations, one way is to solve them with fluctuations included, which will take enormous computer time. This is a direct solution of Navier-Stokes equations, termed DNS. Instead a turbulence model can be adopted which is a computational procedure to close the system of mean flow equations, RANS.

Turbulence models allow the calculation of the mean flow without first calculating the full time-dependent flow field. Usually, it is sufficient to know how turbulence affects the mean flow.

When we want the effects of turbulence, we need expressions for the Reynolds stresses. It is common to adopt a turbulence model. They are based upon the Boussinesq hypothesis based on experimental observations that turbulence decays unless there is shear in isothermal incompressible flows. It was also observed that turbulence increases as the mean rate of deformation increases. In 1877, he proposed that the Reynolds stresses could be linked to the mean rate of deformation.

### 7.2.2 Boussinesq Hypothesis

Using the tensor notation, viscous stresses given by Eq. (3.29) are

$$\tau_{ij} = \mu e_{ij} = \mu\left(\frac{\partial u_i}{\partial x_j} + \frac{\partial u_j}{\partial x_i}\right) \tag{3.29}$$

In a similar manner, Reynolds stresses are linked to the mean rate of deformation:

$$\tau_{ij} = -\rho\overline{u_i' u_j'} = \mu_t\left(\frac{\partial U_i}{\partial x_j} + \frac{\partial U_j}{\partial x_i}\right) \tag{7.9}$$

In the above, the turbulent viscosity (eddy viscosity) $\mu_t$ is used. Its unit is the same as that of the molecular viscosity, Pa s. We can also define a kinematic turbulent viscosity, $\nu_t = \mu_t/\rho$. Its unit is $m^2/s$. The turbulent viscosity is not homogeneous, i.e. it varies in space, and however we assume it to be isotropic. It is the same in all directions. This assumption is valid for many flows, but not for all (e.g. flows with strong separation or swirl).

If we can determine the turbulent viscosity $\mu_t$ we can use Boussinesq hypothesis to determine the Reynolds stresses of (7.7) from (7.9) using RANS solution without finding the fluctuating components. Turbulence models are developed to achieve this. The simplest one is Prandtl's mixing length model developed in 1925.

### *7.2.3 Prandtl's Mixing Length Model*

We noted that the kinematic turbulent viscosity, $\nu_t = \mu_t/\rho$, units are m$^2$/s. On dimensional grounds one can express the kinematic turbulent viscosity $\nu_t$ as the product of a velocity scale $\vartheta$ (m/s) and length scale $\ell$ (m), therefore the associated name *mixing length model.*

$$\nu_t \left(\mathrm{m}^2/\mathrm{s}\right) \propto \vartheta\ (\mathrm{m/s})\ell\ (\mathrm{m}) \tag{7.10}$$

We assume further that the velocity scale $\vartheta$ is proportional to the length scale $\ell$ and the gradients in the velocity $\left|\frac{\partial U}{\partial y}\right|$ (shear rate, which has dimension 1/s):

$$\vartheta \propto \ell\left|\frac{\partial U}{\partial y}\right| \tag{7.11}$$

Using (7.11) in (7.10) we can derive Prandtl's mixing length model:

$$\nu_t = \ell_m^2\left|\frac{\partial U}{\partial y}\right| \tag{7.12}$$

Algebraic expressions exist for the mixing length $\ell_m$ for simple 2-D flows, such as pipe and channel flow. Though simple and easy to implement, it is incapable of describing flows where the turbulent length scale varies: anything with separation or circulation. This is rarely used these days.

There are several, some of those based on Reynolds Averaged Navier-Stokes (RANS) equations (time averaged) which have wide applicability, accurate, simple and economical to run. A discussion on these and other turbulence models is out of scope here. We will discuss briefly one of the most popularly used *k*-ε style models where ε is the rate at which the turbulent kinetic energy *k* dissipates.

### *7.2.4* **k-ε** *Model*

The *k*-ε model focuses on the mechanisms that affect the turbulent kinetic energy (per unit mass) *k*. The instantaneous kinetic energy *k(t)* of a turbulent flow is the sum of mean kinetic energy *K* and turbulent kinetic energy *k*

$$\begin{aligned} K &= \frac{1}{2}\left(U^2 + V^2 + W^2\right) \\ k &= \frac{1}{2}\left(\overline{u'^2} + \overline{v'^2} + \overline{w'^2}\right) \\ k(t) &= K + k \end{aligned} \tag{7.13}$$

ε is the dissipation rate of $k$. On dimensional grounds

$$\nu_t\left(\frac{\mathrm{m}^2}{\mathrm{s}}\right) \propto \vartheta\left(\frac{\mathrm{m}}{\mathrm{s}}\right) \times \ell(\mathrm{m}) \propto k^{1/2}\left[\left(\frac{\mathrm{m}^2}{\mathrm{s}^2}\right)^{1/2}\right] \times \frac{k^{3/2}\left[\left(\frac{\mathrm{m}^2}{\mathrm{s}^2}\right)^{3/2}\right]}{\varepsilon\left(\frac{\mathrm{m}^2}{\mathrm{s}^2}\frac{1}{\mathrm{s}}\right)} = \frac{k^2}{\varepsilon} \tag{7.14}$$

If $k$ and ε are known, we can model the turbulent viscosity as

$$\nu_t = \frac{k^2}{\varepsilon} \tag{7.15}$$

We now need equations for $k$ and ε.
Equation for $k$:
In terms of mean and turbulent kinetic energies per unit mass, instantaneous kinetic energy per unit mass is given by

$$\begin{aligned} k(t) &= K + k \\ K &= \frac{1}{2}\left(U^2 + V^2 + W^2\right) \\ k &= \frac{1}{2}\left(\overline{u'^2} + \overline{v'^2} + \overline{w'^2}\right) \end{aligned} \tag{7.16}$$

Following the idea of transport equation in Chap. 4, we can write the equation for the mean kinetic energy $K$ as follows

$$\underset{\text{(I)}}{\frac{\partial(\rho K)}{\partial t}} + \underset{\text{(II)}}{div(\rho K\mathbf{U})} = div\Big(\underset{\text{(III)}}{-P\mathbf{U}} + \underset{\text{(IV)}}{2\mu\mathbf{U}E_{ij}} - \underset{\text{(V)}}{\rho\mathbf{U}\overline{u_i'u_j'}}\Big) - \underset{\text{(VI)}}{2\mu E_{ij}\cdot E_{ij}} - \underset{\text{(VII)}}{(-\rho\overline{u_i'u_j'}\cdot E_{ij})} \tag{7.17}$$

In the above $E_{ij}$ is the mean rate of deformation tensor. This equation can be read as:

The rate of change of $K$ (I), plus the transport of $K$ by convection (II) **equals** the transport of $K$ by pressure (III), plus the transport of $K$ by viscous stresses (IV), plus the transport of $K$ by Reynolds stresses (V), minus the rate of dissipation of $K$ (VI), minus the turbulence production (VII).

In a similar manner, the transport equation for turbulence kinetic energy $k$ is written with $e'_{ij}$ as fluctuating component of rate of deformation tensor.

$$\underset{\text{(I)}}{\frac{\partial(\rho k)}{\partial t}} + \underset{\text{(II)}}{div(\rho k\mathbf{U})} = div\Big(\underset{\text{(III)}}{-\overline{p'\mathbf{u}'}} + \underset{\text{(IV)}}{2\mu\overline{\mathbf{u}'e'_{ij}}} - \underset{\text{(V)}}{\rho\frac{1}{2}\overline{u_i'\cdot u_i'u_j'}}\Big) - \underset{\text{(VI)}}{2\mu\overline{e'_{ij}\cdot e'_{ij}}} + \underset{\text{(VII)}}{\Big(-\rho\overline{u_i'u_j'}.E_{ij}\Big)} \tag{7.18}$$

The viscous dissipation term (VI) $2\mu \overline{e'_{ij} \cdot e'_{ij}}$ in the $k$ equation above describes the dissipation of $k$ because of the work done by the smallest eddies against the viscous stresses.

Equation (7.18) can be written by combining (III)–(V) into one of diffusion and using Boussinesq hypothesis for item (VI) to give

$$\underset{\text{(I)}}{\frac{\partial(\rho k)}{\partial t}} + \underset{\text{(II)}}{div(\rho k\mathbf{U})} = \underset{\text{(III)}}{div\left[\frac{\mu_t}{\sigma_k} grad\, k\right]} + \underset{\text{(IV)}}{2\mu_t E_{ij} \cdot E_{ij}} - \underset{\text{(V)}}{\rho\varepsilon} \tag{7.19}$$

This equation can be read as:

The rate of change of $k$ (I), plus the transport of $k$ by convection (II) **equals** the transport of $k$ by diffusion (III), plus the rate of production of $k$ (IV), minus the rate of destruction of $k$ (V). In the above, $\sigma_k$ is Prandtl number which connects the diffusivity of $k$ to the eddy viscosity. Typically a value of 1.0 is used.

Equation for ε

We can now define the rate of dissipation per unit mass ε as

$$\varepsilon = 2\nu\overline{e'_{ij} \cdot e'_{ij}} \tag{7.20}$$

A model equation for ε is derived by multiplying the $k$ equation by $\frac{\varepsilon}{k}$ and introducing model constants. The following (simplified) model equation for ε is commonly used.

$$\frac{\partial(\rho\varepsilon)}{\partial t} + div(\rho\varepsilon\mathbf{U}) = div\left[\frac{\mu_t}{\sigma_\varepsilon} grad\, \varepsilon\right] + C_{1\varepsilon}\frac{\varepsilon}{k} 2\mu_t E_{ij} \cdot E_{ij} - C_{2\varepsilon}\rho\frac{\varepsilon^2}{k} \tag{7.21}$$

The Prandtl number $\sigma_\varepsilon$ connects the diffusivity of ε to the eddy viscosity. Typically a value of 1.30 is used. Also, typically values for the model constants $C_{1\varepsilon}$ and $C_{2\varepsilon}$ of 1.44 and 1.92 are used.

Reynolds stresses from $k$ and ε

The turbulent viscosity is calculated from:

$$\mu_t = C_\mu \frac{k^2}{\varepsilon} \tag{7.22}$$

We can take value of $C_\mu = 0.09$. The Reynolds stresses are then calculated as follows:

$$-\rho\overline{u'_i u'_j} = \mu_t\left(\frac{\partial U_i}{\partial x_j} + \frac{\partial U_j}{\partial x_i}\right) - \frac{2}{3}\rho k\delta_{ij} = 2\mu_t E_{ij} - \frac{2}{3}\rho k\delta_{ij} \tag{7.23}$$

Most commonly the procedure one adopts to account for turbulence in Navier-Stokes equations is to adopt RANS approach to get the mean values and then determine the Reynolds stresses using a turbulence model such as the one described above.

## 7.3 Nozzle Flow with a Normal Shock in the Divergent Portion

In Chap. 6, we considered isentropic flow through converging-diverging nozzles, with Mach number at its throat reaching one and pure subsonic flow in the diverging portion with a back pressure of 9.795 MPa as well as perfect expansion supersonic flow in the diverging portion with a back pressure 0.3825 MPa. When the back pressure is reduced from 9.795 to 0.3825 MPa gradually, the diverging portion experiences a normal shock (normal to the direction of quasi-one-dimensional flow) and then an oblique shock before it becomes a perfect expansion isentropic flow. Here, we will study the occurrence of a normal shock by quasi-one-dimensional flow and check the result of a simulation of the nozzle flow with *k*-ε model.

### *7.3.1 Normal Shock*

Consider a steady supersonic one-dimensional flow in which a normal shock wave is located as shown in Fig. 7.6. The shock wave is a thin region and is an adiabatic process since there is no heat exchange from its surroundings. However the temperature increases because of the conversion of kinetic energy to internal energy across the shock wave. In this thin region, high velocity and temperature gradients occur; friction and thermal conduction play an important role on the flow within the shock.

Let the control volume enclose the shock as shown in Fig. 7.6 in the regions 1 and 2, the flow is isentropic (though the shock itself is non-isentropic) with different stagnation conditions. The pressure, density, temperature, Mach number, velocity, stagnation pressure, stagnation enthalpy, stagnation temperature and entropy are

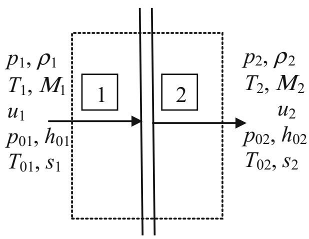


**Fig. 7.6** Normal shock (thin region of highly viscous flow)

given in region 1 ahead of the shock and region 2 behind the shock with respective subscripts. We can write down the following.

$$\begin{aligned}
&\text{Continuity:} && \rho_1 u_1 = \rho_2 u_2 \\
&\text{Momentum:} && p_1 + \rho_1 u_1^2 = p_2 + \rho_2 u_2^2 \\
&\text{Energy:} && h_1 + \frac{1}{2}u_1^2 = h_2 + \frac{1}{2}u_2^2 = h_{01} = h_{02} \\
&\text{Enthalpy:} && h_2 = c_p T_2 \\
&\text{Equation of State:} && p_2 = \rho_2 R T_2
\end{aligned} \tag{7.24}$$

Knowing the conditions in region 1, we can obtain $p$, $\rho$, $T$, $u$ and $h$ in region 2 from the above five Eqs. (7.24).

Divide the momentum equation by the continuity equation

$$\begin{aligned}
&\frac{p_1}{\rho_1 u_1} + u_1 = \frac{p_2}{\rho_2 u_2} + u_2 \Rightarrow \\
&\frac{p_1}{\rho_1 u_1} - \frac{p_2}{\rho_2 u_2} = u_2 - u_1
\end{aligned} \tag{7.25}$$

From (6.32) $\frac{p}{\rho} = \frac{a^2}{\gamma}$ and the above can be written as

$$\frac{a_1^2}{\gamma u_1} - \frac{a_2^2}{\gamma u_2} = u_2 - u_1 \tag{7.26}$$

Instead of energy equation in (7.24) we will use the special form derived for adiabatic flow given by (6.34)

$$\frac{a^2}{\gamma - 1} + \frac{1}{2}u^2 = \frac{\gamma + 1}{2(\gamma - 1)}a^{*2} \tag{6.34}$$

to give in both the regions 1 and 2 as

$$\begin{aligned}
a_1^2 &= \frac{\gamma + 1}{2}a^{*2} - \frac{\gamma - 1}{2}u_1^2 \\
a_2^2 &= \frac{\gamma + 1}{2}a^{*2} - \frac{\gamma - 1}{2}u_2^2
\end{aligned} \tag{7.27}$$

Note that $a^*$ is same in both the regions, as the flow is adiabatic across the shock. We use the above values for $a_1$ and $a_2$ in (7.26) to give

$$\begin{aligned}
&\frac{\gamma+1}{2}\frac{a^{*2}}{\gamma u_1}-\frac{\gamma-1}{2\gamma}u_1-\frac{\gamma+1}{2}\frac{a^{*2}}{\gamma u_2}+\frac{\gamma-1}{2\gamma}u_2=u_2-u_1 \Rightarrow\\
&\frac{\gamma+1}{2\gamma u_1 u_2}a^{*2}+\frac{\gamma-1}{2\gamma}=1 \Rightarrow\\
&\frac{\gamma+1}{2\gamma u_1 u_2}a^{*2}=1-\frac{\gamma-1}{2\gamma}=\frac{\gamma+1}{2\gamma} \Rightarrow\\
&a^{*2}=u_1 u_2
\end{aligned} \tag{7.28}$$

This relation is derived by Prandtl and known as Prandtl equation. This relation can also be expressed as

$$\begin{aligned}
1&=\frac{u_1}{a^*}\frac{u_2}{a^*} \Rightarrow\\
1&=M_1^* M_2^* \Rightarrow\\
M_2^*&=\frac{1}{M_1^*}
\end{aligned} \tag{7.28a}$$

Squaring both sides and using (6.43a) $M^{*2}=\frac{(\gamma+1)M^2}{2+(\gamma-1)M^2}$, we get

$$\begin{aligned}
\frac{(\gamma+1)M_2^2}{2+(\gamma-1)M_2^2}&=\frac{2+(\gamma-1)M_1^2}{(\gamma+1)M_1^2} \Rightarrow\\
M_2^2&=\frac{1+\frac{\gamma-1}{2}M_1^2}{\gamma M_1^2-\frac{\gamma-1}{2}}
\end{aligned} \tag{7.29}$$

This result is significant in that the Mach number behind the shock $M_2$ is function of the Mach number $M_1$ ahead of the shock wave alone. It also shows that $M_2 = 1$ if $M_1 = 1$, which is the case of an infinitely weak normal shock defined as Mach Wave. We also note that $M_2 < 1$ if $M_1 > 1$, i.e., the flow behind the shock wave is subsonic. If the flow ahead of the shock is subsonic, i.e., $M_1 < 1$, a solution for $M_2$ can be obtained from (7.29) However such a solution is not practicable.

To obtain the density and velocity ratios, we can write the continuity equation in (7.24) with the help of (7.28) as

$$\begin{aligned}
\frac{\rho_2}{\rho_1}&=\frac{u_1}{u_2}=\frac{u_1^2}{u_1 u_2} \Rightarrow\\
\frac{\rho_2}{\rho_1}&=\frac{u_1}{u_2}=\frac{u_1^2}{a^{*2}}=M_1^{*2}
\end{aligned} \tag{7.30}$$

Using (6.43a), the above can be rewritten as

$$\frac{\rho_2}{\rho_1} = \frac{u_1}{u_2} = \frac{u_1^2}{a^{*2}} = \frac{(\gamma+1)M_1^2}{2+(\gamma-1)M_1^2} \tag{7.31}$$

We then derive a relationship for the pressure ratio by using the momentum equation and continuity equation in (7.24)

$$\begin{aligned} p_2 - p_1 &= \rho_1 u_1^2 - \rho_2 u_2^2 \\ &= \rho_1 u_1 (u_1 - u_2) \\ &= \rho_1 u_1^2 \left(1 - \frac{u_2}{u_1}\right) \end{aligned} \tag{7.32}$$

Dividing the above equation by $p_1$ and noting that $a = \sqrt{\frac{\gamma p}{\rho}}$ from (6.32), we have

$$\begin{aligned} \frac{p_2 - p_1}{p_1} &= \frac{\gamma \rho_1 u_1^2}{\gamma p_1}\left(1 - \frac{u_2}{u_1}\right) \\ &= \frac{\gamma u_1^2}{a_1^2}\left(1 - \frac{u_2}{u_1}\right) \\ &= \gamma M_1^2 \left(1 - \frac{u_2}{u_1}\right) \end{aligned} \tag{7.33}$$

Substituting velocity ratio $\frac{u_2}{u_1} = \frac{2+(\gamma-1)M_1^2}{(\gamma+1)M_1^2}$ from (7.31) we obtain the pressure ratio across the shock as

$$\begin{aligned} \frac{p_2 - p_1}{p_1} &= \gamma M_1^2 \left(1 - \frac{2+(\gamma-1)M_1^2}{(\gamma+1)M_1^2}\right) \Rightarrow \\ \frac{p_2}{p_1} &= 1 + \frac{2\gamma}{\gamma+1}\left(M_1^2 - 1\right) \end{aligned} \tag{7.34}$$

The temperature ratio can be obtained directly from the equation of state in (7.24)

$$\frac{T_2}{T_1} = \left(\frac{p_2}{p_1}\right)\left(\frac{\rho_1}{\rho_2}\right) \tag{7.35}$$

Using (7.31) and (7.34) for density and pressure ratios respectively and noting that $h = c_p T$ the temperature ratio is obtained as

$$\frac{T_2}{T_1} = \frac{h_2}{h_1} = \left\{1 + \frac{2\gamma}{\gamma+1}\left(M_1^2 - 1\right)\right\} \frac{2+(\gamma-1)M_1^2}{(\gamma+1)M_1^2} \tag{7.36}$$

The Mach number, density, pressure and temperature behind the shock as given in Eqs. (7.29), (7.31), (7.34) and (7.36) show that they are all functions of the upstream Mach number for a given gas with specific heat ratio, $\gamma$. This is a striking phenomenon and shows how powerful it is for the Mach number in governing the compressible flows. Once again when the upstream Mach number is 1, the pressures, densities and temperatures remain same across the weak shock, which is termed Mach wave.

It may be reiterated here that Eq. (7.29) that physically acceptable solutions for normal shock are possible only in supersonic flows, though theoretically, solutions can be obtained for upstream Mach number less than 1 from the Eqs. (7.29), (7.31), (7.34) and (7.36) above. To understand as to why the subsonic flows cannot produce a normal shock, we refer to II law and calculate the entropy change across normal shock. The entropy change across a normal shock can be obtained from Eq. (2.54)

$$s_2 - s_1 = c_p \ln\frac{T_2}{T_1} - R\ln\frac{p_2}{p_1} \tag{2.54}$$

Substituting for Temperature ratio from (7.36) and pressure ratio from (7.34), we get

$$\begin{aligned} s_2 - s_1 = c_p \ln\left\{1 + \frac{2\gamma}{\gamma+1}\left(M_1^2 - 1\right)\right\}\frac{2 + (\gamma-1)M_1^2}{(\gamma+1)M_1^2} \\ - R\ln\left\{1 + \frac{2\gamma}{\gamma+1}\left(M_1^2 - 1\right)\right\} \end{aligned} \tag{7.37}$$

We note from the above that $s_2 - s_1 = 0$ when the normal shock is a Mach wave, i.e., $M_1 = 1$. $s_2 - s_1 > 0$ for supersonic flow $M_1 > 1$. Both these flows are possible according to the II law of thermodynamics. However, when $M_1 < 1$, i.e., the flow is subsonic, $s_2 - s_1 < 0$ and according to the II law, this process is not admissible.

The normal shock is always compressible in nature. This can be verified from Eq. (7.34) that the pressure increases across the shock, so also the temperature and enthalpy in Eq. (7.36) and the density in Eq. (7.31).

Since the flow across the shock is adiabatic, it is obvious that the stagnation temperature remains same for the flow ahead of the shock as well as the flow behind the shock. Both the flows ahead and behind the shock are isentropic by themselves, but have different stagnation pressures. To obtain a relation for the stagnation pressures of the flow ahead and behind the shock, let the local conditions for the flow ahead of the shock in region 1 be $M_1$, $p_1$, $T_1$ and $s_1$. Let us imagine a fluid element with these properties in region 1 to be brought to rest isentropically. Call this state 1a and with properties, $M_{01} = 0$, $p_{01}$, $T_{01}$ and $s_{01} = s_1$. Similarly in the region 2, behind the shock, assume an element with properties $M_2$, $p_2$, $T_2$ and $s_2$ to be brought to rest isentropically which then will have $M_{02} = 0$, $p_{02}$, $T_{02}$ and

$s_{02} = s_2$. The fact that stagnation temperature across the adiabatic shock is same can be demonstrated from Eq. (6.38) as

$$c_p T_{01} = c_p T_{02} = c_p T_0 \tag{7.38}$$

To determine the stagnation pressure behind the shock region, consider Eq. (2.54) for the two imaginary states of stagnation conditions ahead and behind the shock, which is

$$s_2 - s_1 = c_p \ln \frac{T_{02}}{T_{01}} - R \ln \frac{p_{02}}{p_{01}} \tag{7.39}$$

Therefore

$$\frac{p_{02}}{p_{01}} = e^{\frac{-(s_2 - s_1)}{R}} \tag{7.40}$$

Since $s_2 > s_1$, $p_{02} < p_{01}$. Hence there is a loss in stagnation pressure across the shock. Also since $s_2 - s_1$ is a function of Mach number $M_1$ ahead of the shock, the loss in stagnation pressure is a function of $M_1$ only.

*Rocket Nozzle Example in Fig. 6.17 with a Normal Shock*

We have seen in Sects. 6.10–6.12 that isentropic flow occurs through the nozzle when the back pressure is either 9.795 MPa with sonic flow at the throat and subsonic flow in the rest of the nozzle, or 0.3825 MPa, when there is perfect expansion in the nozzle, with sonic conditions at the throat and supersonic conditions in the diverging duct of the nozzle.

When perfect expansion takes place, the back pressure and the pressure at section 8 match exactly well.

When the back pressure is lower than 0.3825 MPa, there is under expansion, since the pressure at section 8 remained same at 0.3825 MPa. The nozzle has not expanded enough to match with the back pressure.

Prandtl-Meyer expansion takes place to bridge the gap in pressure. This expansion is out of scope in the present context.

Normal or oblique shocks take place when $9.795 > p_b > 3.375$ MPa.

The concerned equations are

$$M_2^2 = \frac{1 + \frac{\gamma - 1}{2} M_1^2}{\gamma M_1^2 - \frac{\gamma - 1}{2}} \tag{7.29}$$

$$\frac{\rho_2}{\rho_1} = \frac{(\gamma + 1) M_1^2}{2 + (\gamma - 1) M_1^2} \tag{7.31}$$

$$\frac{u_2}{u_1} = \frac{2 + (\gamma - 1) M_1^2}{(\gamma + 1) M_1^2} \tag{7.31a}$$

$$\frac{p_2}{p_1} = 1 + \frac{2\gamma}{\gamma + 1}\left(M_1^2 - 1\right) \tag{7.34}$$

$$\frac{T_2}{T_1} = \left\{1 + \frac{2\gamma}{\gamma + 1}\left(M_1^2 - 1\right)\right\}\frac{2 + (\gamma - 1)M_1^2}{(\gamma + 1)M_1^2} \tag{7.36}$$

The solution procedure is easier, if we start with location of normal shock because the way in which Eq. (7.29) is set up. Let us assume the shock at section 8.

*Normal Shock at Section* 8: From Table 6.4 with perfect expansion solution, the Mach number is 2.776; Note that the flow prior to the section 8 is entirely governed by the supersonic isentropic solution given in Table 6.4. For the shock to occur at section 8, we need two different flows, prior to the shock region 1 and flow across the shock region 2. So we denote $M_{81}$ = 2.776. The Mach number immediately after the shock here is then given by (7.29).

$$M_{82} = \sqrt{\frac{1 + 0.2M_{81}^2}{1.4M_{81}^2 - 0.2}} = \sqrt{\frac{1 + 0.2 \times 2.776^2}{1.4 \times 2.776^2 - 0.2}} = 0.4899$$

From Table 6.4, the pressure prior to the shock location can be obtained as

$$p_{81} = 0.0724 \times 5.2828 = 0.3825 \text{ MPa}$$

From (7.34)

$$\frac{p_{82}}{0.3825} = 1 + \frac{2.8}{2.4}\left(2.776^2 - 1\right) \Rightarrow$$
$$p_{82} = 3.375 \text{ MPa}$$

Therefore a normal shock will occur at section 8, when the back pressure is 3.375 MPa. The nozzle itself has already expanded to give a pressure at the exit equal to 0.3825 MPa. Therefore the nozzle has expanded to a level more than necessary to match with the back pressure or the nozzle has overexpanded.

The normal shock at section 8, takes care of this gap and compresses the flow to the required value. Suppose the back pressure is in the range of 0.3825–3.375 MPa, what will happen? We have another phenomenon that an oblique shock occurs at the exit of the nozzle. A consideration of an oblique shock is not discussed here.

*Normal Shock at Section* 5: We first note that the flow remains the same as in Table 6.4 up to this section 5. The Mach number before the shock $M_{51}$ is 1.4319; The Mach number immediately after the shock is then

$$M_{52} = \sqrt{\frac{1 + 0.2 \times 1.4319^2}{1.4 \times 1.4319^2 - 0.2}} = 0.7267$$

The pressure prior to the shock location is

$$p_{51} = 0.5686 \times 5.2828 = 3.0038 \text{ MPa}$$

Therefore

$$p_{52} = 3.0038\left[1 + \frac{2.8}{2.4}\left(1.4319^2 - 1\right)\right] = 6.6846 \text{ MPa}$$

The flow behind the shock is isentropic by itself, however with a different stagnation pressure in comparison to the isentropic flow ahead of the shock. Therefore we determine the flow properties by first determining the $A_e^*$ for the post shock flow in the nozzle exit portion. We first note that $\frac{A_5}{A^*} = 1.1331$ for the pre-shock flow. With the help of (6.66)

$$\frac{A_5}{A_e^*} = \frac{1}{M_{52}}\left[\left(\frac{2}{\gamma+1}\right)\left(1 + \frac{\gamma-1}{2}M_{52}^2\right)\right]^{\frac{\gamma+1}{2(\gamma-1)}} \Rightarrow$$
$$\frac{A_5}{A_e^*} = \frac{1}{0.7267}\left[\frac{1}{1.2}\left(1 + 0.2 \times 0.7267^2\right)\right]^3 = 1.0763$$

The area ratios for the sections 6–8 are given by

$$\frac{A_6}{A_e^*} = \frac{A_6}{A_5}\frac{A_5}{A_e^*} = 1.5093$$
$$\frac{A_7}{A_e^*} = 2.3950$$
$$\frac{A_8}{A_e^*} = 3.2501$$

The corresponding values of Mach numbers from Eq. (6.66a) by an iteration process are

$$M_6 = 0.4259$$
$$M_7 = 0.2509$$
$$M_8 = 0.1816$$

The stagnation pressure for post shock flow is determined from Eq. (6.39)

$$\frac{p_{02}}{p_{52}} = \left(1 + \frac{\gamma-1}{2}M_{52}^2\right)^{\frac{\gamma}{\gamma-1}} \Rightarrow$$
$$p_{02} = 6.6846\left(1 + 0.2 \times 0.7267^2\right)^{3.5} = 9.499 \text{ MPa}$$

For the shock at location 5, the pressure at the exit section 8 can now be obtained as

$$p_8 = \frac{9.4994}{(1 + 0.2 \times 0.1816^2)^{3.5}} = 9.2833 \text{ MPa}$$

In other words, a normal shock occurs at station 5, when the back pressure is lowered from 9.795 to 9.2833 MPa. As the pressure is lowered further, the shock travels along the diverging duct, finally reaching the exit location when the back pressure $p_b = p_{82} = 3.375$ MPa.

Recall that the normal shock is adiabatic and therefore there is no loss in stagnation temperature. From (6.37), we have

$$\frac{T_0}{T_4} = 1.2$$

The temperature ratio of any section with that of the throat can be obtained from

$$\frac{T}{T_4} = \frac{T_0}{T_4}\frac{T}{T_0} = \frac{1.2}{(1 + 0.2M^2)}$$

Tables 7.1, 7.2, 7.3, 7.4 give the flow properties behind the shock when it is located at sections 5–8 respectively.

**Table 7.1** Flow properties behind the shock located at section 5

| Station | $M$ | $\frac{p}{p_4}$ | $\frac{T}{T_4}$ |
|---|---|---|---|
| 51 | 1.4318 | 0.5686 | 0.8510 |
| 52 | 0.7267 | 1.2650 | 1.0854 |
| 6 | 0.4269 | 1.5863 | 1.1578 |
| 7 | 0.2509 | 1.7210 | 1.1851 |
| 8 | 0.1816 | 1.7571 | 1.1921 |

**Table 7.2** Flow properties behind the shock located at section 6

| Station | $M$ | $\frac{p}{p_4}$ | $\frac{T}{T_4}$ |
|---|---|---|---|
| 61 | 1.9267 | 0.2711 | 0.6887 |
| 62 | 0.5905 | 1.1288 | 1.1218 |
| 7 | 0.3235 | 1.3292 | 1.1754 |
| 8 | 0.2813 | 1.3769 | 1.1873 |

**Table 7.3** Flow properties behind the shock located at section 7

| Station | $M$ | $\frac{p}{p_4}$ | $\frac{T}{T_4}$ |
|---|---|---|---|
| 71 | 2.4520 | 0.1194 | 0.5448 |
| 72 | 0.5177 | 0.8176 | 1.1389 |
| 8 | 0.3509 | 0.9014 | 1.1712 |

**Table 7.4** Flow Properties behind the shock located at section 8

| Station | $M$ | $\frac{p}{p_4}$ | $\frac{T}{T_4}$ |
|---|---|---|---|
| 81 | 2.7700 | 0.0724 | 0.4722 |
| 82 | 0.4800 | 0.6385 | 1.1450 |

## 7.4 CFD Solution of Flow in Converging-Diverging Nozzles with a Normal Shock

We will now consider the nozzle example given in Sect. 6.13 in Fig. 6.19 with a back pressure 5 MPa. Because of the shock occurrence in the diverging portion, it is necessary to solve Navier-Stokes equations. As discussed before we use $k$-ε model of turbulence in RANS solution. The results obtained are given here.

The velocity contours in the mid-plane in m/s are given in Fig. 7.7. At the throat the velocity reached is around 800 m/s, sonic velocity, it then increases to a maximum of 1600 m/s before dropping down to 120 m/s at the exit. From the throat, the flow is supersonic till the shock location; beyond the shock the flow becomes subsonic. When the back pressure is 3.375 MPa the shock occurs at the exit. Since the back pressure 5 MPa is more than this value, the normal shock occurs at a location prior to the exit as shown in Fig. 7.7.

The Mach number contours are given in Fig. 7.8. The throat section is clearly under sonic conditions. We notice that these contours are not exactly normal to the central axis of the nozzle, but are convex in the diverging duct and concave in the

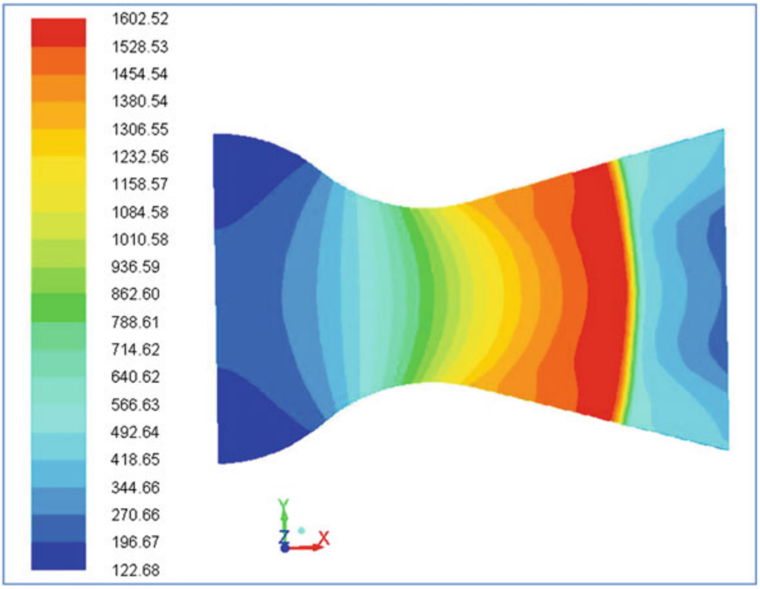


**Fig. 7.7** Velocity contours at the mid-plane

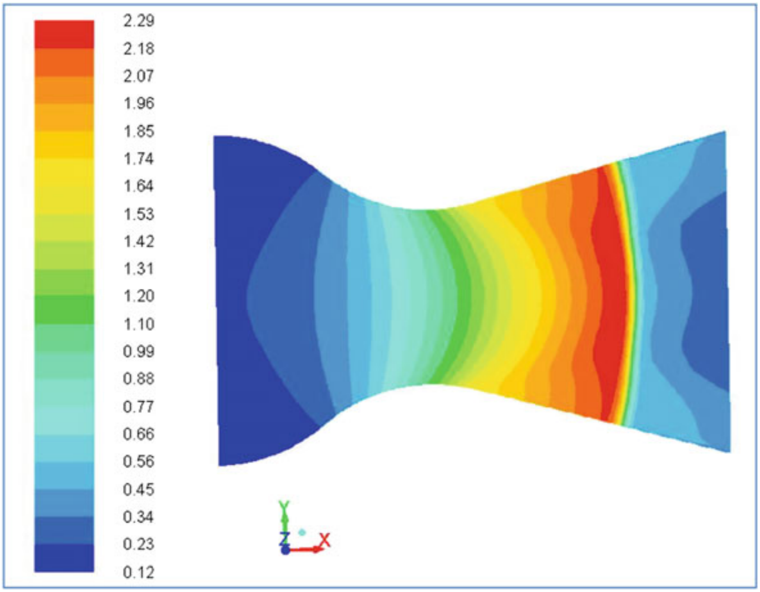


**Fig. 7.8** Mach number contours at the mid-plane

converging nozzle duct. This is because the flow is not exactly one dimensional it is three dimensional in nature. The analysis is conducted for quasi one dimensional flow and we have an ideal shock normal to the one dimension of the flow. The flow near the walls can be seen to be normal to the walls, not normal to the equivalent one dimensional flow direction. Along the central axis the flow is normal to this axis but not to the nozzle walls.

Figure 7.9 gives the velocity vector contours. On the nozzle walls the flow tugs to the walls and that is why the shock wave is convex in nature in the diverging duct and the velocity contours are concave in the converging duct.

The static pressure is almost same as stagnation pressure at the entry which decreases as the velocity keeps increasing. At the shock location the velocity reaches a high value and in the post shock flow the velocity falls and therefore the static pressure increases. This can be seen in Table 7.2. The value of pressure at the throat is determined earlier to be 5.2828 MPa and the value in Fig. 7.10 is the same. Prior to the shock, the pressure is the lowest 0.776 MPa which increases towards the exit to match with the back pressure 5 MPa.

Figure 7.11 gives the static temperature contours; initially it is the same as the total temperature at the entry with stagnation conditions and continuously decreases and post shock it raises again.

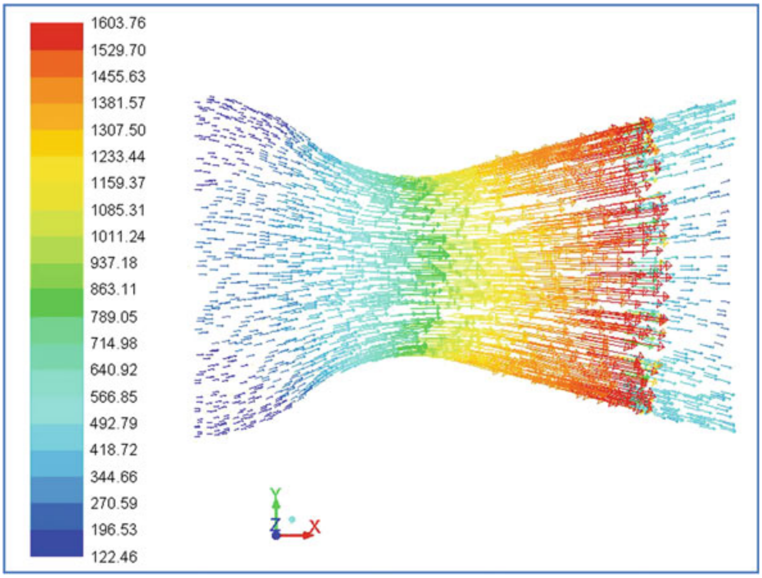


**Fig. 7.9** Velocity Vector contours at the mid-plane

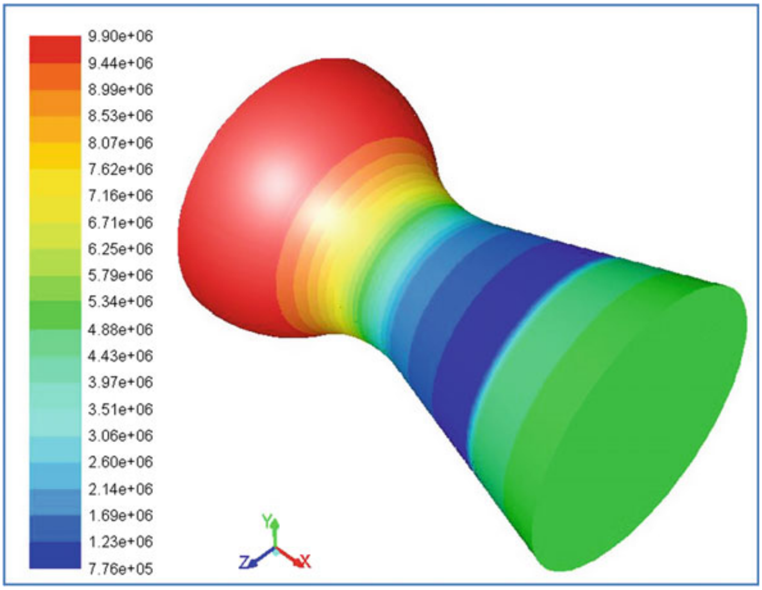


**Fig. 7.10** Static pressure contours

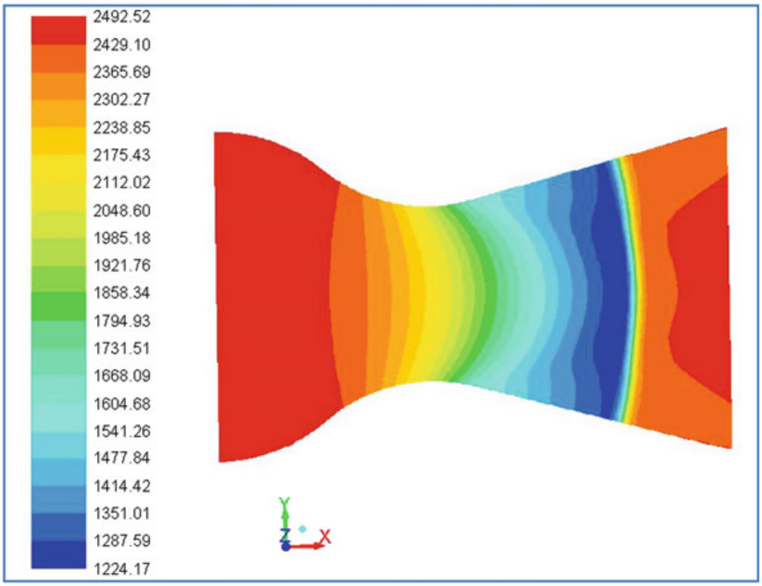


**Fig. 7.11** Static temperature contours at the mid-plane

## Exercises 7

7.1 What is turbulence? How is that connected to Reynolds number?
7.2 Discuss characteristics of turbulence.
7.3 Decompose the velocities in a turbulent flow into steady and time dependent terms and discuss what Reynolds stresses are.
7.4 What is RANS? Explain how this is accomplished and why?
7.5 Discuss Boussinesq hypothesis and how this is helpful in modelling turbulence.
7.6 What is Prandtl mixing model in simplifying turbulent flow?
7.7 What is turbulent kinetic energy and how its dissipation is modelled? Discuss the concept of turbulent viscosity.
7.8 When does a normal shock occur in a flow in nozzle flow? Using the continuity equation, momentum equation, energy equation, enthalpy and equation of state, determine relations between the state quantities before and after normal shock.
7.9 Derive Prandtl's equation and the relation between Mach number before and after a normal shock.
7.10 Show that a shock cannot occur in a subsonic flow.
7.11 Continue the problem 6.17 and discuss the conditions when a normal shock occurs in the diverging portion. Pay your attention to the conditions at the throat and the flow in converging portion of the nozzle. Show that the flow before and after are isentropic and determine the stagnation properties of these isentropic flows.

# Chapter 8
# Epilogue

**Abstract** Here we summarize the need to introduce 21st century approach of SBES with HPC at an early stage of UG education in place of approximate engineering approach evolved a century ago using Log Tables and Slide Rules.

The world of science changed our lives from the 17th century. The science revolution brought a culture of scientific thinking through parameterization of Physics that we have been observing over millennia. It brought the realm of engineering directly to our doorstops. The industrial revolution became a reality. Initially the design remained as engineering practice and testing but with the advent of rotating machinery at the turn of 20th century, analytical design became a necessity. Unfortunately we did not yet have computational capabilities beyond using logarithmic tables and hand calculations.

Therefore approximation of five coupled partial differential equations of fluids was simplified drastically to one dimension and approximate methods were evolved to get along with the design of rotating machinery.

This scenario has changed since high performance computing became common. This has brought back fundamental sciences of scientific revolution over three centuries ago. Yet many educational institutions continue to emphasize century old approximations rather than turning to current industrial practices. This has meant that commercial codes are still simply tools, and engineers of the day very rarely know what happens in a code. The codes are merely replacing log tables or slide rules of yesteryear, using the same science, more accurately rather than through the approximations.

This book presents an approach that brings science directly to the fore. It will be of immense benefit in in helping the young mind to understand better what the commercial codes do and bring the student to current engineering practices more intelligibly; Simulation Based Engineering Science (SBES) Approach.



J.S. Rao, *Simulation Based Engineering in Fluid Flow Design*,
DOI 10.1007/978-3-319-46382-7_8

**Acknowledgments** I am basically a solid mechanics person through my initial stages after graduation. During the mid-1970s I began to research work on excitation forces acting on moving turbo-machine blades which led me to Theodore von Karman's work on isolated airfoils and this aerodynamics was alien to me. I then contacted Professor William Sears of Ithaca, who had retired and settled in Tucson, Arizona from Rochester, NY. Being 35 years of age at that time, I was nervous about talking to him; true to the character of great teachers, he made me feel at ease and over 3–4 long distance calls he explained the physics behind interfering stage flow. I am deeply indebted to Professor Sears. That was my entry into fluid mechanics.

My large body of dedicated students worked hard in filling the empty areas of the puzzle that was an integrated approach to bringing to life the world of machine components. These students worked long hours in labs, computer centers and my home. They became a part of my family. I am extremely indebted to their devotion to the subject.

I began to realize slowly and steadily that Solids, Fluids and Electromagnetism are interdisciplinary was astounding to see that our forefathers, Newton, Euler, Faraday amongst others have bequeathed us such a rich legacy of science over three centuries. In the absence of computational means, engineering disciplines and practices grew separately over the last century; this scenario is rapidly changing in the last decade or two with basic sciences providing accurate solutions, thus giving rise to Simulation Based Engineering Science to the forefront. This necessitates a rethinking of the approach to inculcate approximate methods to engineering students and replace those by SBES.

My teacher and mentor Professor B.M. Belgaumkar talked to me about this science 54 years ago. Frankly I didn't follow him then. After a continuous exposure to industrial problems in the last two decades I recall his industrial service after retirement in the 1970s. I am very grateful for his guidance in my life.

I am thankful to my colleague Ashok Kumar for helping in solving problems on computer. I am thankful to my Kumaraguru College of Technology office and their help in preparing the materials.

Finally, I would like to express deepest gratitude to Arutselvar Padmabhushan Dr. Nachimuthu Mahalingam. He is a freedom fighter, Gandhian, educationalist, a great Tamil scholar and above all a visionary providing guidance to people like me. He shaped my spiritual part of life in the last decade, particularly during the last 2 years. I have the honor to be associated with him in my academics. I thank him very much for giving me the opportunity to partaking in promoting scientific thinking and temperments to younger generations of faculty and students. He is no longer with us now and I have the privilege to dedicate this book in his memory.

# Index




J.S. Rao, *Simulation Based Engineering in Fluid Flow Design*,
DOI 10.1007/978-3-319-46382-7